National Aeronautics and
Space Administration

**Lyndon B. Johnson Space Center**

# ARES

## Astromaterials Research & Exploration Science

# Biennial Report 2009-2010

## Cover image

*Photomicrograph of a thin section of the Martian meteorite (nakhlite) Miller Range (MIL) 03346, a specimen from the U.S. Antarctic meteorite collection managed in part by JSC, taken in crossed polarized light. The large crystals are clinopyroxene, and they are surrounded by a fine grained mesostasis of crystals and recrystallized glass. This sample formed in a shallow magma chamber on Mars approximately 1.3 billion years ago, and was found in Antarctica in 2003. The thin section is 30 micrometers thick, and the width of view is 3.5 millimeters.*

# Contents

# *Astromaterials Research and Exploration Science Directorate*

## Eileen K. Stansbery, Ph.D.

Since the return of the first lunar samples, what is now the Astromaterials Research and Exploration Science (ARES) Directorate has had curatorial responsibility for all NASA-held extraterrestrial materials. Originating during the Apollo Program (1960s), this capability at Johnson Space Center (JSC) included scientists who were responsible for the science planning and training of astronauts for lunar surface activities, as well as experts in the analysis and preservation of the precious returned samples. Today, ARES conducts research in basic and applied space and planetary science, and its scientific staff represents a broad diversity of expertise in the physical sciences (physics, chemistry, geology, astronomy), mathematics and engineering organized into three offices (figure 1), Astromaterials Research (KR), Astromaterials Acquisition and Curation (KT), and Human Exploration Science (KX).

Scientists within the Astromaterials Acquisition and Curation Office preserve, protect, document and distribute samples of the current astromaterials collections. Since the return of the first lunar samples, ARES has been assigned curatorial responsibility for all NASA-held extraterrestrial materials (Apollo lunar samples, Antarctic meteorites—some of which have been confirmed to have originated on the Moon and on Mars—cosmic dust, solar wind samples, comet and interstellar dust particles, and space-exposed hardware). The responsibilities of curation consist not only of the long-term care of the samples, but also the support and planning for future sample collection missions and research and technology to enable new sample types. Curation provides the foundation for research into the samples. The Lunar Sample Facility and other curation cleanrooms, data center, laboratories, and associated instrumentation are unique NASA resources that, together with our staff's fundamental understanding of the entire collection, provide a service to the external research community, who rely on access to the samples.

The curation efforts are greatly enhanced by a strong group of planetary scientists who conduct peer-reviewed astromaterials research. Astromaterials Research Office scientists conduct peer-reviewed research as Principal or Co-Investigators in planetary science (e.g., cosmochemistry, origins of solar systems, Mars fundamental research, planetary geology and geophysics) and participate as Co-Investigators or Participating Scientists in many of NASA's robotic planetary missions. Since the last report, ARES has achieved several noteworthy milestones, some of which are documented in detail in the sections that follow.

Within the Human Exploration Science Office, ARES is a world leader in orbital debris research, including modeling and monitoring the debris environment, designing debris shielding, and policy development to control and mitigate the orbital debris population. ARES has aggressively pursued refinements in the knowledge of the debris environment and hazards that it represents to spacecraft. Additionally, the ARES Image Science and Analysis Group has been recognized as

world class as a result of the high quality of near-real-time analysis of ascent and on-orbit inspection imagery to identify debris shedding, anomalies, and associated potential damage during space shuttle missions. ARES Earth scientists manage and continuously update the database of astronaut photography that is predominantly from Shuttle and ISS missions, but also includes the results of 40 years of human space flight. The Crew Earth Observations web site (http://eol.jsc.nasa.gov/Education/ESS/crew.htm) continues to receive several million hits per month. ARES scientists are also influencing decisions in the development of the next generation of human and robotic spacecraft and missions through lab tests on optical qualities of materials for windows, micrometeoroid/orbital debris shielding technology, and analog activities to assess surface science operations.

ARES serves as host to numerous students and visiting scientists as part of the services provided to the research community and conducts a robust education and outreach program. ARES scientists are recognized nationally and internationally by virtue of their success in publishing in peer-reviewed journals and winning competitive research proposals. ARES scientists have won every major award presented by the Meteoritical Society, including the Leonard Medal, the most prestigious award in planetary science and cosmochemistry, the Barringer Medal, recognizing outstanding work in the field of impact cratering, the Nier Prize for outstanding research by a young scientist, and several recipients of the Nininger Meteorite Award. One of our scientists received the DoD Joint Meritorious Civilian Service Award (the highest civilian honor given by DoD). ARES has established numerous partnerships with other NASA Centers, universities, and national laboratories. ARES scientists serve as journal editors, members of advisory panels and review committees, and society officers, and several scientists have been elected as Fellows in their professional societies.

This biennial report summarizes a subset of the accomplishments made by each of the ARES offices and highlights participation in the support of on-going human and robotic missions as well as development of new missions and planning for human and robotic exploration stepping out into the solar system beyond low Earth orbit.

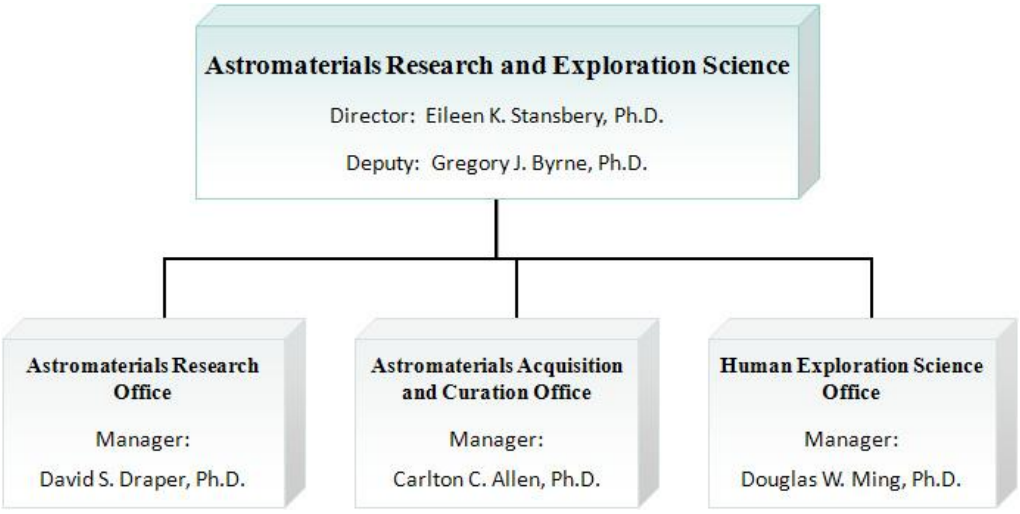


*Figure 1.– ARES organization chart*

# *Astromaterials Research Office (KR)*
# Overview

**David S. Draper, Ph.D., Manager**
**http://ares.jsc.nasa.gov/ares/indexkr.cfm**

The staff of the Astromaterials Research Office conducts peer-reviewed research in astromaterials. Scientists are funded through basic science disciplines of the NASA ROSES NRA (link below), including Cosmochemistry, Origins of Solar Systems, Astrobiology & Exobiology, Planetary Geology & Geophysics, Mars Fundamental Research, Lunar Advanced Science and Exploration Research and Planetary Astronomy. Further funding comes from planetary missions, instrument development, and data analysis programs.

http://nspires.nasaprs.com/external/solicitations/summary.do?method=init&solId={AEF75D0F-2272-7DE7-D52A-295B47C8F5CF}&path=open

The fundamental goal of our research is to understand the origin and evolution of the solar system, particularly the terrestrial, "rocky" bodies. Our research involves analysis of, and experiments on, astromaterials in order to understand their nature, sources, and processes of formation. Our state-of-the-art analytical laboratories include four electron microbeam labs for mineral analysis, four spectroscopy labs for chemical and mineralogical analysis, and four mass spectrometry labs for isotopic analysis. Other facilities include the experimental impact laboratory and both one-atmosphere gas mixing and high-pressure experimental petrology labs. Recent research has emphasized a diverse range of topics, including:

- Study of the solar system's primitive materials such as carbonaceous chondrites and interplanetary dust,
- Study of early solar system chronology using short-lived radioisotopes and of early nebular processes through detailed geochemical and isotopic characterizations,
- Study of large-scale planetary differentiation and evolution through study of siderophile and incompatible trace element partitioning, magma ocean crystallization simulations, and isotopic systematics,
- Study of the petrogenesis of martian meteorites through petrographic, isotopic, chemical, and experimental melting and crystallization studies,
- Interpretation of remote sensing data, especially from current robotic lunar and mars missions, and study of terrestrial analog materials, and
- Study of the role of biological systems and processes in evolution of astromaterials and the extent to which they constrain potential habitability.

**The following reports give examples of astromaterials research done by members of this and other ARES offices.**

## *JSC Probes the Life History of Meteorite From Early Solar System*

*Justin Simon*

JSC and colleagues at Lawrence Livermore National Laboratory, the University of California, Berkeley and the University of Chicago have performed a micro-probe analysis of the core and outer layers of a pea-size fragment meteorite some 4.6 billion years old to reconstruct the history of its formation, providing the first evidence that dust grains experienced wildly varying environments during the planet-forming years of our solar system. These dust grains, called calcium-, aluminum-rich inclusions (CAIs), are understood to have formed very early in the evolution of the Solar System and in contact with nebular gas, either as solid condensates or as molten droplets. On the basis of the oxygen isotope record found, the team interpreted these findings in the context of models about how matter formed in the early protoplanetary nebula and reported their implications for the formation of terrestrial planets in the March 2011 issue of the journal Science.

Their micrometer-scale analyses of a CAI, and the characteristic mineral bands mantling the CAI, reveal that the outer parts of this primitive object have a large range of oxygen isotope compositions. The variations are systematic; the relative abundance of $^{16}O$ first decreases toward the CAI margin, approaching a planetary-like isotopic composition, then shifts to extremely $^{16}O$-rich compositions through the surrounding rim. The variability implies that CAIs formed from several oxygen reservoirs, likely located in distinct regions of the solar nebula. The observations support early and short-lived fluctuations of the environment in which CAIs formed, either because of transport of the CAIs themselves to distinct regions of the solar nebula or because of varying gas composition near the proto-Sun.

To investigate intra-CAI oxygen isotopic variations, a component of the primitive meteorite Allende (the CAI called A37) and its surrounding concentric rim were measured by NanoSIMS, an ion microprobe with nanometer-scale spatial resolution. An image of A37 can be seen in the figure. The core of A37 extending well beyond the field of view to the upper left consists of the minerals melilite, spinel and perovskite. The rim consists of a sequence of mono-mineral layers a few micrometers thick (hibonite, perovskite, spinel, melilite/sodalite, pyroxene, and olivine). A spinel-rich micro-inclusion appears to have been entrapped while the rim was forming. The ion microprobe measurements were obtained as ~2 μm spot analyses spaced every 7–10 μm across the rim and the outer ~150 μm of the interior. At the resolution that is accessible with the NanoSIMS, both A37 and its rim exhibit more than 20‰ variation in $\Delta^{17}O$, a range that is close to the full range thought to exist among solids formed in the entire Solar System. These data imply that A37 was transported among several different nebular oxygen isotopic reservoirs, potentially as it passed through and/or into various regions of the protoplanetary disk.

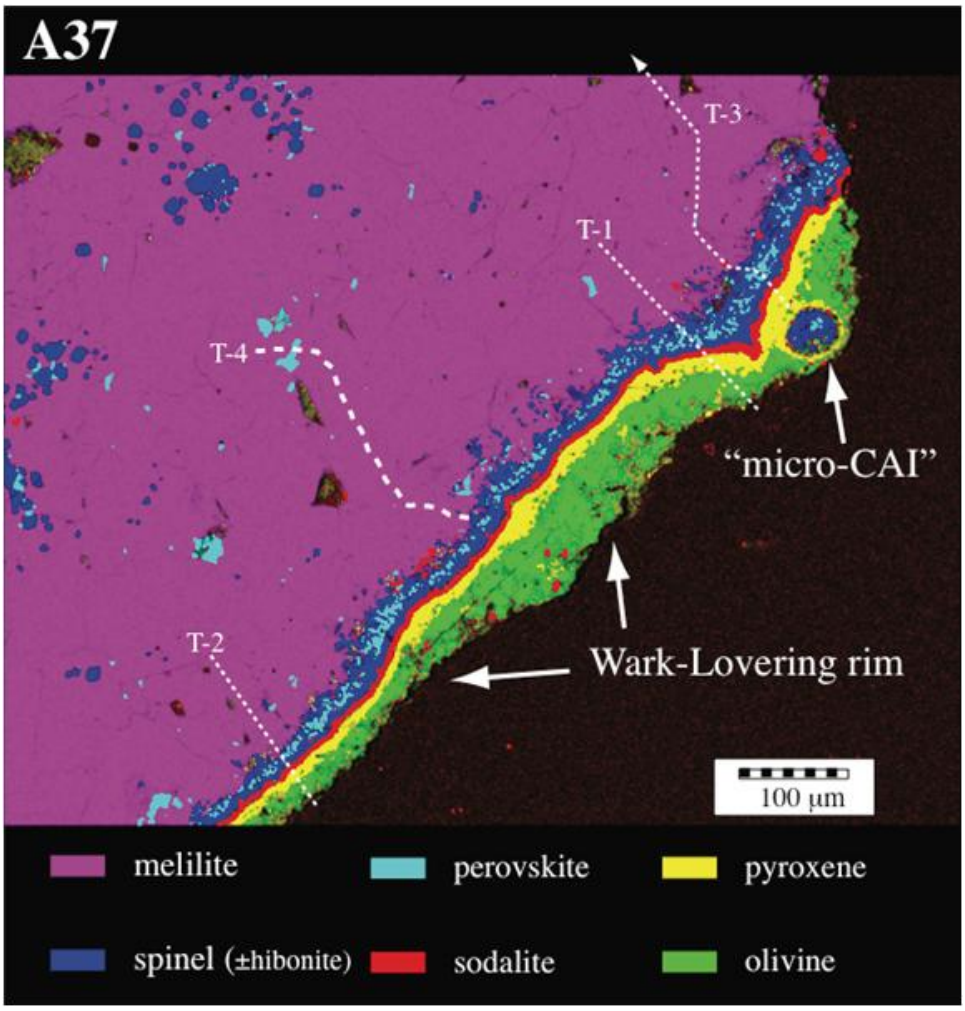


*Figure 1.– Compositional x-ray image of the rim and margin of a ~4.6 billion year old calcium aluminum rich refractory inclusion (CAI) from the Allende carbonaceous chondrite.*

The evidence for transport of solid matter reported by the team supports the inference from theoretical studies that outward radial transport of solid matter is a basic consequence of protoplanetary disk evolution. Large-scale radial circulation of nebular solids is also consistent with the reports of crystalline material located in the outer reaches of our Solar System, and in the outer, cool regions of distant stars. The variable but largely $^{16}$O-rich composition of the rim suggests that after transport out of the inner Solar System, CAIs either continued to form within a region in the outer Solar System that varied in composition, or that they were returned back to the inner Solar System.

## *Theoretical Cosmochemistry*

*Thomas Wilson, David Mittlefehldt*

ARES is leveraging its strong background in theoretical physics to study the mysterious, unknown carrier phase in carbonaceous chondrites that transports their noble gases. This phase is known in meteoritics as Q-phase (figure 1).

The directorate realized that the field has been primarily focused on experimental analysis and has felt that a computational analysis group could fit in well with basic ARES laboratory programs. A collaboration has been initiated with a theoretical chemistry group at Rice University, and together they hope to define a new analytical approach that may help experimentalists in the ultimate discovery of Q: *What is Q and what information can it shed regarding the origin and evolution of the Solar System?* Since experimental scientists have failed to identify Q after 35 years of trying, perhaps it is time that they get some help from their colleagues in the theoretical science community.

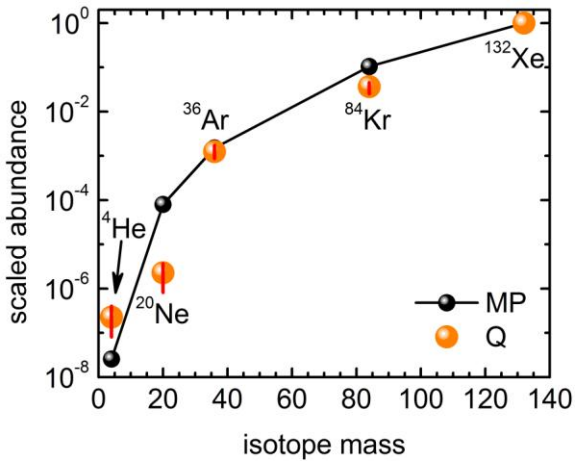


*Figure 1.– Q-phase.*

## *How Tiny Amounts of Water in the Deep Earth Saved Continents*

*Anne Peslier, Alan Woodland (University of Frankfurt), David Bell (Arizona State University), Marina Lazarov (University of Frankfurt)*

The Earth is unique in our solar system not only because of its water-filled oceans and its oxygen rich atmosphere, but also because of its plate tectonic engine. The layer on which the tectonic plates float is called the asthenosphere and is made of very slowly deformable rock. Riding on it, huge chunks of the crust and mantle sink constantly into the asthenosphere when they become old and dense at subduction zones, while new crust is being made at mid-ocean ridges. Finally continents break up and collide over 100 of million year cycles, churning up even more crust at their edges. And yet, over its 4.5 Ga history, the Earth has managed to preserve some very old rocks, some more than 3 Ga years old. What prevented these rocks from being recycled into the asthenosphere? Recent work published in the Sept 2$^{nd}$ issue of *Nature* by JSC and colleagues at the University of Frankfurt, and Arizona State University bring answers to this puzzle.

For this study they turned their attention to the ancient cores of continents, called cratons, where the oldest rocks can be found. Cratons are also part of tectonic plates and therefore also float on the asthenosphere. They resemble icebergs in an ocean with deep keels (down to 200 km) protruding into the asthenosphere. Samples from these keels, brought up by magmas that traverse them called kimberlites, are available. The latter are incidentally famous for also bringing up diamonds. It is known that these roots are as old as the rocks found at the surface, around 3 Ga. Scientists have long tried to explain why these roots exist, as it would be expected that they would be eroded away by the surrounding hot and dynamic asthenosphere. It has been proposed that the keels float because they are less dense than the asthenosphere. Over their billion years history magmas have removed dense elements (iron, aluminium, calcium) from them. Geologists also think that their cold temperature compared to that of the asthenosphere make the roots stiff and resistant. Finally, scientists have long proposed that water, or more exactly, the absence of it in the keel, could make it also strong and resistant. The last hypothesis has never been proven until this study.

JSC has a specialty in measuring tiny amounts of water locked up in minerals. The main mineral of rocks from the root of the Kaapvaal craton located in South Africa was analyzed. The more this mineral, called olivine, contains water, the softer it becomes. On the contrary, the olivines from the very bottom of the craton are very dry, making them very hard to deform and break (see figure). So here is a mechanism for rendering the keels of cratons resistant: they have a shell of very hard dry olivines. This work has crucial implications on our understanding of Earth plate tectonics, why continents exist and the evolution of planetary interiors since the formation of the solar system.

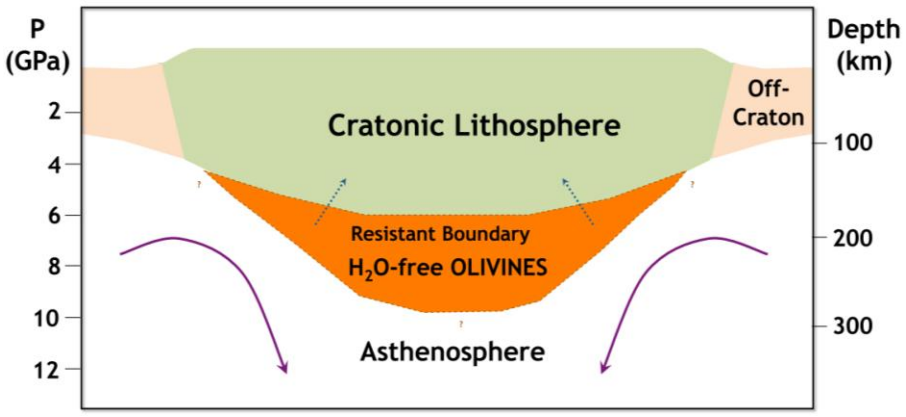


*Figure 1.– A sketch of a cross-section of a craton. A layer of resistant dry rock (orange) and the bottom of the cratonic keel prevents it from being eroded away over billions of years by the convection in the asthenophere (purple arrows).*

# *Early Life on Earth and the Search for Extraterrestrial Biosignatures*

*Dorothy Z. Oehler, Everett K. Gibson*

An understanding of earliest terrestrial life is of astrobiological importance, as knowledge of early evolutionary processes on Earth could provide insight to development of life on other planets. Yet, the nature of early life on Earth is difficult to assess because the oldest potential biosignatures are commonly poorly preserved.

JSC has been using the relatively new technique of NANOSIMS to evaluate ancient microorganisms preserved on Earth. Results from well-preserved and non-controversial microfossils (figure 1) have provided new criteria for assessing the origin of poorly preserved organic materials. These criteria were applied to controversial organic microstructures from a 3 billion year old sedimentary rock in Australia. Results (figure 2) suggest that the organic structures are biogenic and the same age as the rock. More importantly, the results from NANOSIMS add to a growing body of data suggesting that by 3 billion years ago, life on Earth was multifaceted and diverse. This view of early terrestrial evolution may increase the likelihood that primitive life on other planets could survive and adapt to adverse or unusual conditions by ready development of diversity in form and biochemistry.

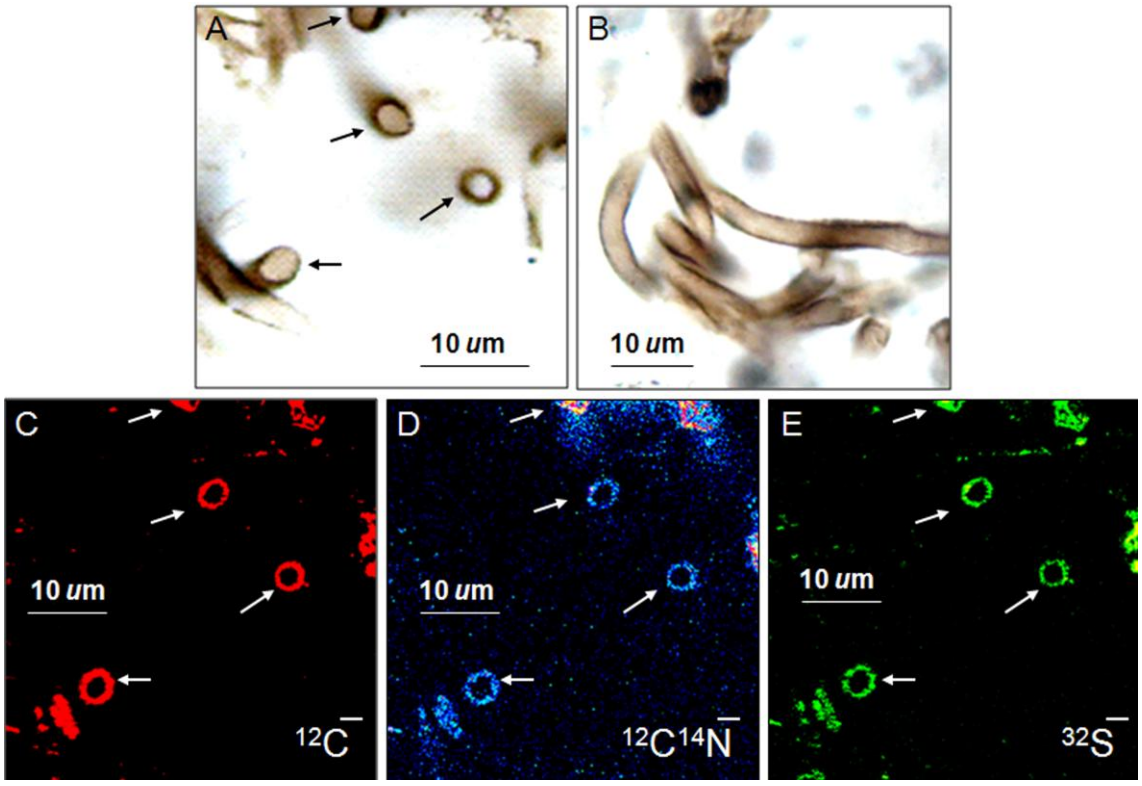


*Figure 1.– Well-preserved, 1 billion year old organic microfossils, Bitter Springs Formation, Australia. A-B, optical photomicrographs in transmitted light of filamentous microfossils in a thin section. C-E, NanoSIMS element maps of the three filaments imaged in cross-section in (A).*

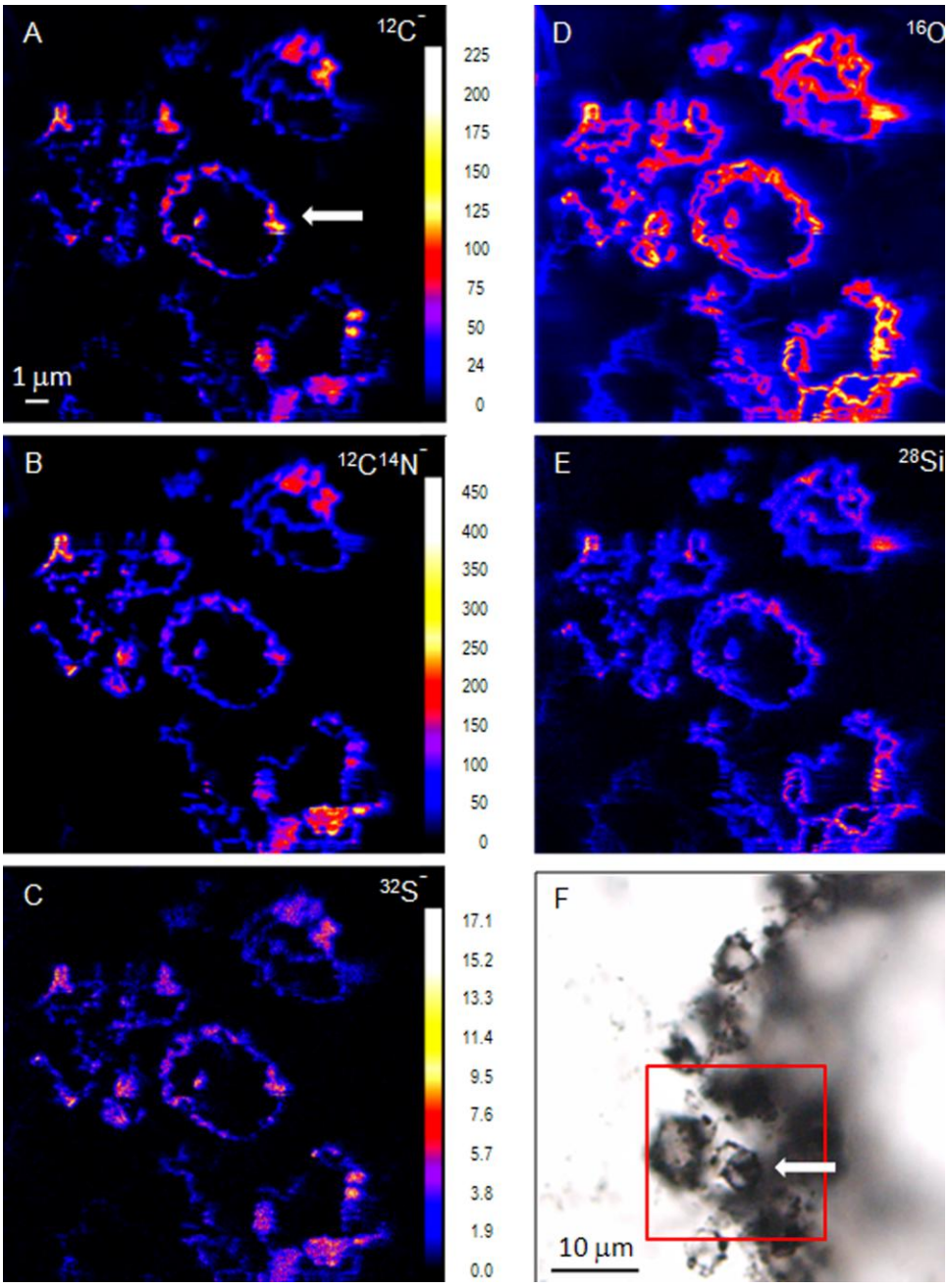


*Figure 2.– Controversial, organic microstructures in a 3 billion year old rock from the Pilbara of Australia. A-E, NanoSIMS element maps of the spheroidal structures within the red rectangle of (F). F, optical photomicrograph in transmitted light of a thin section showing spheroidal, microfossil-like structures.*

# *Fluids and Their Effect on Measurements of Lunar Soil Particle Size Distribution*

*Bonnie L. Cooper, David S. McKay, W. T. Wallace, Carla P. Gonzalez*

**Introduction**

From the late 1960s until now, lunar soil particle size distributions have typically been determined by sieving—sometimes dry, and at other times with fluids such as water or Freon. Laser diffraction instruments allow rapid assessment of particle size distribution, and eventually may replace sieve measurements. However, when measuring lunar soils with laser diffraction instruments, care must be taken in choosing a carrier fluid that is compatible with lunar material.

**Background**

Distilled water is the fluid of choice for laser diffraction measurements of substances when there is no concern about adverse effects of water on the material being measured. When JSC began the analyses of lunar soils using laser diffraction, the first measurements were made with distilled water. Although the medians measured were comparable to earlier sieve data, the means tended to be significantly larger than expected.

The effect of water vapor on lunar soil has been studied extensively. The particles interact strongly with water vapor, and subsequent adsorptions of nitrogen showed that the specific surface area increased as much as threefold after exposure to moisture. It was observed that significant porosity had been generated by this exposure to water vapor. The possibility of other physical changes in the surfaces of the grains was not studied.

**Investigation**

A dispersion test showed that the use of distilled water resulted in clumping of lunar soil (figure 1). When a size-fractionated sample from lunar soil 14003,96 was measured in water, the volumetric mean was 121.1 micrometers, and the median was 98.04 micrometers (figure 2). When another sample of the same material was measured with isopropanol, the volumetric mean was 59.63 micrometers, and the median was 57.30 micrometers. Variation in aliquots could not be invoked as the cause of this difference.

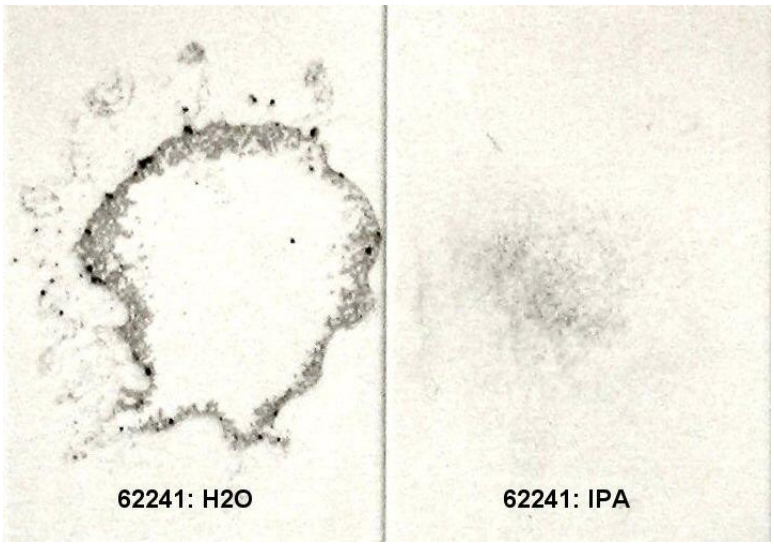


*Figure 1.– Dispersion tests with drops of water (left) and isopropanol (right) on a microscope slide, followed by application of a few mg of lunar soil 62241.*

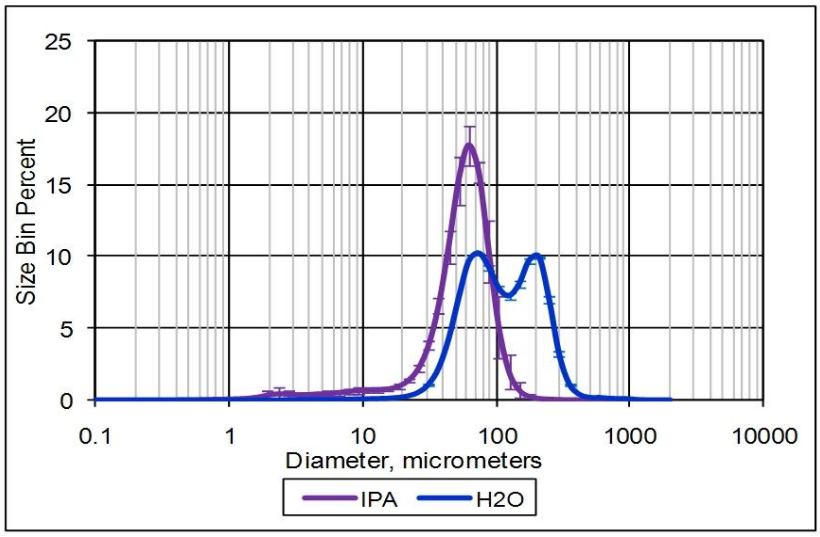


*Figure 2.– Measurements of a size-fractionated sample from Apollo 14 soil 14003,96 in water (blue) and in isopropanol (purple). Note the secondary peak at large (~200 micro-meters) particle size in the histogram that was measured in water, thought to be caused by clumping.*

A measurement of Apollo 11 soil 10084,2006 also showed significant variations related to the fluid that was used for measurement (figure 3). Moreover, when comparing three separate measurements of the sample in water, the standard error was seen to be significantly larger than the standard error produced when isopropanol was used.

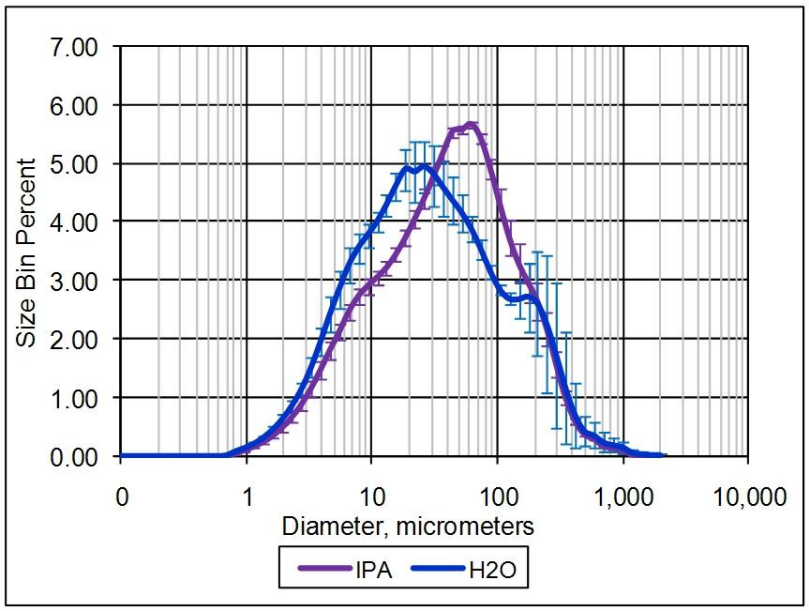


*Figure 3.– Measurements of Apollo 11 soil 10084 in water (blue) and isopropanol (purple).*

It was found that the use of isopropyl alcohol resulted in little or no clumping. However, there was concern that the isopropyl alcohol might partially dissolve and disaggregate the agglutinates because of their high proportion of potentially reactive glass, and thus create smaller particles than would have occurred naturally. To address this concern, JSC performed dissolution tests on lunar soil 14003,96 using isopropanol and water, and also using an acidic citrate-phosphate buffer (pH 4). The

solutions were analyzed with ICP-MS. It was observed that neutral pH water had a strong tendency to dissolve the silicon, calcium, and aluminum in lunar soil, and that the isopropanol dissolved a negligible amount of these elements when corrected for the blank control (figure 4).

| Element | Water | $H_2O$ Control | Isopropanol (IPA) | IPA Control | pH 4 buffer Solution | pH 4 buffer Solution Control |
|---|---|---|---|---|---|---|
| **Silicon** | 304.5 | 9 | 1280 | 1500 | ~35,000 | ~700 |
| **Calcium** | 0.53 | 0.14 | 0.1 | 0.2 | | |
| **Aluminum** | 3 | 2 | 8 | 8 | ~22,500 | ~100 |
| **Magnesium** | 0.32 | 0.04 | 0.04 | 0.04 | | |
| **Iron** | 5 | 8 | 20 | 20 | ~17,000 | ~100 |
| **Sulfur** | 0.7 | 0.7 | 1.6 | 1.6 | | |
| **Titanium** | 1 | 1 | 4 | 4 | ~1700 | ~100 |

*Figure 4.– Dissolution of lunar soil 14003 in water, isopropanol, and in a pH 4 buffer solution. Controls were $H_2O$, isopropanol (IPA), and pH 4 buffer solution without soil or other solute.*

**Discussion and Conclusion**

During the studies of lunar soils 10084, 14003, 62241 and 61141, it was found that water tends to cause clumping in the soil particles which cannot be de-agglomerated by sonication or by dispersant. Dissolution also occurs when lunar soil samples are placed in water. The finest fraction of lunar soil is known to concentrate both glass particles and plagioclase-rich particles. The dissolution studies show that the major elements of plagioclase are the elements most affected by dissolution in water at neutral pH, but are not detectibly dissolved by isopropyl alcohol. Dissolution and clumping can apparently create a spurious bimodal distribution in water-exposed lunar soil. It is therefore recommended to use alternative fluids of lesser polarity for particle size measurements. Isopropyl alcohol appears to have negligible chemical effect on lunar soil grains and its use avoids spurious rain size artifacts.

# *Size Separation of Dry Lunar Soil for Inhalation Toxicology Studies*

*Bonnie L. Cooper, David S. McKay, L. A. Taylor (University of Tennessee), J. James, W. T. Wallace, Carla P. Gonzalez*

Lunar dust (defined as grains <20 µm diameter) is formed by collisions of micrometeorites (<1 mm) with the lunar surface. This process causes mechanical fracturing of the dust into smaller grains, and melting of smaller grains into agglutinates. Dust is gradually redistributed on the lunar surface by these impacts and by levitation of the smallest grains due to electrostatic forces acting at the day-night terminator. Particles in the micron range are levitated a few centimeters above the surface, whereas ultrafine grains (~0.1 µm) can be levitated many kilometers above the surface. As these grains settle, the surface becomes covered with fine dust derived from mechanical processes that have chemically activated the dust's surface. Since the moon is devoid of an atmosphere, this reactivity will remain until the dust encounters an atmosphere.

Dust in the ultrafine to few-micron size is of particular concern to toxicologists because of the potential for adverse health effects. Mechanically-ground mineral dusts have been shown to be more toxic than their un-ground counterparts. NASA's experience during the Apollo missions was that lunar dust adhered to the extravehicular activity (EVA) suits and was unintentionally brought into the lander in large quantities. Limited data on the grain size brought into the Lander on EVA suits suggest that a major portion of that dust was in the respirable range. Apollo crews occasionally reported adverse effects from exposure to the dust, but their exposures were brief, episodic, and occurred over just a few days. Space faring nations envision stays of at least 6 months on the lunar surface with many short 'expeditions' to collect samples and study these within a lunar habitat. Thus, we set out to determine the potential health effects of long-term, episodic exposure to lunar dust, knowing that the amount of authentic lunar dust available in the respirable size range for research would be quite small.

**Preparation of Lunar Dust for Toxicology Studies**

We must use actual lunar material for our tests because there is no simulant that mimics the necessary properties of lunar soil. Available lunar simulants do not take into account the possible effects of nanophase iron, solar wind impingement, or galactic cosmic ray bombardment—factors which seem likely to alter the surface chemistry of the soil grains. Lunar dust *in situ* is likely to have grain surfaces that are chemically reactive, potentially increasing its toxicity. The Apollo lunar samples have been carefully preserved in nitrogen and, although some degree of degradation may have occurred, they provide the most realistic experiment possible at this time.

Our previous work has shown that physically-induced grain surface reactivity is greatly reduced ("passivated") over the course of a few hours when in contact with humidity and atmospheric oxygen. Consequently, we performed all separation procedures in a dry nitrogen (0.5 ppm $H_2O$, 20.6 ppm $O_2$) atmosphere. Although particle size separators (such as impactors or cyclones) can be utilized in conjunction with the instruments and systems developed for inhalation toxicology

experiments, it was desirable to separate the lunar dust prior to placing it in the inhalation system, because of the uncertainty in the amount of respirable dust that could be extracted from this specific sample. The number of test animals could be adjusted based on the amount of respirable dust obtained. We build on previous work on dry separation of the respirable fraction of lunar soil, adding additional components to accommodate the large amount of material that must be processed.

**Dust Separation System**

When inhalation toxicology experiments are performed using terrestrial materials, the processing steps typically do not need to be efficient with respect to retaining all of the feed material. However, because lunar dust is a national treasure, a review of the standard techniques was warranted. The primary difference between our dust separation system and others is that our system is designed to keep the dust from being contaminated or changed in reactivity properties, while maximizing dust recovery and minimizing contamination and losses. Each of the first three components of our system produces a significant size fractionation, and the final component collects the desired respirable product for use in subsequent toxicology testing. The operational system is shown in figure 1 inside a nitrogen cabinet. The components are described below.

*Figure 1.– Operational system.*

**Fluidized Bed**

The fluidized bed offers the advantage of continuous mechanical impingement of grains upon each other. To determine the effectiveness of the fluidized bed, we compared the particle size distribution of the original material to the material that remained in the fluidized bed after four hours of operation. The starting material had a mean grain size of 31.35 micrometers and a geometric standard deviation of 3.012, whereas the material left behind in the fluidized bed had a mean grain size of 60.26 micrometers and a geometric standard deviation of 1.626. The median diameter had increased because the smaller particles had been removed.

**Settling Flask**
Following the fluidized bed is a settling flask, in which the input is directed via a tube to the bottom of the flask. The settling flask contains a large volume compared to the tubing which feeds dust into it. The expansion of size in the flask reduces the speed of the dust-filled airstream, allowing heavier particles to settle out of the flow. Smaller particles will remain in the air stream and move to the top of the flask, where they are carried to the next component—the cyclone.

**Cyclone**
A cyclone separator consists of a cylindrical shell with a tangential inlet through which dusty gas enters; an exit pipe for discharging the processed gas, and a cup at the bottom of a conical base where oversized particles are collected. A dual vortex is created inside the cyclone because of its geometry. The main vortex spirals downward and carries most of the coarser dust particles. The inner vortex, created near the bottom of the cyclone, spirals upward and carries finer dust particles. Its performance was characterized by measuring the particle size distribution of the material that entered the cyclone (the flask material), the material found in the cyclone cup and cyclone body after processing, and the material that was delivered to the filter.

**Membrane Filter**
The membrane filter is the final component in the system. Here, the product dust is collected. Filters have collection efficiencies of more than 99% for very fine particulates. We used a membrane (Nuclepore™ polycarbonate) filter with a pore size of 0.45 micrometers. The membrane filters are robust: a single filter is used throughout a four-hour system operation. The filter is capable of trapping particles that are only 10% of the pore size, thus we expect to find particles as small as 0.045 micrometers (45 nanometers) in the collected material. Many particles smaller than this which reach the growing filter cake may be trapped, so there is no definitive lower cutoff to the collection size.

**Collection of Respirable Dust from Lunar Soil 14003,96**
By extrapolating sieve data, we had previously estimated that 1–3% by mass of typical mature lunar soils are in the respirable size range, and demonstrated that this is indeed the case for Apollo 11 lunar soil 10084. We estimated that we could recover at least 2 gm of respirable dust from our initial charge of 200 gm of lunar soil. The total collected dust from all runs was 2.54 grams. Figure 2 shows the volumetric particle size distribution of the soil separates that we collected.

| Sample: 14003,96 | Geometric Mean, micrometers | Median, micrometers | Geometric Standard Deviation | Skewness | Kurtosis |
|---|---|---|---|---|---|
| Starting Material 14003,96 | 31.35 | 44.04 | 3.012 | -0.471 | 1.012 |
| Recovered from Fluidized Bed | 60.26 | 62.38 | 1.626 | -0.221 | 1.321 |
| Recovered from Flask | 17.3 | 19.73 | 2.4 | -0.202 | 1.053 |
| Recovered from Cyclone | 4.212 | 4.086 | 1.768 | 0.141 | 1.355 |
| Recovered from Filter | 2.186 | 2.224 | 1.509 | -0.069 | 1.008 |

*Figure 2.– Particle size distributions of materials recovered from each component of the dust separation system.*

**Grinding Lunar Dust to Respirable Size**

The next phase of the project involved the grinding of additional lunar soil from the remaining (coarser) sample, in order to obtain material that would be chemically reactive to the same (or greater) extent as the natural lunar dust.

**Jet Mill**

The main advantage of a jet mill over other kinds of mills is its ability to grind a material to sizes of 1 to 10 micrometers diameter, in a narrow particle size range. Contamination is reduced because grinding is accomplished by colliding particles into each other, rather than using a metal or mineral device to mechanically crush the grains. The jet mill was modified with a dust catcher made in or laboratory, utilizing membrane filter material rather than fiber, to minimize the amount of material that would be lost to the filter. Because the instrument was operated inside a pressurized glove box its pressure gradient was reduced, resulting in a product that was somewhat larger (~2.6 micrometers) than would have been otherwise obtained.

We obtained 54.9 grams of material in the 2.6 micrometers size range, and calculated that it would provide sufficient material for our inhalation toxicology experiments, in which an additional cyclone would be used in the final separation step.

However, in addition to the inhalation toxicology test, several precursor tests required lunar dust in mouse-respirable particle sizes. Thus we separated some of the ground material using a modified aerosolizer and cyclone system, again collecting the product dust on a membrane filter as described above. The modifications included bypassing some of the circuitry in the aerosolizer controller such that no feedback was required to keep the instrument operating at full capacity. This procedure allowed for the collection of a limited amount of respirable material (~1.4 micrometers median diameter) that did not require additional separation by the cyclone in the inhalation chamber system.

**Ball Mill**

A ball-mill grinder consists of a sealable container, into which is placed the material to be ground and one or more grinding balls, which may be made of the same material as the jar liner. The sealed jar is placed on a mechanical sample holder which vibrates at a selectable frequency for the desired amount of grinding time. Because there was some evidence that the ball mill grinder could produce dusts that were more chemically reactive than did the jet-mill grinder, we used this instrument to grind a second batch of size-fractionated material from our original sample allocation. When samples were removed from the grinder, we observed that spheroids of agglomerated dust grains were in the jar, which, if passed through a sieve, would re-form into spheroids in the sieve pan (figure 3). Particle size measurements on this material showed that significant agglomeration of grains had occurred: from a starting material with a median grain diameter of 3.89 μm, we obtained a finished product of median diameter 4.81 μm. However, when this material was passed through the modified aerosolizing/cycloning separator described above, the material de-agglomerated to a median grain diameter of ~1.7 micrometers.

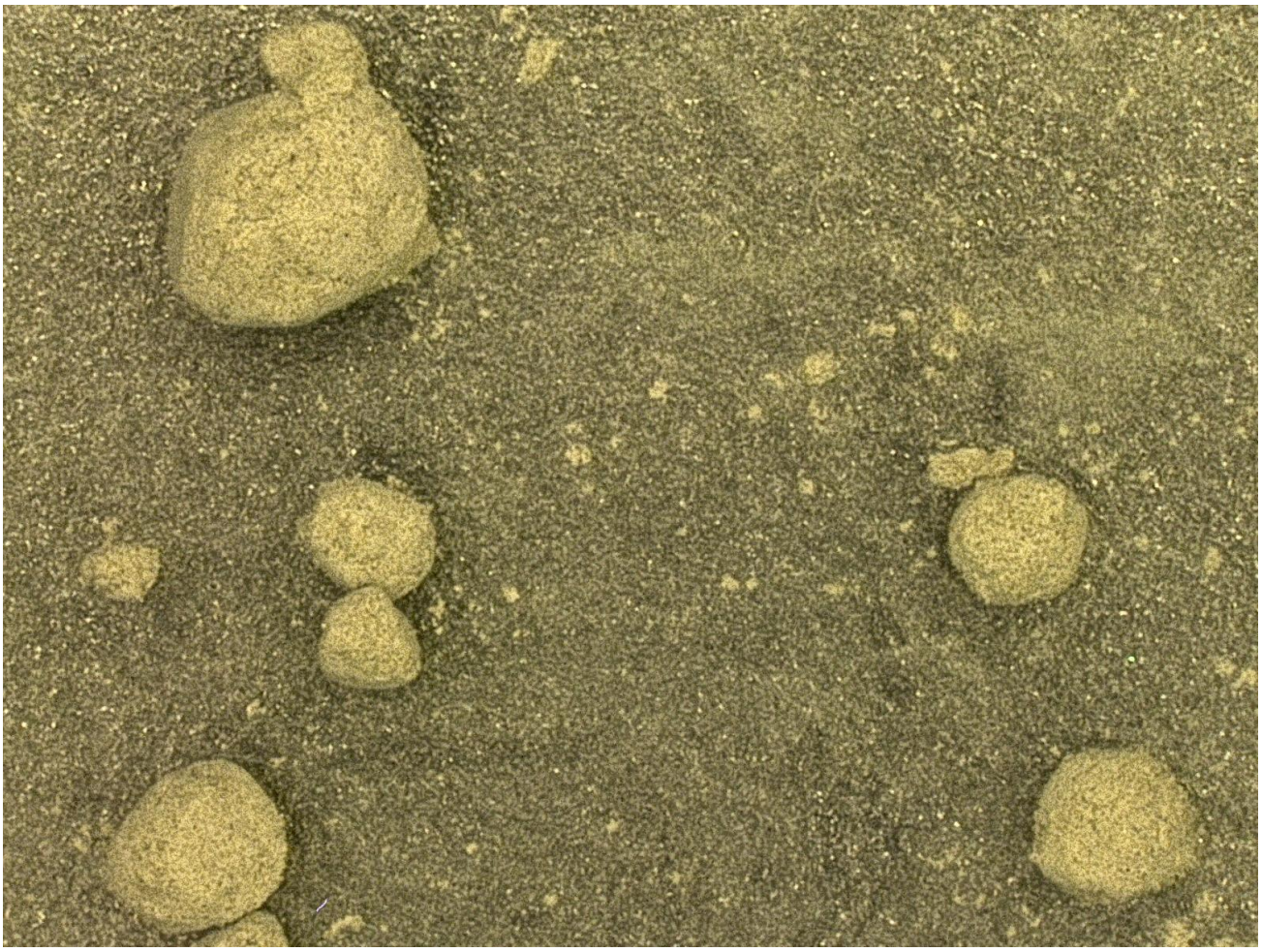

*Figure 3.– Sub-spherical agglomerates of ball-mill-ground particles prior to separation by aerosolization.*

**Conclusions**

We separated a total of 2.54 grams of natural respirable dust from the 200-gm lunar sample 14003,96. This fine-grained material is intended primarily for toxicology studies but will also be characterized for bulk chemistry, grain chemistry, mineralogy, optical reflectance, nanophase iron content, and other critical properties. Our method meets stringent requirements: the soil is kept dry, and is only exposed only to pure nitrogen gas. The soil has been conserved and recovered to the maximum extent possible. In addition, we have developed a method for grinding coarser lunar soil to produce sufficient respirable soil for animal toxicity testing while preserving the freshly-exposed grain surfaces in a pristine state. The separation method can be used for other purposes, and can be modified to handle larger or smaller quantities of material. It is particularly useful for isolating statistically representative particles for Transmission Electron Microscopy (TEM) studies.

## *Computational Radiation Analysis*

*Thomas Wilson*

ARES analyzes the effects of cosmic rays and space radiation (figure 1), and how these influence the human exploration of space. The directorate is collaborating, through the University of Houston, with European physicists at CERN in Geneva on the development of a powerful Monte Carlo program known as FLUKA for simulating the cosmic and solar radiation environment in space and in particular on the Moon, Mars and asteroids. Two related ARES applications are the effects of cosmic rays on the protosolar disk during the evolution of the Solar System and remote albedo analysis of planetary surfaces.

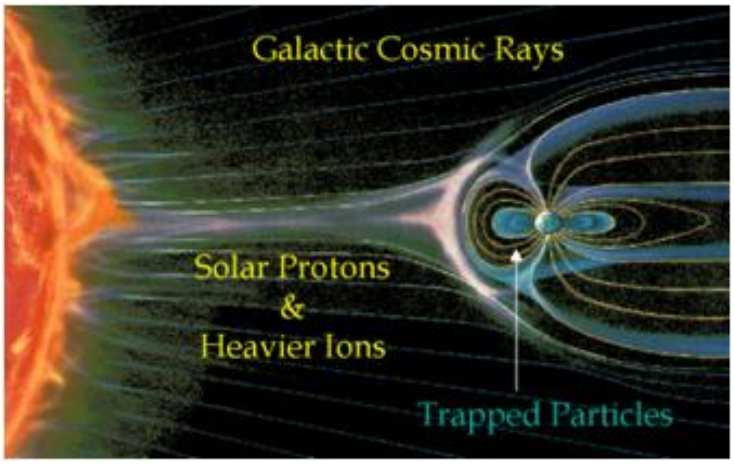


*Figure 1.– Cosmic rays.*

## *Magnetic Dynamo Action in Magnetohydrodynamic Turbulence*

*John V. Shebalin*

JSC conducted research that may help solve the "dynamo problem", that is, the problem of explaining how the generally turbulent magnetofluids (*i.e.*, plasmas) contained in stars and planets (and some laboratory devices) produce large-scale magnetic fields. There have been a number of complicated attempts to solve this problem and there have also been quite intricate numerical simulations that reproduce solar- and geo-magnetic phenomena. What has been found is a general mechanism that does this in relatively simple way and that could be applicable to more realistic cases.

In brief, most researchers have long believed that if you take a magnetofluid and stir it up, as it relaxes it produces turbulent magnetohydrodynamic (MHD) fluctuations at all length scales, but the

average direction of any of these fluctuations, over a reasonably long time, will be zero, in keeping with ensemble predicitions based on the statistical mechanics of ideal (*i.e.*, non-dissipative) turbulence. (When time averages and ensemble averages match, the system has "ergodicity".)

What JSC has found is a mechanism that breaks the ergodicity (hence, "broken ergodicity") and produces quasi-stationary large-scale magnetic fields. This is a qualitatively new result and a conceptual change with regard to a long-held paradigm (the so-called mean-field dynamo theory) concerning the origin of magnetism in planets and stars. The results pertain to the plasmas associated with plasma engines and other plasma confinement devices, if these can maintain a relatively stable plasma for a long enough period of time, as is the case for stars and planets (see figure).

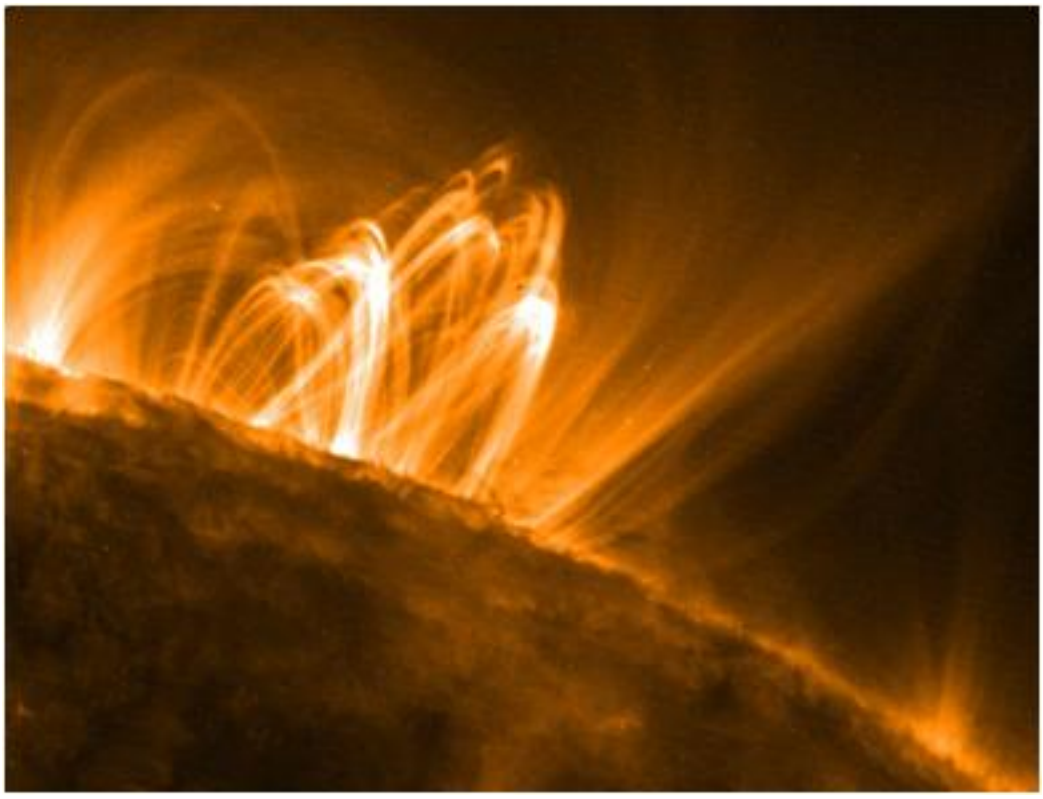

*Figure 1.– NASA Transition Region and Coronal Explorer (TRACE) image of Sun on September 12, 2000.*

# *Windows in the Ancient Martian Atmosphere*

*Paul Niles*

Using data returned from NASA's Mars Reconnaissance Orbiter (MRO) spacecraft and the Phoenix Lander, researchers associated with Johnson Space Center have made several important discoveries that help understand the ancient climate of Mars and the fate of carbon dioxide in its atmosphere.

A deposit of carbonate rocks that once existed 6 km below the surface of Mars was uplifted and exposed by an ancient meteor impact and has now been identified using the Compact Reconnaissance Imaging Spectrometer for Mars (CRISM) (figure 1). The carbonate minerals exist along with hydrated silicate minerals of a likely hydrothermal origin. Carbonate rocks have long been a Holy Grail of Mars exploration for several reasons: 1) because carbonates form from liquid water on the surface and such deposits could indicate past seas that were once present on Mars, and 2) because these minerals are the primary means for removing $CO_2$ from the atmosphere and abundant carbonates suggest that ancient Mars may have supported a denser $CO_2$ atmosphere with a much stronger greenhouse effect.

*Figure 1.– The central peak of Leighton crater located at 57 E, 3 N contains layered materials that have been uplifted from depth and tilted on-end, displaying one of the best exposures of deep crust seen on Mars. Bedrock exposed in the uplifted central peak of the 65-km crater contains clay minerals and carbonates suggesting hydrothermal alteration.*

While this is not the first detection of carbonates on Mars, this particular detection is special because carbonates coexist along with hydrothermal silicate minerals, indicating that a hydrothermal system existed in the presence of $CO_2$ deep in the Martian crust. This is exactly the type of environment that could be capable of sustaining microbiological life in the subsurface of Mars, protected from the harsh surface environment.

The Martian atmosphere is mainly composed of carbon dioxide and is less than 1% of the terrestrial atmosphere (figure 2). NASA's Mars Exploration Program has put a high priority on learning more about the history of the atmosphere on the planet, especially whether the modern atmosphere is a remnant of an older, thicker atmosphere or whether the modern atmosphere represents the conditions that have always been present on the planet.

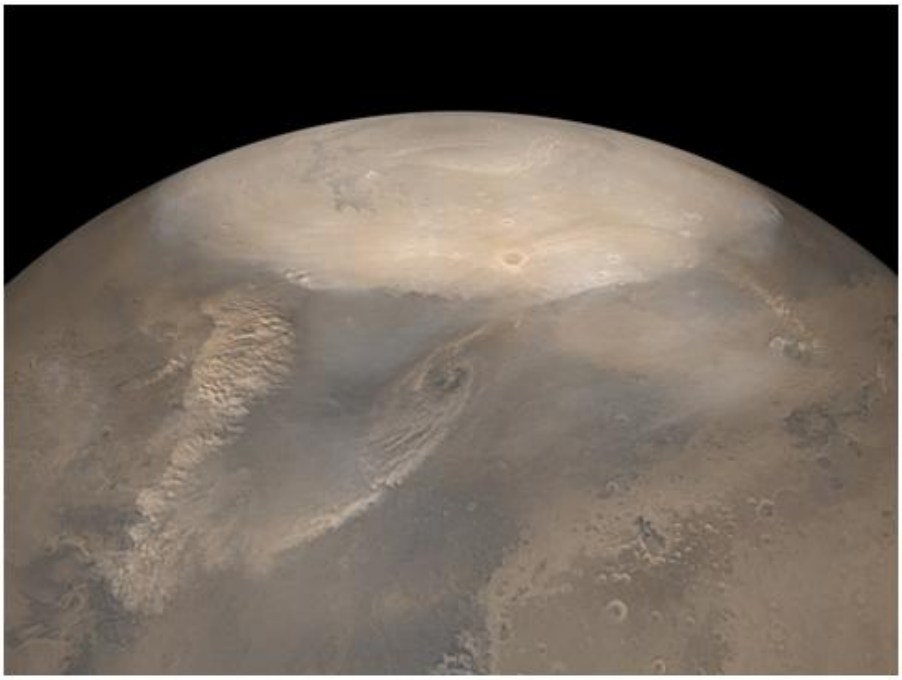

*Figure 2.– During spring on the martian north pole, condensed $CO_2$ ice begins to thaw and return to the atmosphere. During martian winter up to 25% of the atmospheric carbon dioxide can be frozen at one of the poles. This is a mosaic of images taken by the Mars Global Surveyor spacecraft in 2002. Credit: NASA/JPL/Malin Space Science Systems*

In addition to trying to discover ancient carbonate deposits, measurements of the isotope ratios in Martian carbon dioxide can also address these questions. The Phoenix Mars lander made these measurements in the summer of 2008 with unprecedented precision and they revealed that carbon dioxide on Mars has proportions of carbon and oxygen isotopes similar to carbon dioxide in Earth's atmosphere. This unexpected result reveals that Mars is a much more active planet than previously thought. In fact, results suggest that Mars has replenished its atmospheric carbon dioxide relatively recently, and that the carbon dioxide has reacted with liquid water present on the surface.

The low gravity and lack of a magnetic field on Mars mean that as carbon dioxide resides in the atmosphere it will be lost to space, a process that favors loss of the lighter carbon-12 isotope compared to carbon-13. Although an older atmosphere on Mars should contain much more carbon-13, it doesn't. This suggests the Martian atmosphere has been recently replenished with carbon

dioxide emitted from volcanoes and volcanism has been an active process in Mars' geologically recent past—within millions of years rather than billions.

However, a volcanic signature is not present in the proportions of oxygen-18 and oxygen-16 in Martian carbon dioxide. This suggests that the carbon dioxide has reacted with liquid water, enriching the oxygen in carbon dioxide with heavier oxygen-18. These findings also suggest that the liquid water has primarily existed at temperatures near freezing and that hydrothermal systems similar to Yellowstone hot springs on Earth have been rare on Mars throughout its history. The findings do not reveal specific locations or dates of liquid water and volcanic vents, but geologically recent occurrences of those conditions provide the best explanations for the isotope proportions we found.

The comparisons of the Phoenix atmosphere measurements to measurements of Martian meteorites collected on Earth provide confirmation of key findings. The meteorites contain carbonate minerals similar to those detected from orbit. Certain meteorites contain carbonates with isotopic proportions that match the atmospheric measurements by Phoenix. This provides supporting evidence that the watery conditions associated with carbonate formation have continued even under Mars' current cold and dry conditions.

## *New Research on Purported Martian Biosignatures in Meteorite Allan Hills 84001: From 1996 to 2011*

*Everett Gibson, Kathie Thomas-Keprta, Simon J. Clemett, David S. McKay*

Utilizing the latest and most advanced analytical instrumentation available, a research team at Johnson Space Center has reexamined the hypothesis about potential biosignatures in the Martian Meteorite Allan Hills 84001 (ALH84001). The team's results and conclusions present strong evidence for possible biological activity on Mars during its first 600 million years of evolution.

By reassessing the leading alternative non-biologic hypothesis that heating produced the tiny magnetites, the results of this study of Martian meteorite ALH84001 reinforce the original hypothesis that biology played a role in the formation of the carbonate disks and their associated tiny magnetite crystals. This heating hypothesis for the formation of the magnetites has been favored by many researchers for about a decade, but is now shown by this research to be an implausible explanation not supported by either theory or by new detailed observations of the ALH84001 meteorite.

It is well known that the Martian meteorite ALH84001 preserves evidence of interaction with water while on Mars in the form of microscopic carbonate disks present in many cracks and crevices in this meteorite. These carbonate disks are believed to have precipitated 3.9 Ga ago on Mars at the beginning of the Noachian epoch, the time of the oldest, still-exposed Martian surface, and perhaps

the time when Martian oceans were present. Embedded in cracks and veins throughout these carbonate disks are nanocrystal magnetites ($Fe_3O_4$) with unusual chemical and physical properties, whose origins have become the source of considerable scientific debate. Various research teams from around the world have suggested that these magnetites are the product of partial thermal decomposition of the host carbonate, in which the iron-rich carbonate was heated by meteorite impacts and thermal events, resulting in the loss of some of its carbon dioxide. This process is theorized to leave only the iron oxide behind as magnetite crystals. Alternatively, the origins of magnetite and carbonate may be unrelated; that is, magnetite is not directly related to or formed from the carbonate, but has been washed into the carbonate disks during and after the time when the disks were formed from Martian ground or surface water.

The team sought to resolve these hypotheses through the detailed characterization of the compositional and structural relationships of the carbonate disks and associated magnetites within the cracks and crevices of the rock in which they are embedded. Extensive use of state-of-the-art focused ion beam milling techniques along with microanalysis by high-resolution transmission electron microscopy has been utilized for sample preparation and analysis. The team then compared their observations with those from experimental thermal decomposition studies of iron carbonates under a range of plausible geological heating scenarios.

The JSC team concludes that the vast majority of the nanocrystal magnetites present in the carbonate disks could not have formed from the host carbonate by any of the currently proposed thermal decomposition or shock scenarios. Instead, they found there is considerable evidence in support of an alternative origin for the magnetite, unrelated to any shock or thermal processing of the carbonates. In the favored hypothesis, the magnetites were brought in from somewhere else and added to the carbonates as the carbonates crystallized.

In natural iron-rich carbonate systems minor and trace elements such as manganese and magnesium are often associated with the carbonates and when these carbonates are decomposed by thermal processes, the resulting $Fe_3O_4$ will contain trace levels of the host carbonate's minor and trace elements. However, for magnetites produced from biological processes, the resulting $Fe_3O_4$ will contain no contaminant trace elements such as manganese (Mn) and magnesium (Mg). In some kinds of Earth bacteria (magnetotactic bacteria), Darwinian-derived processes purify magnetites, even in the presence of magnesium and manganese, by excluding the contaminant elements, making these magnetites more efficient detectors of the Earth's magnetic field. Detailed analysis of selected magnetites within ALH84001 shows no trace element contaminants for the majority of the magnetites (figure 1). Most are identical to the unique population of magnetites known to be formed on Earth by biology. A few ALH84001 magnetites contain minor chromium (Cr) and/or aluminum (Al); neither element is present in the host carbonate. This indicates these impure magnetites formed elsewhere before being incorporated into the carbonate and are not a product of thermal decomposition (figure 2). Additionally, a fraction of magnetites are present in carbonate that contains little to no iron (Fe) indicating they had to form elsewhere prior to being embedded in carbonate.

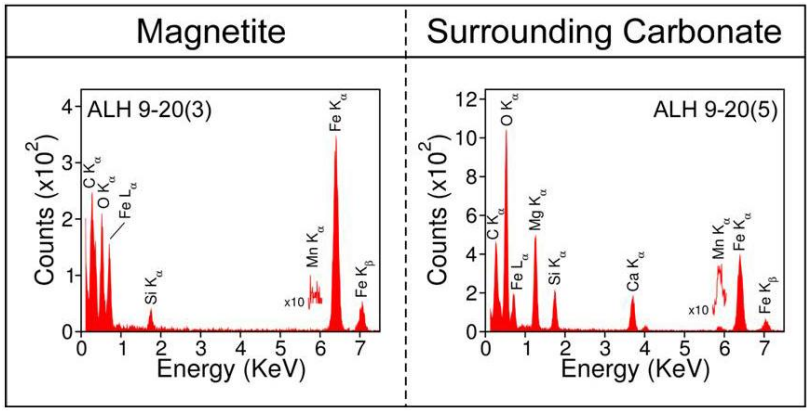


*Figure 1.– EDX spectra of chemically pure magnetite (left) and host carbonate (right). While the carbonate contains both Mg and Mn, the magnetite crystal is chemically pure and contains neither element as would be expected if the magnetite was a product of carbonate decomposition.*

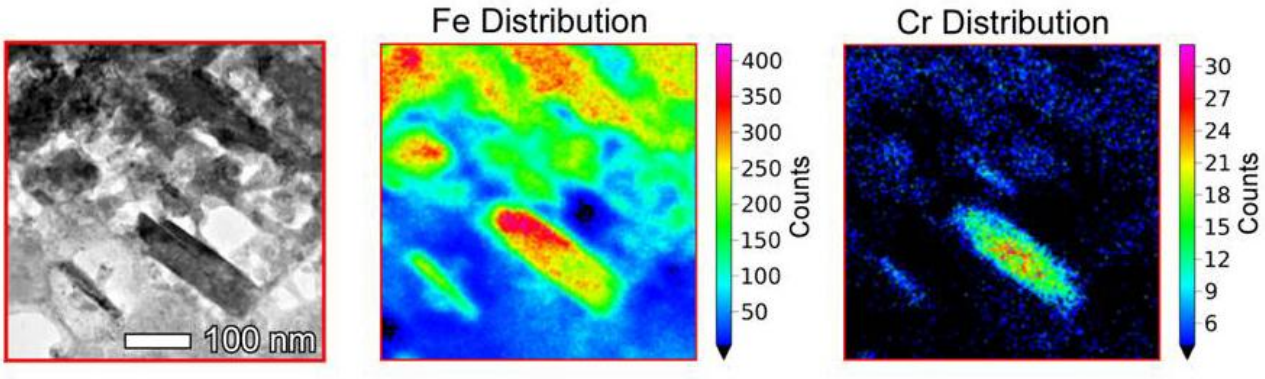


*Figure 2.– Magnetite embedded in carbonate (left); EDX maps of region at left showing the distribution of Fe and Cr (center and right). This magnetite crystal is impure, containing minor Cr.*

The scientific results offer strong support to the original 1996 hypothesis and show that most of the alternative arguments are invalid. The original hypothesis advanced by the JSC team was that 3.9 Ga ago, the carbonates were precipitated in cracks and hollows of a cooled martian volcanic rock with the help of martian microbes and these carbonates trapped or included tiny crystals of magnetite identical in specific properties to those known to be formed on earth by specialized bacteria. The original hypothesis proposed that there could have been conditions on Mars favoring habitability for life and which could have supported active biogenic processes.

While the new work does not prove that the biogenic hypothesis is true, it does show that the most popular alternative non-biologic hypotheses (thermal decomposition or shock decomposition of iron-rich carbonate) to explain the properties of ALH84001 simply does not fit the evidence in the meteorite. By showing that the thermal decomposition models are unlikely, this new discovery removes the single most important obstacle to the acceptance of the original hypothesis of the JSC group who proposed that ALH84001 contained evidence of past life on Mars. The evidence supporting the possibility of past life on Mars which has been slowly building during the past decade

including signs of past surface water such as the remains of rivers, lakes, and possibly oceans, signs of current water near or at the surface, water-derived deposits of clay minerals and carbonate outcrops in old terrain, and the identification of methane in the Martian atmosphere.

## *Mars Habitability, Biosignature Preservation, and Mission Support*

*Dorothy Z. Oehler, Carlton C. Allen*

JSC has been studying the Martian surface to identify areas of past habitability with enhanced potential to preserve biosignatures. One area has been singled out in the southern Acidalia Planitia/northern Chryse Planitia area of the martian lowlands. This area is predicted to have accumulated thick sequences of fine-grained sediments that could include preserved biosignatures. The area also contains tens of thousands of mud-volcano-like mounds (figure 1). Mud volcanoes on Mars could have provided long-lived conduits for fluid movement from depth to the surface (figure 2), microhabitats for *in-situ*, endolithic life (figure 3), and a mechanism for transporting samples from depth to the surface where they could be accessed by future Rovers. Results of this work were reported in a recent peer-reviewed article in *Icarus* (Oehler and Allen, 2010). In response to a call by the Mars Program for imaging targets for future landing site candidates, JSC submitted multiple sites from the Chryse/Acidalia region of potential mud volcanism.

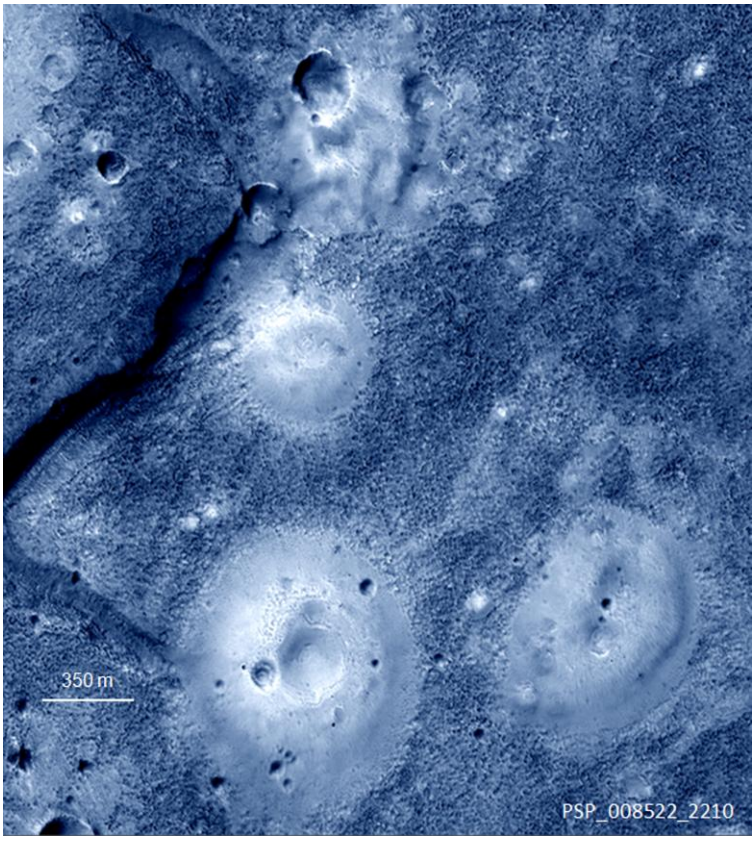


*Figure 1.– Mounds in Acidalia Planitia, Mars. These features have been compared to terrestrial mud volcanoes.*

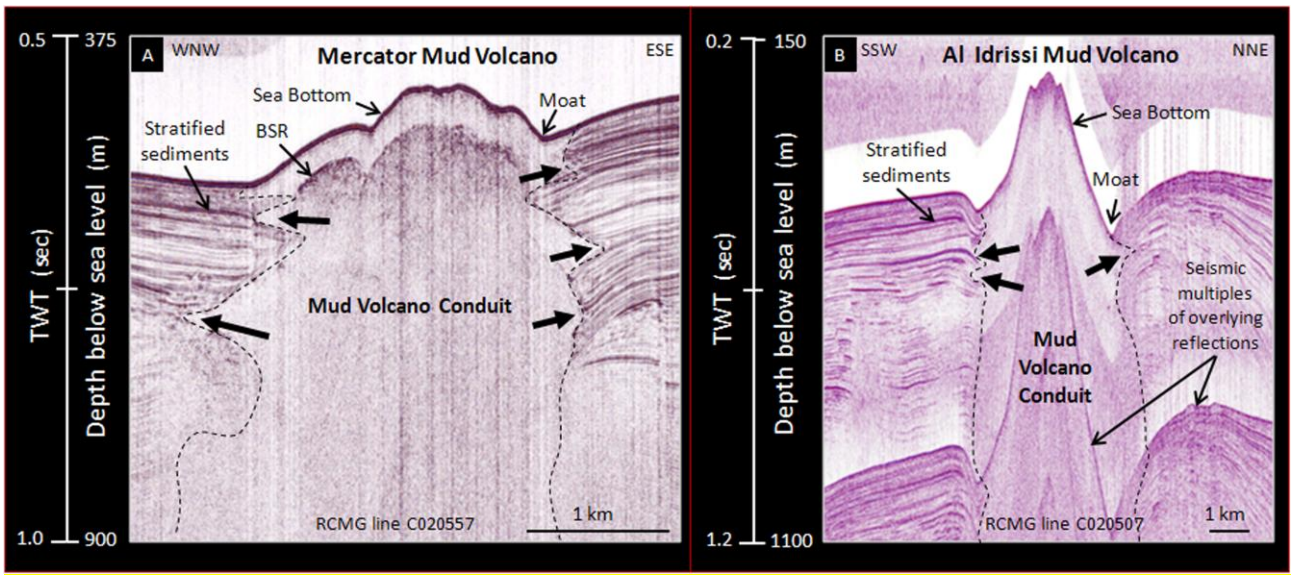


*Figure 2.– Seismic profiles of mud volcanoes in the Gulf of Cadiz, offshore Morocco, illustrating the conduits to the surface created by these types of structures. Thick arrows point to levels where mud flows interfinger with stratified sediments in the subsurface.*

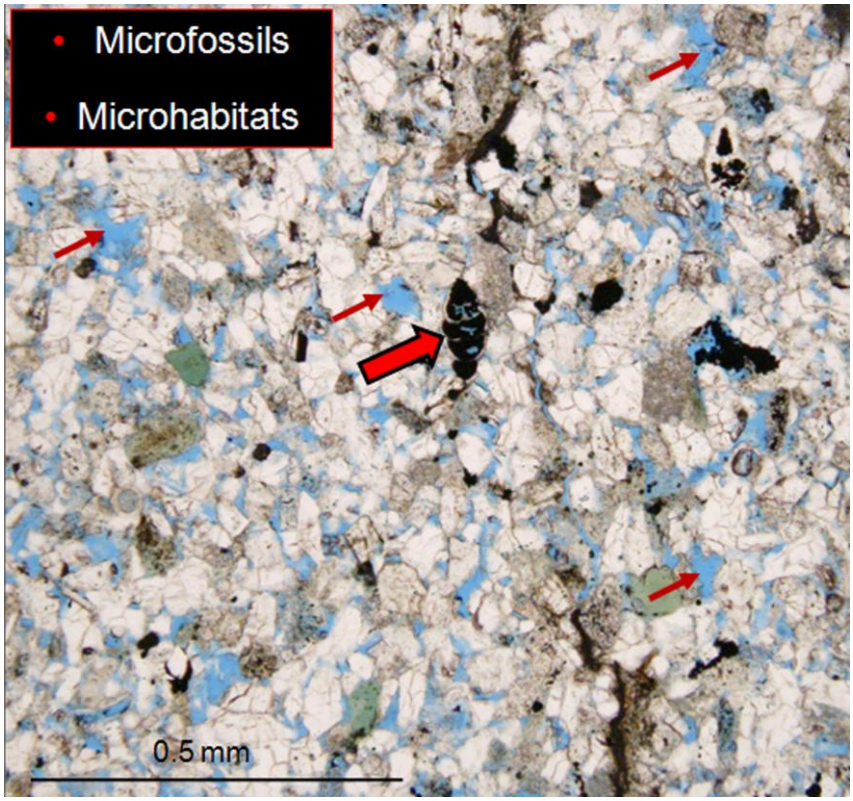


*Figure 3.– Coarse-grained sediment brought to the surface by a terrestrial mud volcano, illustrating microhabitats. Optical photomicrograph in transmitted light of a thin section. Large red arrow points to microfossil. Small red arrows illustrate potential microhabitats in porosity (shown in blue from tinted epoxy).*

# *The History of Mars Revisited Via the Petrological and Geochemical Study of Martian Meteorites*

*Anne Peslier; Dan Hnatyshin, Chris Herd (University of Alberta); Erin Walton (Grant McEwan University); Alan D. Brandon, Thomas Lapen, John Shafer, Minako Righter (University of Houston); Vinciane Debaille (Université Libre de Belgique); Brian Beard (University of Wisconsin)*

Understanding the geological history of Mars makes key advances via the study of Martian meteorites, our only samples from this planet. Each time a new meteorite from this planet is found, potential huge strides in this science can be made. Here the team concentrated on the petrological study of a Martian meteorite found in Antarctica in 2006 called LAR 06319. Detailed petrological study revealed that this meteorite represents a sample from a lava erupted at the surface of Mars. The importance of this meteorite is that its minerals represent an entire sequence of snapshots of the history of the magma from the time it left the depths of the Martian mantle to the time it reached the surface of the planet. By carefully determining the temperature and oxygen fugacity conditions at which these minerals formed at these various times throughout the history of this magma, JSC and scientists at the University of Alberta and University of Houston could show that information about the chemical and physical conditions in the source of Martian magmas can be lost during the evolution of the magma after it has left the Martian mantle. This particular meteorite, however, having preserved most of the information from its source to its eruption could be used by the team to redefine the conditions pertaining at the source of Martian magmas. This study makes it easier to model the magmatic history of Mars, in particular by narrowing the range of oxygen fugacity of the source of Martian magmas. See figure 1.

JSC also collaborated with University of Houston scientists in refining the timeline of volcanic activity on Mars with the precise dating of the oldest Martian meteorite ALH 94001 and the age determination of the meteorite described above LAR 06312. These studies affirm that only one Martian meteorite is very old (ALH 94001 more than 4 Ga), while all others are samples of magmas erupted on the martian surface much later, less than 600 million years ago. All these results constrain models of planetary formation and evolution.

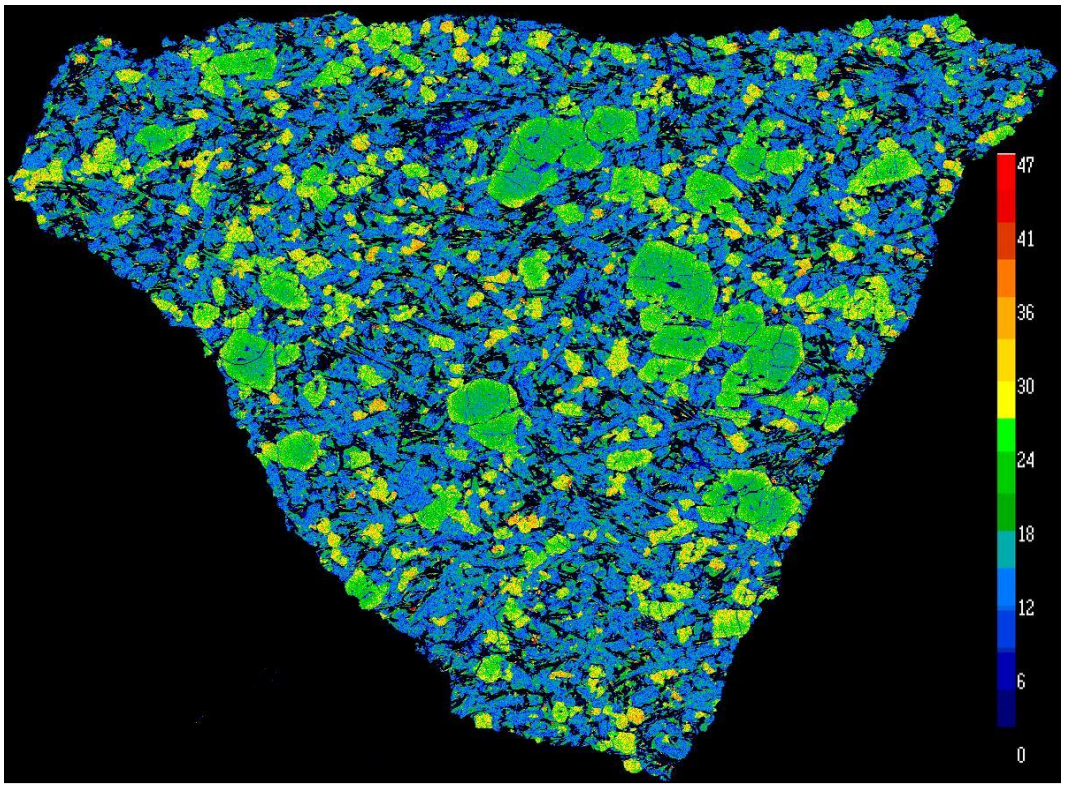


*Figure 1.– The figure shows a map of the iron content of a thin slice of the Martian meteorite LAR 06319. The sample is about 2 cm at its widest side. The large green minerals formed first in conditions closed to that of the source of the magma deep in the Martian mantle, while the thin needle-like black ones most likely formed at eruption at the Martian surface. Blue indicates low amounts of iron, while orange-reds means large amounts of iron.*

# *Astromaterials Acquisition and Curation Office (KT)*
# Overview


## Carlton Allen, Ph.D., Astromaterials Curator, Manager

**http://curator.jsc.nasa.gov/index.cfm**


The Astromaterials Acquisition and Curation Office has the unique responsibility to curate NASA's extraterrestrial samples—from past and forthcoming missions—into the indefinite future. Presently curation includes documentation, preservation, preparation and distribution of samples from the Moon, asteroids, comets, the solar wind and the planet Mars. Each of these sample sets has a unique history and comes from a unique environment. The curation laboratories and procedures developed over forty years have proven both necessary and sufficient to serve the evolving needs of a worldwide research community. A new generation of sample return missions is being planned and proposed to destinations across the solar system. We are developing the tools and techniques to meet the challenges of these new samples.

Extraterrestrial samples pose unique curation requirements. These samples were formed in environments strikingly different from that on the Earth's surface. Terrestrial contamination would destroy much of the scientific significance of extraterrestrial materials. In order to preserve the research value of these precious samples, contamination must be minimized, understood, and documented. In addition the samples must be preserved—as far as possible—from physical and chemical alteration. The elaborate Curation facilities at JSC were designed and constructed, and have been operated for many years, to keep sample contamination and alteration to a minimum.

At the current time JSC curates six collections of extraterrestrial samples:

- Lunar rocks and soils collected by the Apollo astronauts
- Meteorites collected on NSF-funded expeditions to Antarctica
- "Cosmic dust" collected by high altitude NASA aircraft
- Solar wind atoms collected by the Genesis spacecraft
- Comet particles collected by the Stardust spacecraft
- Interstellar dust particles collected by the Stardust spacecraft

Within the next year we anticipate receiving and curating 10% of the asteroid dust samples collected by the Japanese Hayabusa mission.

Each of these sample sets has a unique history and comes from a unique environment. We have developed specialized laboratories and practices over many years in order to preserve and protect the samples, not only for current research but "for studies that may be carried out in the indefinite future."

**The following reports provide insight into the Curation team's work and research in 2009 and 2010.**

## *Recovery After Mishap—Salvaging Genesis Solar Wind Sample Science*

*Judith Allton*

The collectors returned by the Genesis mission contain solar wind atoms which can be analyzed in sophisticated laboratory instruments to measure very precisely the composition of the Sun. Since the Sun contains >99% of the mass in the solar system, knowing its elemental and isotopic composition is a good average measure of the composition of the solar nebula at the time when the planets were forming. Scientists already have rocks from the Moon, Mars and the asteroids and dust particles from comets. Genesis' solar data allows new insights in tracing the chemical evolution of diverse planetary samples, most of which came from a common starting material, the solar nebula. Separate collections were made of high speed solar wind, coronal mass ejection solar wind and interstream low speed solar wind. Information from these different solar regimes adds to the understanding of solar physics (figure 1).

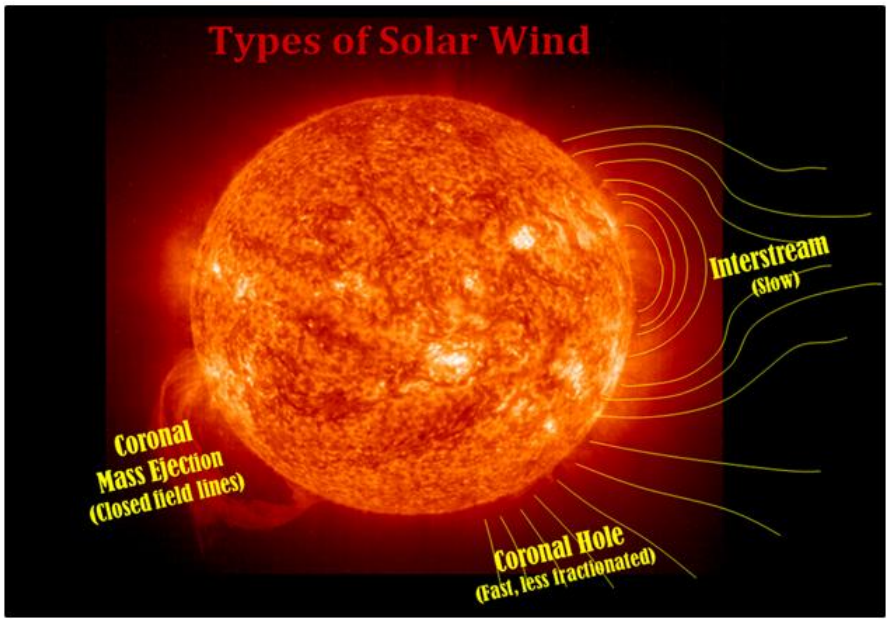


*Figure 1.– Genesis mission collected separately three regimes of the solar wind: Interstream slow solar wind, coronal hole high speed solar wind, and coronal mass ejection solar wind.*

Genesis solar wind collectors are highly polished surfaces into which solar wind nuclei are implanted, typically 40 to 100nm below the surface (figures 2 and 3).

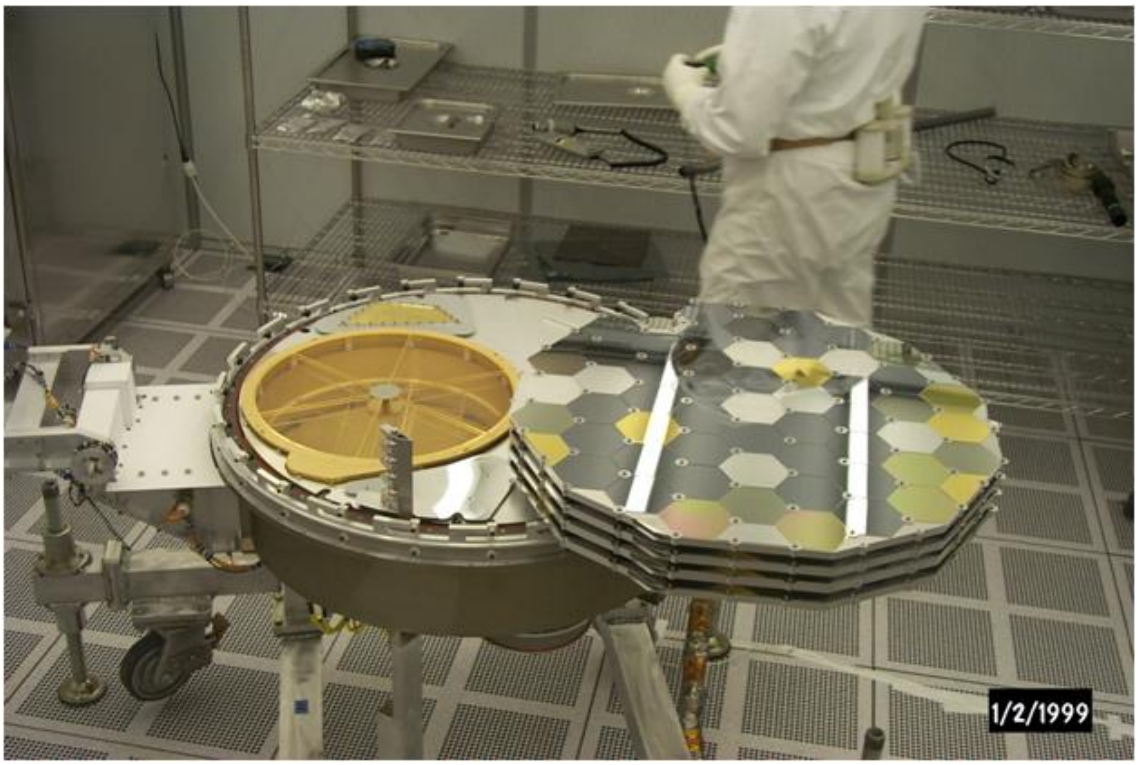


*Figure 2.– Hexagonal polished collectors of pure materials accumulated solar wind from three regimes over a 28 month period at Earth-Sun L1.*

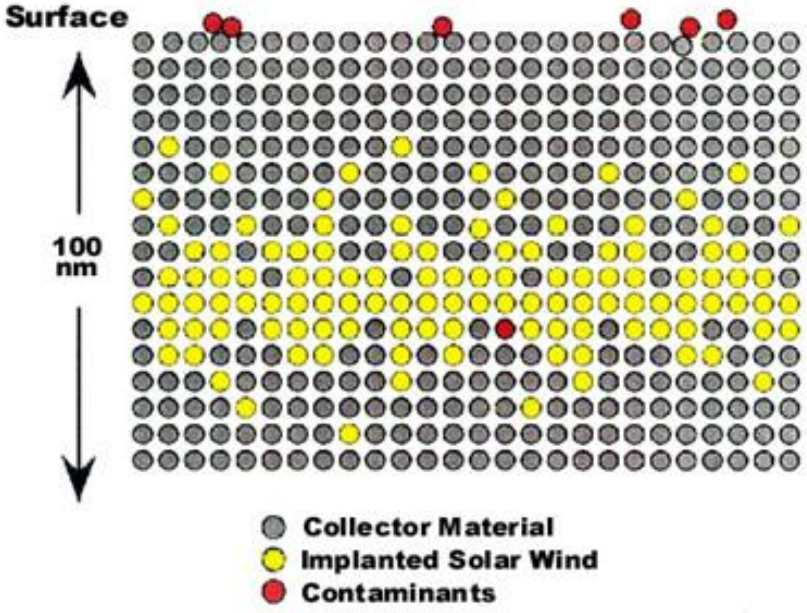


*Figure 3.– Solar wind nuclei are implanted just below the surface of the polished collectors.*

The advantages of returning samples to the laboratory are many. State-of-the-art instrumentation can be used for analysis to very high precision, different techniques can be used to verify the same measurement, multiple teams can confirm or dispute the results, and evolving science questions can be addressed through new types of analyses. To this list of advantages of returned samples, add one more: recovery from mishaps is greatly enhanced.

Genesis Mission was launched August 2001, collected solar wind at Earth-Sun L1 location for 28 months, and returned to Earth September 2004. The parachute did not deploy and the return capsule hit the ground at an estimated 300 kph, which resulted in the collector canister breaking open and exposing the collectors to the environment. Many of the collectors were fragmented and contaminated with particulate debris and a molecular film.

**Early Design Choices Proved Useful During Recovery**

Because the analytical goals were challenging, the solar collectors were comprised of very pure, very clean materials and assembled under ISO Class 4 conditions. Fifteen distinct materials were used for collectors, allowing overlap in analysis for specific elements on a variety of materials. Some materials survived the hard landing better than others. Sapphire-based collectors survived in larger pieces. Diamond surfaces were more resistant to scratching.

After return, a variety of collector cleaning processes were tested to remove the contaminant particles and molecular film. Some collector materials proved more easily cleaned than others. Thus, the variety of collector materials not only provided an analytical redundancy, but also more options for cleaning the surface without disturbing the solar wind.

Flight-like collector reference materials were preserved. These specimens proved crucial as "blanks" for subtracting background components of measured parameters. These reference materials were also used in development of cleaning processes.

The thickness of the hexagonal solar collectors was unique for each solar wind regime: 700 μm for bulk solar wind, 650 μm for coronal mass ejection, 600 μm for high speed, and 550 μm for low speed. Since collectors were dislodged and fragmented upon the hard landing, collector thickness is the only direct way to determine solar wind regime.

**Characterization of Collector Fragments**

Collector fragments can be easily identified by optical observation, except for silicon. The two types of silicon are distinguished by use of an FT-IR to observe a carbon-oxygen bond, present only in Czochralski method silicon. A catalog of the collector fragments is available on the internet. The catalog contains an image, the material, the dimensions and area, the solar wind regime, and a qualitative assessment of surface condition (figures 4 and 5). Cataloging is an ongoing process with 1600 samples displayed as of 2011.

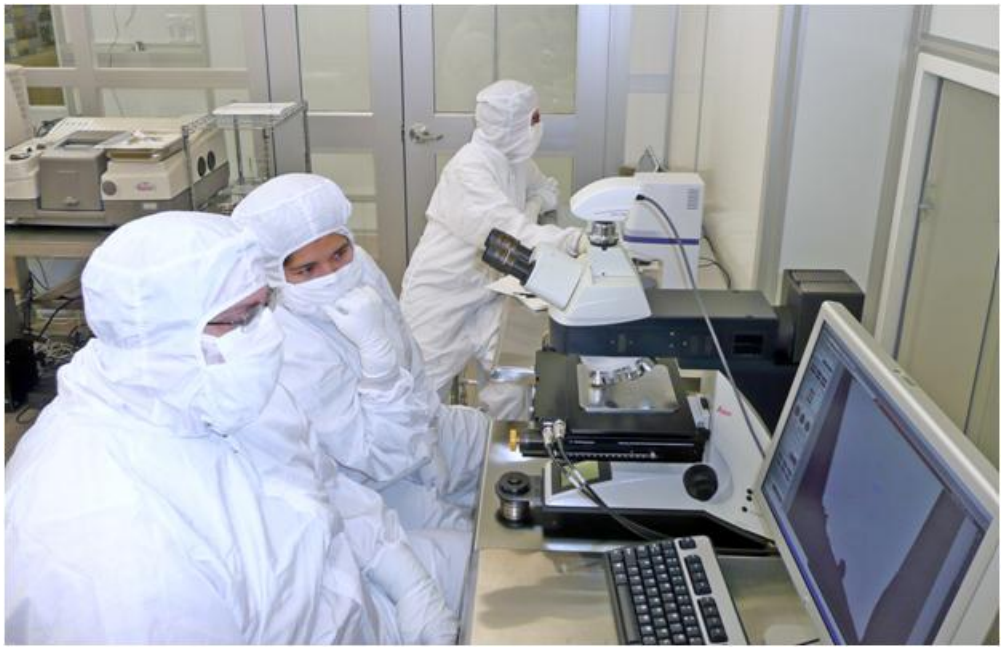

*Figure 4.– Recovered collector fragments are imaged and measured for the online catalog.*

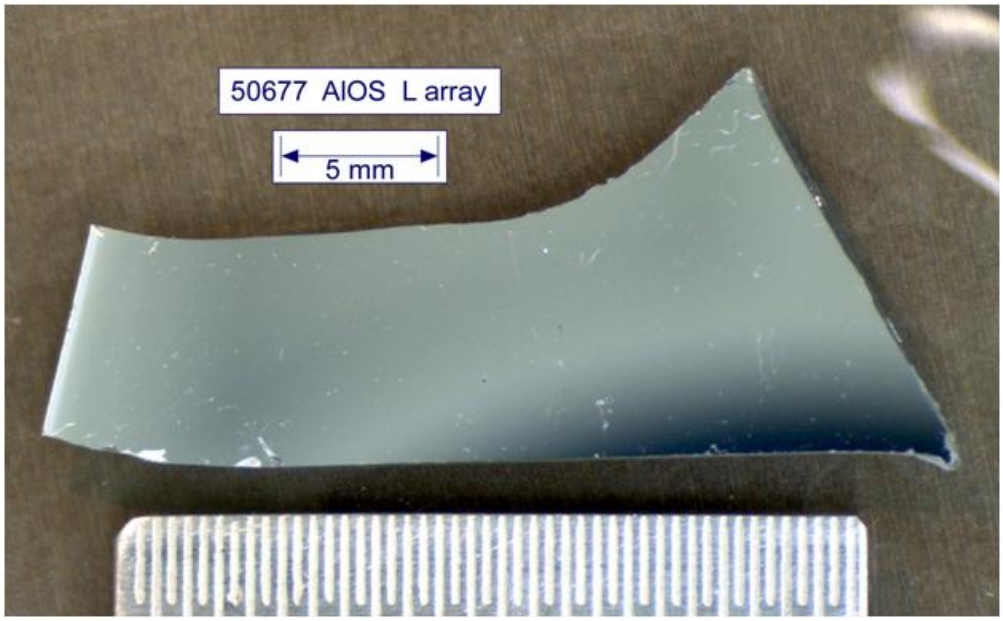


*Figure 5.– An example from the online catalog is this aluminum-on-sapphire sample.*

**Cleaning of Collectors Fragments**

Megasonically energized ultrapure water (UPW), which was successfully used to clean the payload prior to launch, was adapted to remove particulate contamination from solar wind collectors. The continuous flow process produces water of 18Ω–cm resistivity (ionic concentrations in the low parts per trillion). To apply UPW cleaning to small irregular collector fragments, a megasonic cleaning head was mounted to a single wafer spin processor. In this configuration a small collector fragment

held by a vacuum chuck is spun up to 3000 rpm. Megasonically energized UPW is applied for 30 seconds to 15 minutes, depending on material. Extra spin time effectively dries the collector fragment. Particles greater than 5 µm are efficiently removed, leaving no solvent residue.

A commercial UV lamp device creates a UV ozone cleaning atmosphere which effectively removes the 5 nm film found on some collector fragments. Typical UV exposure times are 30 minutes.

Cleaning performed at the JSC Genesis curation facility is first order cleaning. Members of the science team have developed second round cleaning with strong acids, such as hydrofluoric and aqua regia. JSC curation assists with documentation and logistics for this iterative process with the science community.

**Science Results**

Important science results are emerging from analysis of the Genesis solar wind samples. This challenging work is being done by the science community on the 400 Genesis solar wind samples allocated for research purposes. Investigators have the capability to choose a measurement site on a given collector sample in order to avoid damaged areas and to make multiple analyses. Figure 6 shows a silicon carbide collector which has been analyzed for two different elements by two different research groups. The number one and two science goals of determining the solar oxygen isotope and nitrogen isotope compositions have been published.

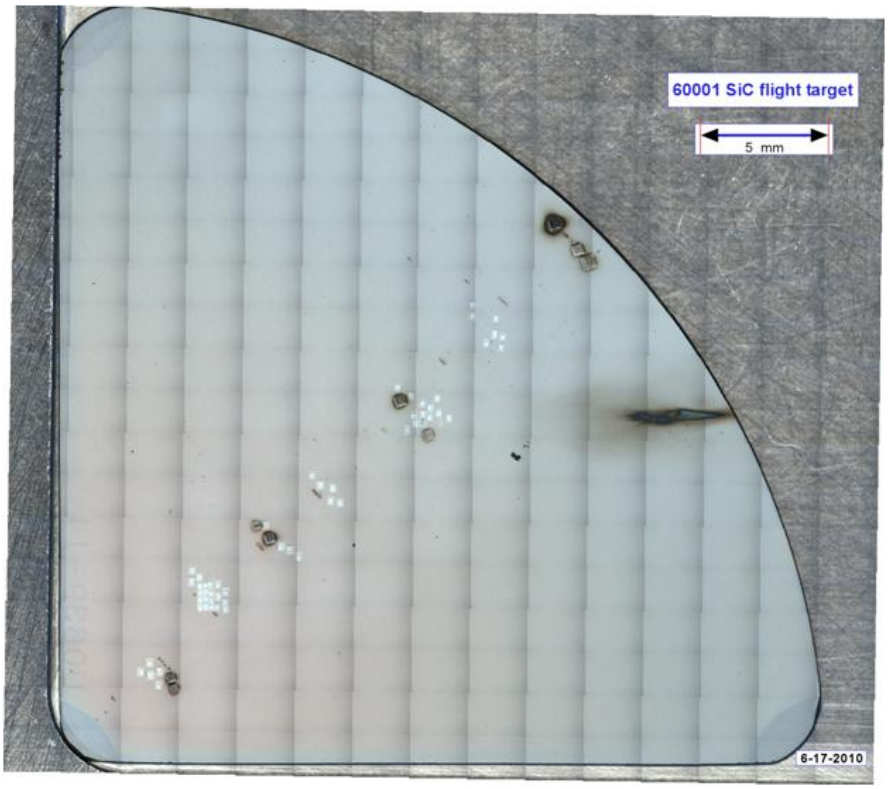


*Figure 6.– This mosaic image of a Genesis silicon carbide collector shows the effects of ion beam analyses by two science groups.*

# *Stardust—Searching for Contemporary Interstellar Dust*

*David Frank, Mike Zolensky, Bradley De Gregorio, Ron Bastien, Jack Warren*

In 2006, the Stardust Mission returned the first samples from a primitive solar system body. This NASA Discovery class mission, along with the Apollo and Genesis Missions, represents NASA's third sample return from a celestial body. The Stardust spacecraft made a close encounter (at 6 km/s) with comet Wild-2 and successfully captured thousands of dust grains ejected from the comet's coma. The collector was an array of silica aerogel and aluminum foils arranged in the approximate size and shape of a tennis racket.

Although the primary (and successfully completed) objective of the mission was to capture these Wild-2 comet samples, a second similar collector was flown on the same payload and exposed to the stream of "contemporary interstellar dust"; particles that originate from other stars, planetary systems, and nebulae. This very low flux of μm and sub-μm sized dust grains pass through our solar system at speeds in excess of 20 km/s as the sun revolves around the center of the Milky Way Galaxy. While thousands of particles in the size range of a few μm up to ~150 μm were collected from comet Wild-2, it is expected that only perhaps a few dozen dust grains approximately a few μm *and less* were captured from the interstellar medium. The extremely low particle flux and tiny grain size make locating these particles a colossal challenge. To overcome this "needle in a haystack" search, we conduct automated scanning of the aerogel at high resolution using an optical compound microscope equipped with a live video feed and computer controlled stage. To date, we have scanned almost one half of the collector and created roughly one quarter of a million "focus movies," each of which represents a field of view of 0.24 $mm^2$. These movies are distributed for inspection to volunteers around the world via the web-based Stardust@home project. With >29,000 volunteers, it is the largest ever collaboration in planetary science.

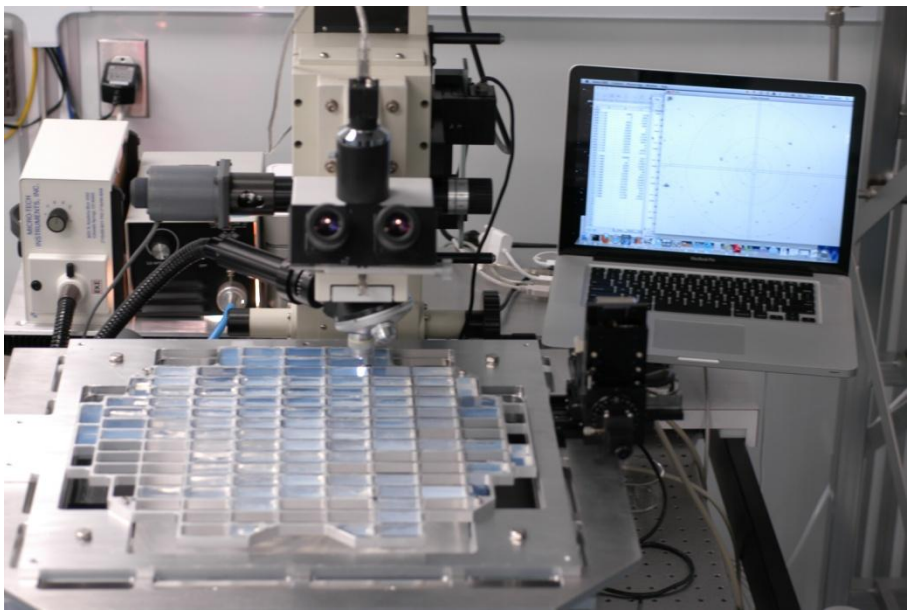

*Figure 1.– The Stardust aerogel scanning system at JSC with the interstellar collector mounted for automated scanning.*

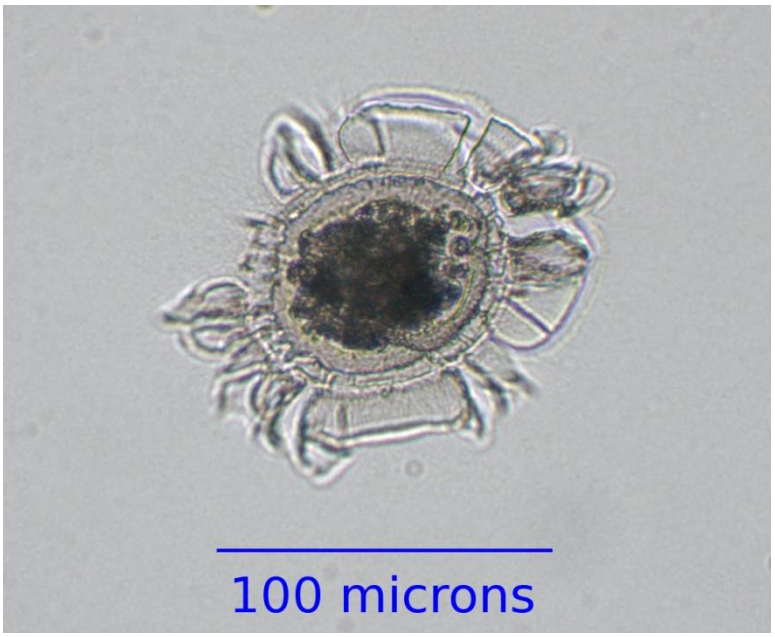


*Figure 2.– A cavity seen through the aerogel scanning system, possibly created by the hypervelocity impact of an interstellar dust grain.*

Potential features identified by Stardust@home are closely examined. Real particle impacts are extracted from the collector in tiny wedges of aerogel less than 0.5 mm thick, using glass needles formed to a µm-sized tip. The needles are programmed to repeatedly poke into the aerogel via computer controlled micromanipulators, eventually creating a series of precise "cuts" in the aerogel. These samples are extracted and prepared for investigators around the globe. The Stardust Laboratory at JSC is one of two laboratories in the world with this specialized capability.

*Figure 3.– An aerogel wedge cut and mounted to a silicon "micro-fork", containing a microscopic particle impact that may be one of the first identified contemporary interstellar dust samples.*

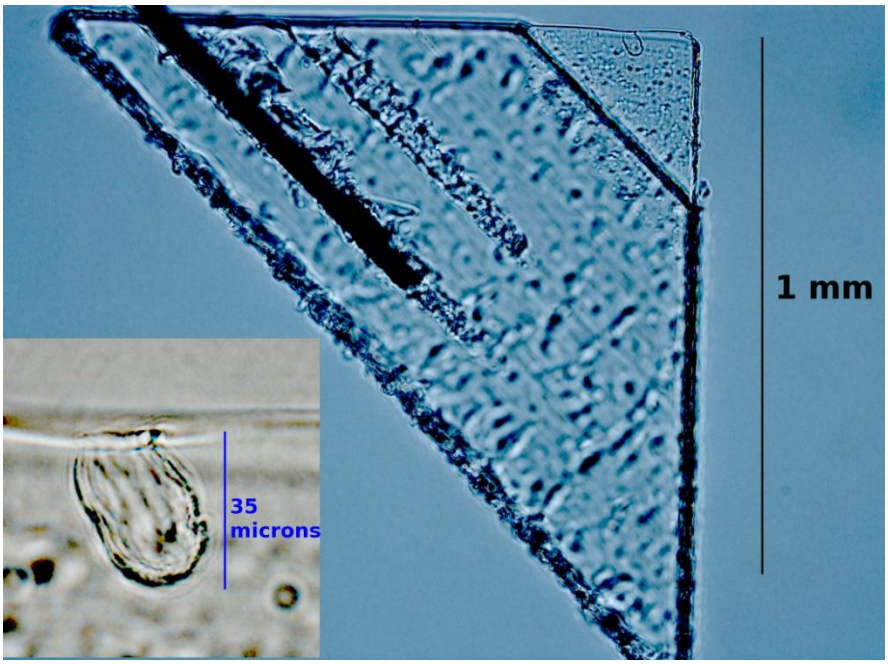

External scientists analyze the compositions of candidate interstellar grains using synchrotron-based, X-ray spectroscopy, and attempt to determine which particles are real interstellar dust and which originate from the spacecraft, other contaminants, or from within our own solar system. At the March 2011 Lunar and Planetary Science Conference, the Stardust Interstellar Preliminary Analysis Teams reported that four of these identified, extracted, and analyzed particles may be the first of the rare and elusive interstellar dust grains.

We will continue to conduct automated scanning and particle extraction in order to identify and analyze impacts by interstellar dust. These samples will complement the highly successful and dramatic collection of Wild-2 comet dust. Taken together, they will increase our understanding of our own solar system and its early history, how it compares to other planetary systems and galactic materials, as well as the astrophysical environment of interstellar space in between.

## *Analysis of the First Direct Samples of Early Solar System Water*

*Mike Zolensky*

Over the past three decades we have become increasingly aware of the fundamental importance of water, and aqueous alteration, on primitive solar-system bodies. Liquid water is apparently as essential to life as is carbon. All classes of the most primitive astromaterials we have studied show some evidence of interaction with aqueous fluids. We can also observe cryovolcanism of several small solar system bodies (e.g. Saturnian and Jovian moons), and so are certain of the continuing and widespread importance of aqueous processes across the solar system. Nevertheless, we still lack fundamental information such as the location and timing of the aqueous alteration and the detailed nature of the aqueous fluid itself. A major impediment to our understanding of aqueous alteration has been the apparent absence of direct samples of aqueous fluids in meteorites.

Our understanding of early solar system fluids took a dramatic turn 10 years ago with the discovery of fluid inclusion-bearing halite (NaCl – common table salt) crystals in the matrix of two freshly-fallen brecciated H chondrite (meteorite) falls, Monahans and Zag. The halites were dated by K-Ar, Rb-Sr and I-Xe systematics to be 4.5 billion years old. Collaborating with a Virginia Polytechnic Institute scientist, JSC began examining both meteorites for the presence of aqueous fluid inclusions, which were immediately found.

Fluid inclusions are micro-samples of fluid that are trapped at the crystal/fluid interface during growth (primary) or some later time along a healed fracture (secondary) (figure 1). Both varieties of fluid inclusions are found in Monahans and Zag halite. The presence of secondary inclusions in the halite indicates that aqueous fluids were locally present following halite deposition, suggesting that aqueous activity could have been episodic. In any fluid inclusion analysis it is thus critical to separately analyze the primary and secondary inclusions, if possible, yielding temporal information on fluid compositional changes. Heating/freezing measurements were made on the halite fluid

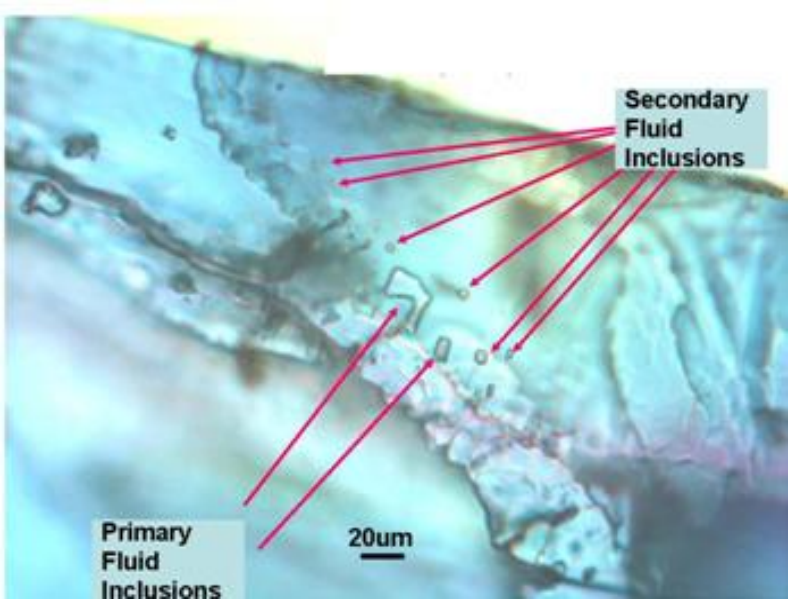


*Figure 1.– Monahans halite with target fluid inclusions indicated. Scale bar measures 20 micrometers.*

inclusions for both Monahans and Zag, determining that the fluids were trapped at ~25 degrees C. These are the first direct measurements of aqueous alteration temperature in any astromaterial, and are also important because they demonstrate unequivocally that these halites have never been subsequently heated. A disadvantage of halite is that it is so readily dissolved in the terrestrial atmosphere, unless extreme care is taken with the samples. Understanding this problem, the Monahans and Zag samples were maintained in curation-grade, dry nitrogen-filled cabinets waiting for technology to catch up with the samples, to finally permit chemical and isotopic analyses of the trapped water droplets and to discover their origin. This time has finally arrived.

The first step has been to measure the hydrogen and oxygen isotopic composition of the fluid inclusions aqueous solutions, in order to understand the origin of these fluids. The O and H isotopic composition of the aqueous fluids will be compared to determine which of these bodies were the parent objects: potentially asteroids, comets, or giant planet moons. They will also be compared to the Earth's water. Testing of our hypothesis that the O and H isotopic composition of the aqueous fluids in meteorites (in fluid inclusions) will be shown to be most similar to cometary coma water, and also similar to the water being ejected from cryovolcanoes on Jovian and Saturnian moons. The bulk composition of the fluid inclusion-bearing phases in each meteorite will be measured, as a further guide to the aqueous fluid bulk composition. This will further test our hypothesis that the water was not asteroidal in origin.

Several Zag and Monahans halite crystals have been selected for secondary ion mass spectrometry (SIMS) analysis by a collaborator at Hokkaido University, who modified his Cameca 1270 SIMS with a special internal freezing stage. The aqueous fluid inclusions have to be frozen, before being exposed (by sputtering) for analysis in the SIMS. After a great deal of effort, the correct sample preparation and analytical techniques were developed to obtain quality O and H isotopic measurements of individual aqueous fluid inclusions in the halites. Figure 1 shows one Monahans halite crystal, indicating the fluid inclusions that were analyzed. The SIMS freezing stage holds the

sample temperature of about -150 °C during measurements by liquid nitrogen. Fluid inclusions in the depth of ~50µm from the halite surface have been successfully measured. The sizes of inclusions were about 5µm. Initial results of this work are shown in the figure 2. The observed distribution of isotopic variations of fluid inclusions seems to result from the interaction between comet-like water and meteorite silicates. Now techniques are being optimized to permit a reduction in the errors and to target specific individual fluid inclusions—a necessary capability to permit us to measure temporal changes in aqueous compositions by distinguishing between preselected primary and secondary fluid inclusions. The team now has a unique sample suite, being analyzed by a unique instrument, providing critical information on the activity of water in the early solar system which can be obtained in no other manner.

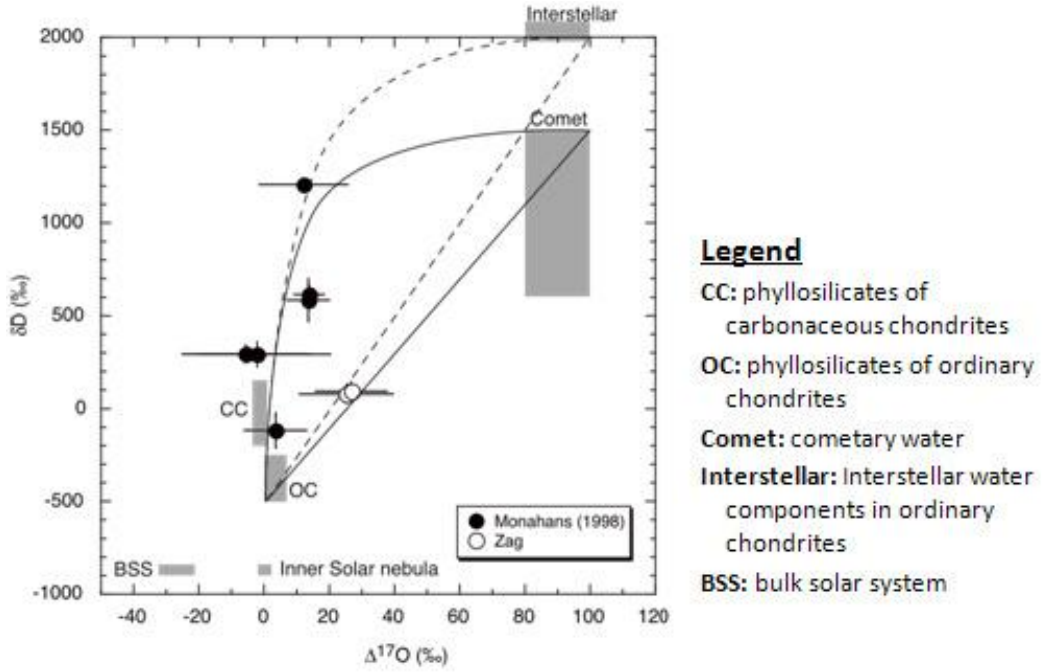


*Figure 2.– Results of the analysis of O and H isotopes of several Monahans and Zag halite fluid inclusions. Lines are expected mixing lines between cometary (or interstellar) water and ordinary chondrite.*

The team hypothesized that organics being carried through the parent body of the halite have been deposited adjacent to the fluid inclusions, where they have been preserved against any thermal metamorphism. We have recently located these organics, and they are being analyzed using confocal Raman spectroscopy, at the Carnegie Geophysical Institution. These organics will be compared with those found in chondrites and Wild-2 comet coma particles to determine whether these classes of organics had an origin within aqueous solutions.

Finally, the team is locating and analyzing fluid inclusions in other meteorites. Fluid inclusions in six other meteorites have already been found, to broaden the scope of the work and extend it to other primitive water-bearing solar system objects.

# *Nanometer-Scale Anatomy of Entire Stardust Tracks*

*Keiko Nakamura-Messenger, Lindsay Keller, Simon Clemett, Scott Messenger*

Analyses of samples returned from Comet 81P/Wild-2 by the Stardust spacecraft have resulted in a number of surprising findings that show the origins of comets are more complex than previously suspected. However, these samples pose new challenges for study because they are diverse and suffered fragmentation, thermal alteration, and fine scale mixing with aerogel. Consequently, fundamental questions remain about the nature of cometary materials, such as the abundances of organic matter, crystalline materials, and presolar grains. To overcome these challenges, JSC researchers have developed new sample preparation and analytical techniques tailored for entire aerogel tracks of Wild2 sample analyses both on "carrot" and "bulbous" tracks. The team has successfully sliced an entire track along its axis while preserving its original shape into 510 thin sections with 70 nm thickness (figure 1). This innovation allowed examination of the distribution of fragments along the entire track from the entrance hole all the way to the terminal particle. Scanning transmission electron microscope (STEM) was used for elemental and detailed mineralogy characterization, NanoSIMS was used for isotopic analyses, and ultrafast two-step laser mass spectrometry (*ultra* L2MS) was used to investigate the nature and distribution of organic phases.

Our most important findings from the analysis of these two Wild2 aerogel tracks and their terminal particles include:

- The terminal particles are dominated by Mg-rich crystalline silicates (forsterite and enstatite) that formed at high temperatures.
- The crystalline silicates have O isotopic compositions within the range of meteoritic materials, implying that they originated in the inner Solar System.
- The forsterite grain shows a $^{16}$O-enrichment of ~40‰, and likely formed in the inner Solar System. This grain may have formed together with amoeboid olivine aggregates in meteorites.
- Submicrometer diamond grains were identified that likely formed in the Solar System.
- Complex aromatic hydrocarbons are distributed along aerogel tracks and in terminal particles. These organics are likely cometary but affected by shock heating.
- Some cometary grains contain N-rich organic matter in the form of aromatic nitriles (R-C≡N). Such materials have potential astrobiological importance because it is believed that comets significantly contributed to the prebiotic chemical inventory of both the Earth and Mars.
- The Stardust organic compounds share some similarities with those of carbonaceous chondrites, but are more similar to interplanetary dust particles. These findings are consistent with the notion that a fraction of interplanetary dust is cometary.

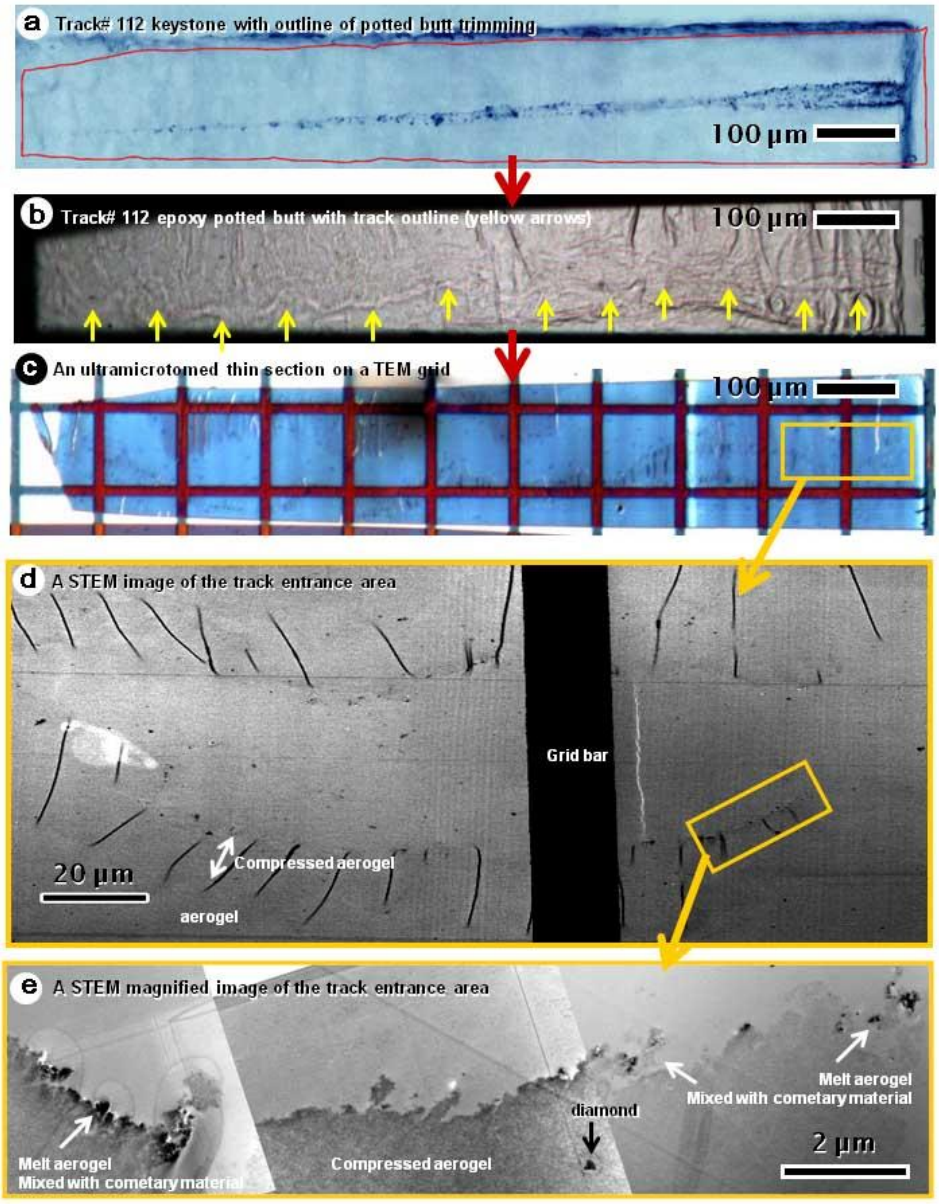


*Figure 1.– Processing flowchart for dissecting the whole track in aerogel.* ***(a)*** *Low magnification optical micro-graph (under transmitted light) of the Track112 keystone after the terminal particle extraction. The red trapezoid indicates the outline of trimmed potted butt.* ***(b)*** *Top view of the epoxy potted butt of Track112 after trimming into trapezoid shape. Yellow allows indicate the track outline visible through the covering epoxy resin.* ***(c)*** *One out of 510 ultramicrotomed thin sections of Track112 mounted on amorphous carbon supported Cu TEM grid.* ***(d)*** *A bright-field STEM micrograph of the boxed area in (c). The track morphology is well-preserved in an ultramicrotome thin section and material is intact. The aerogel within 20 um of the track wall (darker contrast with wrinkles) was compressed by the impact.* ***(e)*** *Photo mosaic of bright-field STEM micrographs of boxed area in (d). Numerous sub-micrometer sized grains are observed along the track wall. Many of these tiny grains consist of melt particles (cometary material intimately mixed with melted aerogel). One of the diamond grains is located in the compressed aerogel (arrowed).*

# *Wassonite: The Discovery of a New Meteoritic Mineral*

*Keiko Nakamura-Messenger, Lindsay Keller, Simon Clemett, Zia Rahman*

Using state-of-the art instruments, researchers in the Robert M. Walker Laboratory for Space Science at JSC discovered a new mineral within a meteorite. The new mineral is a titanium sulfide (TiS) and is named wassonite in honor of meteoriticist Prof. John Wasson (UCLA). The tiny grains of wassonite were found in the Yamato 691 enstatite chondrite, a rare type of meteorite that originated in the asteroid belt and later fell to Earth in Antarctica. The wassonite grains were recognized as a potential new mineral by colleagues at UCLA, who measured the chemical composition of the grains, but were unable to determine its other properties. Using the focused ion beam (FIB) instrument at JSC, a thin slice of one of the wassonite grains was nano-machined and extracted from the meteorite for measurements with the JSC field-emission transmission electron microscope (TEM). The TEM analyses revealed the atomic structure of the grains, showing that wassonite has a relatively simple crystal structure consisting of alternating layers of Ti and S atoms. The chemical composition of wassonite and the speciation of the constituent atoms were measured using X-ray and electron spectroscopies at nearly the atomic scale. The textural relationship between wassonite and the other minerals in the meteorite (figure 1) are remarkably well-preserved in the FIB section. These data were sufficient for the Committee on New Mineral Names of the International Mineralogical Association to give official approval for the name "wassonite". Titanium sulfide has been synthesized and studied by scientists for decades in the semiconductor industry, but it had never before been found in nature.

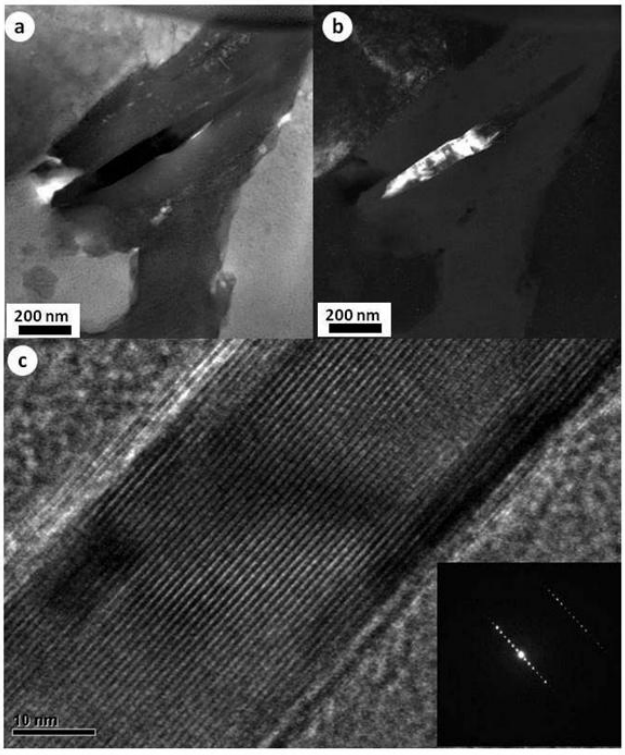


*Figure 1.– Wassonite grain in the Yamato 691 meteorite (a) A bright field TEM image showing a wassonite grain in dark contrast, (b) a high angle annular dark field TEM image of the same grain, (c) a high resolution TEM image of wassonite grain from the boxed area in (a). Inset is the selected area electron diffraction (SAED) pattern of wassonite.*

In the vast majority of minerals, Ti is bonded to oxygen and is referred to as a *lithophile* element. The fact that in wassonite, the titanium is bonded to sulfur indicates that it formed in a strongly reducing (oxygen-poor) environment at high temperatures (>1500K). These conditions existed close to the Sun in the early solar system ~4.5 billion years ago.

## *Hayabusa—The First Asteroid Sample Return Mission*

*Mike Zolensky*

On the evening of June 13, 2010, when the Institute of Space and Astrological Science (ISAS)/Japan Aerospace Exploration Agency (JAXA) Hayabusa spacecraft parachuted into the Woomera Prohibited Area in South Australia, JSC scientists were there to meet it. The JSC participants were members of the science team of the Hayabusa Mission, the first sample return mission to visit an asteroid and only the third sample return mission since the Apollo and Luna Missions of the 1960s and 1970s. The JSC members helped coordinate ground-based observers of the atmospheric entry fireball and served in the field on the capsule recovery team. The atmospheric entry and landing of the spacecraft was flawless, and the capsule landed very near the center of the calculated landing ellipse, an astounding feat considering the difficulties in navigating the spacecraft and steering it into the atmosphere. Figure 1 shows the Hayabusa capsule following reentry under examination by the recovery team. The team was prepared to douse the spacecraft with spemicide liquid in the event the capsule had opened upon landing.

*Figure 1.– The Hayabusa capsule is examined by the recovery team following reentry.*

Those who have been following the mission know about the many nail-biting episodes in its flight both to and from asteroid Itokawa. But even after the safe landing back on Earth, the big question remained, "Would there be any samples inside?" The asteroid regolith sampling mechanism had failed, and all hopes centered on the possibility that stray regolith grains might have been captured during one or more of the spacecraft's forceful touch and-go landings on the asteroid's surface.

Upon recovery, the capsule was flown by chartered jet to a new curation laboratory at ISAS's Sagimihara campus for dissection.

It took weeks of work but science team members found and removed thousands of asteroid regolith grains from the capsule for detailed analysis. Every technique involved in sample removal, handling and preliminary analyses were developed and optimized for these special samples, but the recent experience with the NASA Stardust Mission samples of comet Wild-2 were integral to the success with the Itokawa samples—all leading members of the Hayabusa sample analysis teams were previously involved in the Wild 2 samples. JSC and ARC scientists, the only U.S. team members and leaders of the preliminary analysis of the Wild-2 samples in 2006, are participating in the preliminary Hayabusa analyses in Japan. At the March 2011 Lunar and Planetary Science Conference the Hayabusa preliminary analysis teams reported the first results to packed crowds of planetary scientists. Figure 2, an excerpt from the initial reporting, is an electron backscattered image of one asteroid Itokawa grain.


*Figure 2.– An electron backscattered image of one asteroid Itokawa grain. Bright areas are sulfide and oxide crystals, grey regions are silicates. Scale bar is 10 micrometers.*

After the completion of the preliminary analysis of Itokawa samples, they will be made available to investigators worldwide. At this time 10% of the recovered samples will be permanently transferred to JSC, where they will be housed in a new Hayabusa Curation Laboratory, just down the hall from the comet Wild-2 samples. Together these samples will drive new efforts into understanding the origin and early history of the solar system.

# GeoLab

*Cynthia Evans, Michael Calaway, Mary Sue Bell*

**What is GeoLab?**

GeoLab is a prototype geological laboratory designed for deployment and testing during NASA's analog missions. JSC scientists built GeoLab as part of a technology project to support the development of science operational concepts on future planetary missions. It was integrated into NASA's Habitat Demonstration Unit-1/Pressurized Excursion Module (HDU1-PEM), a first generation exploration habitat testbed (see figure 1).


*Figure 1.– The HDU1-PEM (center) with two docked space exploration rovers. The main HDU-PEM volume includes several workstations. Three circular ports below "Habitat Demonstration Unit" are the antechamber doors that provide access directly into the GeoLab glovebox.*

As a testbed, GeoLab (figure 2) provides a safe, contained working space for crew members to perform preliminary examination and characterization of geologic samples. The GeoLab concept builds from the hardware and protocols used in JSC's Astromaterials Sample Curation laboratories. The centerpiece of the GeoLab is a custom-built glovebox, constructed from stainless steel and polycarbonate, and built to support a positive pressure nitrogen environment. The glovebox is mounted onto the habitat's structural ribs; the unique shape (trapezoidal prism) fits within a pie-shaped section of the cylindrical habitat. A key innovation of GeoLab is the mechanism for transferring samples into the glovebox: three antechambers (airlocks) that pass through the shell of the habitat. These antechambers allow geologic samples to enter and exit the main glovebox chamber directly from (and to) the outside, minimizing potential contamination from inside the

habitat. The glovebox also incorporates a state-of-the-art environmental monitoring system. The main chamber of the glovebox is equipped with sensors that monitor $O_2$ (ppm), pressure (mbar), humidity, and temperature, and each antechamber contains pressure sensors. Four video surveillance cameras provide real-time displays of operations inside the GeoLab workstation and the area around the antechamber doors on the outside the habitat.

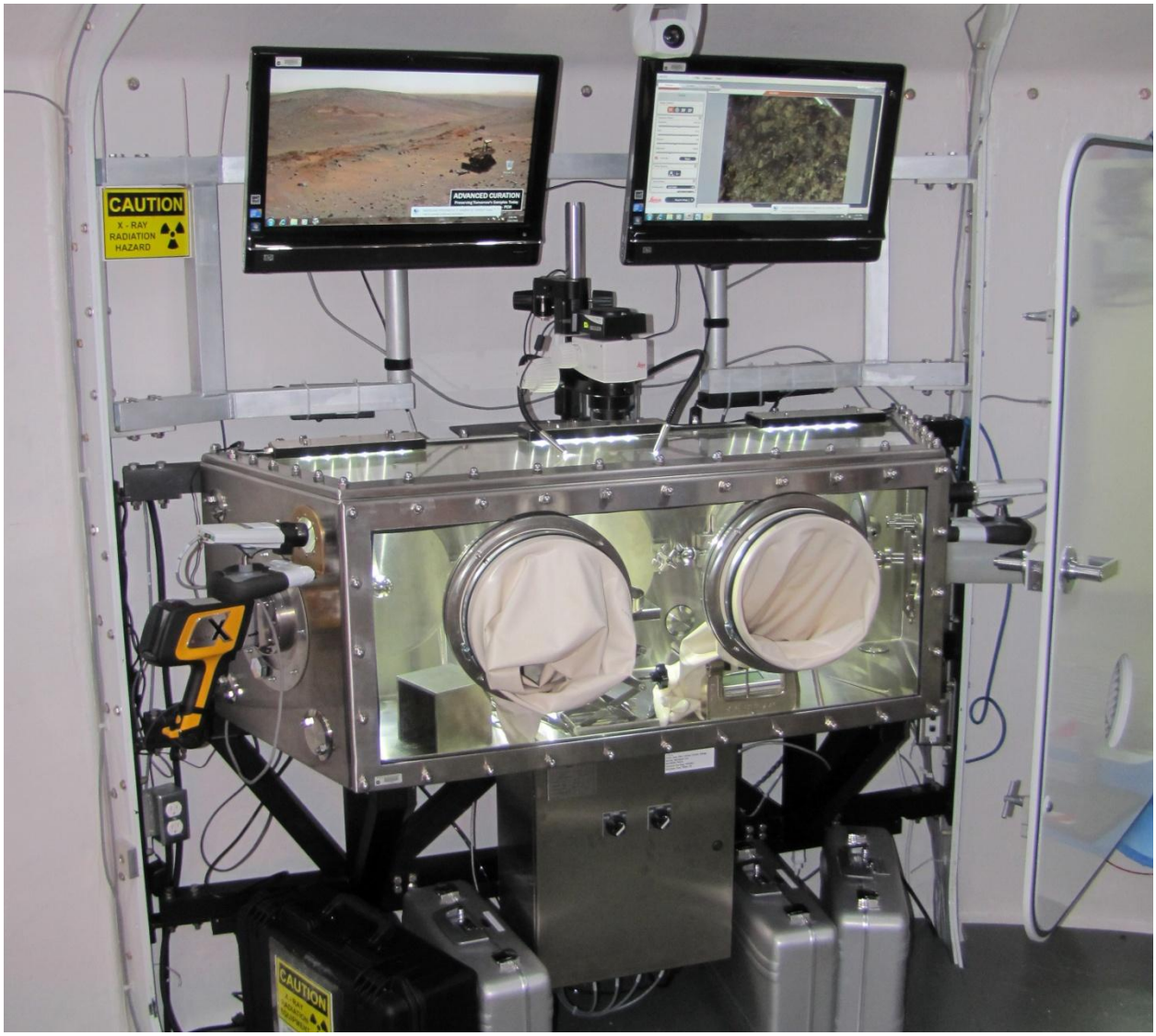


*Figure 2.– GeoLab integrated into the HDU1-PEM. The suite of instruments included a handheld XRF analyzer (far left), stereo microscope (center, above glovebox), network cameras, and touchscreen computers.*

**Configurability**

The GeoLab design includes a large set of ports for rapid reconfiguration with new instruments for sample characterization. Our initial setup included a stereomicroscope (Leica M80) for microscopic examination and image capture of samples, and an Innov-X handheld Delta DP6000 X-ray

Fluorescence (XRF) spectrometer for whole rock geochemical fingerprinting. Images and data from the instruments can be saved and "downlinked" to a remote science team. The glovebox also contains a mass balance and scale for collecting sample mass and size. All instrumentation and cameras are controlled at the workstation with two touchscreen computers (HP Touchsmart 600xt) mounted over the workstation and integrated into the HDU1-PEM avionics system. The cameras and sensor displays can be viewed and controlled in real-time on the remote network, and data from the microscope and XRF can be quickly moved across the network, enabling collaboration between the astronaut crew and a supporting science backroom.

**Field Trials**

The GeoLab and the HDU1-PEM were tested for the first time as part of the 2010 Desert Research and Technology Studies (D-RATS), NASA's analog field exercise in northern Arizona. The demonstration was initially conceived to guide the development of requirements for the Lunar Surface Systems Program and test initial operational concepts for an early lunar excursion habitat that would follow rovers performing geological traverses (figures 1 and 3). GeoLab objectives targeted general support of future planetary surface geoscience activities by providing an infrastructure for preliminary examination of samples, early analytical characterization of key samples, insight into special considerations for curation, and utilizing data for prioritization of samples for return to Earth.

*Figure 3.– Crew member collecting a geological sample during a D-RATS traverse.*

**GeoLab Operations in the Field**

The specific 2010 GeoLab operations included testing basic functions of the glovebox and associated instruments with a variety of operators (figure 4), and supporting the D-RATS science team with additional data on samples that were collected during the rover traverses. When the crews examined samples in the GeoLab, they were testing, at a high level, four major objectives:

- How does the GeoLab function as a workspace, including glovebox and instrument operations?
- How well do the crew and science team work together; what benefits are achieved by crew-scientist interactions during the integrated GeoLab tests?
- Can the data collected in the GeoLab inform the science team about the geologic units and the geologic history of the traverse area?
- Can the data collected in the GeoLab help the science team prioritize samples for decisions regarding future return to earth?

*Figure 4.– During GeoLab operations all data could be viewed in near-real time by a remote science team.*

**Initial GeoLab Results**

Results from the GeoLab 2010 operations provide a first look at both the value and operational constraints associated with human-tended geological operations in a laboratory setting on a planetary surface. Initial assessments suggest that:

- The GeoLab glovebox provided a high fidelity field laboratory, and it performed well. With a trained crew, samples could be examined relatively quickly, and provide additional detailed data for further consideration by the science team.
- GeoLab operations benefited from science team participation. The science team saved valuable crew time by performing certain tasks (for example, camera control), and guided the crew for decisions regarding data collection.
- The detailed data collected in the GeoLab added to the body of evidence applied to understanding the regional geology. Even though initial assessments of the geochemical data include many

uncertainties, the full body of data collected on each sample suggests that similar-looking rock units could be distinguished, providing data useful for geologic interpretation of the area (figure 5). Of note, data collected on alteration surfaces of samples provided additional detail and information that was difficult to obtain in the field. We assume these data would also be useful to the science team for decisions regarding sample handling and prioritization.

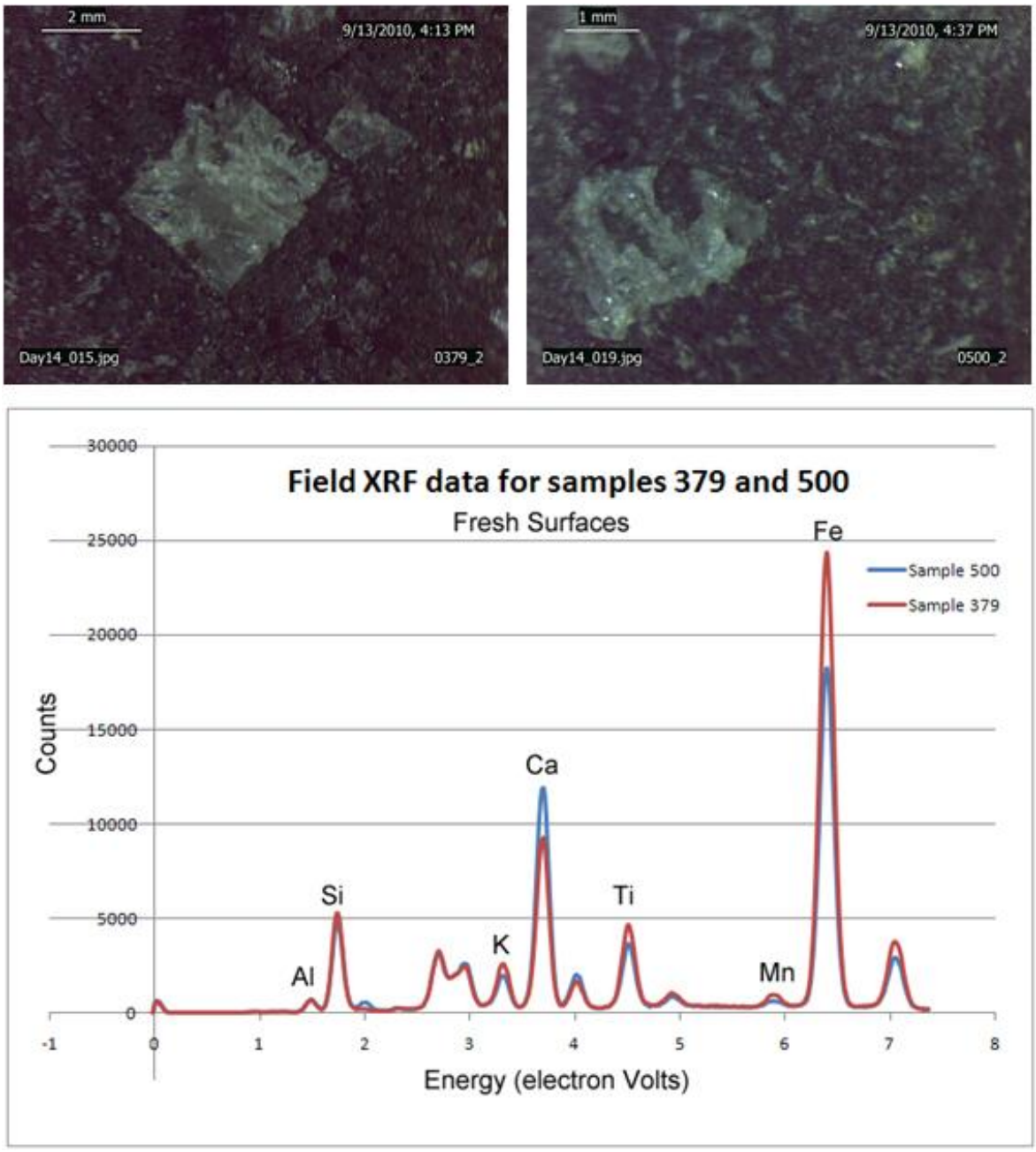


*Figure 5.– Microscopic images (texture and phenocryst assemblage) and XRF spectra for rapid geochemical fingerprinting of two samples from similar-looking units [Sample 379 left, Sample 500 right] suggest compositional differences between the older flow unit (500) and an older cinder cone (379).*

**Future Plans for GeoLab**

There are several areas of continued development for future GeoLab operations. The team is testing best operating practices for the XRF as a field/lab instrument, and assessing how to interpret XRF data for whole rock geochemical fingerprinting. Not surprisingly, the GeoLab XRF data must be interpreted within the context of the field occurrence and detailed visual descriptions (especially texture, homogeneity, surface roughness and alteration, and more), and microscopic imagery. In parallel to analysis of our D-RATS data, the team is characterizing the performance of the XRF spectrometer by conducting tests with rocks of known composition and a variety of surfaces, and building working calibration curves for the major rock-forming elements. The data will be used for analyzing the results of our D-RATS samples. There is also a plan to test the configurability of GeoLab in the 2011 D-RATS field tests by integrating an additional analytical instruments, and upgrading and simplifying the instrument interfaces for remote operations. Collaboration will continue with both the science and operations teams for integrated tests, to take full advantage of the operational environment provided by the field deployment.

Continued testing of GeoLab operations in a field environment will contribute to the development of habitat-based laboratory concepts. The scientific and operational value of additional analytical capabilities will be tested in GeoLab, and in the future, we will compare results to similar analyses using field instruments operated by crew or instruments mounted on robots. The team aims to apply their work toward defining preliminary examination and sample handling protocols required for efficient field campaigns and initial curation efforts that control contamination and preserve pristine samples collected during exploration missions. Assessment of the laboratory operations will drive the definition of requirements and support the advancement of new technologies for handling and examining extraterrestrial samples, and transporting them back to Earth.

# *Human Exploration Science Office (KX)*
# Overview

## Douglas W. Ming, Ph.D., Manager

**http://ares.jsc.nasa.gov/ares/exploration/index.cfm**

The Human Exploration Science Office provides support for human spaceflight and conducts world-class research and technology development in the areas of space orbital debris, hypervelocity impact technology, image science and analysis, crew earth observations and human and robotic exploration science.

NASA's Orbital Debris Program Office (ODPO) is housed in the Human Exploration Science Office. The ODPO provides leadership in orbital debris research, including the development of national and international space policy on orbital debris. The office is recognized internationally for research on measurements and modeling of the Earth's orbital debris environment.

The Hypervelocity Impact Technology (HVIT) project provides evaluation of the risks to spacecraft posed by micro-meteoroid and orbital debris (MMOD) impacts through laboratory testing and software modeling predictions. Research and technology development programs are underway to develop shielding to protect humans from MMOD during spaceflight missions. The project contributes to the safety of the crew on human spaceflight missions by identifying MMOD risks for each mission. Advanced shielding designs are being evaluated for future missions.

NASA Image Science and Analysis Group (ISAG) provide near, real-time imagery analysis of spacecraft flight (Shuttle, ISS, commercial spaceflight) to assess vehicle performance, debris shedding and anomalies. Image analysis protocols are currently being developed to evaluate the performance and anomalies for future spacecraft, i.e., Multi-Purpose Crew Vehicle and commercial spaceflight vehicles. The Crew Earth Observations (CEO) payload onboard the ISS is a function of the ISAG. Earth imagery acquired by astronauts are catalogued and made available to the public through a web-based access site. ISAG scientists conduct research on the interpretation of the CEO imagery.

Human exploration science focuses on science strategies for future human exploration missions to the Moon, Mars, asteroids and beyond. This function provides communication and coordination between the science community and mission planners. ARES scientists continue to support the operation of robotic missions (i.e., Mars Exploration Rovers, Mars Science Laboratory, Dawn) and contribute to the interpretation of data returned by these voyagers to Mars, Asteroids and other planetary bodies.

**Reports on several projects are given in the following pages.**

# *Image Science Support to Commercial Development*

*Tracy Calhoun*

The Image Science and Analysis Laboratory (ISAL) at Johnson Space Center is continually building, honing and adapting its image science capabilities to provide optimum support to NASA customers. Often this evolution is driven by the pace of imaging technology, but sometimes the evolution results from new space policy. NASA's effort to commercialize space transportation to and from the International Space Station (ISS) is a recent example of an agency goal spurring lab evolution.

Under Commercial Orbital Transportation Services, or "COTS", NASA awarded Space Act Agreements to Space Exploration Technologies (SpaceX) and Orbital Sciences Corporation (OSC) to develop systems that can provide cargo to ISS after Shuttle retirement. COTS partners will fly demonstration missions of these systems, culminating in each demonstrating a mission that berths with ISS. Under COTS, NASA provides requirements, funding and high level oversight and the companies provide vehicle design, construction and operation.

To support oversight, NASA secured the services of the ISAL, one of the first JSC teams to support commercialization. The traditional model for ISAL support to a program is to partner with a NASA customer on every step of the image science process—from the design of imagery acquisition, through the meticulous screening of mission imagery and ending with the application of image analysis techniques to investigate significant findings derived from the screening. But now, with the agency removed from day-to-day mission development, the ISAL was tasked to help NASA design an engineering imagery plan that could provide a feel for overall performance but, in the event of a mishap, would be adequate to support accident investigation. The latter is an important element considering that it is fiscally impractical for commercial partners to acquire imaging resources comparable to those already in place at NASA's Kennedy Space Center.

The first mission that ISAL supported was SpaceX's Falcon maiden flight in June of 2010 from launch complex 40 at the Cape Canaveral Air Force Station (CCAFS LC-40). The ISAL worked with NASA managers to establish vehicle events and features of interest. The ISAL then coordinated with KSC imagery teams to design a camera complement, imagery acquisition plan, distribution plan and schedule. This included the acquisition of high quality still images to document the preflight condition of the vehicle and ground structures. This Vehicle Configuration Imagery, or "VCI", is essential to the imagery screening process and any subsequent image analysis.

During and after the launch, the ISAL screened each piece of imagery with an experienced eye from their support to numerous NASA launches. They also leveraged KSC launch experts to screen the same imagery set. Launch findings were documented in a custom data base with access limited to key NASA and SpaceX personnel, due to the proprietary nature of the imagery. NASA managers used the database to identify events of interest but also provided the database to SpaceX for insight into things that cannot be monitored or detected in telemetry. Additionally, a courtesy copy of the NASA imagery was supplied to SpaceX via portable hard drives, delivered by overnight mail.

On December 8, 2010, SpaceX launched a second Falcon from CCAFS with their Dragon capsule as an official demonstration flight for the NASA COTS program, designated as "C1". That mission was again supported by the ISAL (figure 1). In late 2011, the ISAL will support SpaceX's C2 launch and a maiden launch of OSC's Taurus 2 rocket. In 2012 ISAL will support the second Taurus 2 launch, the official demonstration flight for NASA COTS, and possibly a C3 SpaceX demonstration mission. The OSC missions will launch from Virginia's Mid-Atlantic Regional Spaceport (MARS), adjacent to the Wallops Flight Facility.


*Figure 1.– The SpaceX Falcon 9 with the Dragon vehicle demonstration flight on December 8, 2010.*

# *Photogrammetric Analysis of Parachute Tests*

*David Bretz*

The Crew Exploration Vehicle Parachute Assembly System (CPAS) is being designed to land the Orion Crew Module at a safe rate of descent (33 feet-per-second) at splashdown with a cluster of two to three main parachutes. The most important driver of rate of descent is the canopy loading, defined as the suspended weight divided by the total parachute surface area. Parachutes in a cluster distort their shapes when they collide or even when they are close enough for their "spillover" flow to interfere with each other. The reduction in canopy projected area leads to a loss in drag and an increase in descent rate. CPAS main parachutes have a noticeable cyclical expansion and contraction called "breathing" which can measurably affect performance.

The understanding of the cluster dynamics has been improved through the use of image analysis of video obtained during drop tests. High definition video imagery looking upward from a test payload that is released from an aircraft is used to measure several key aspects of parachute behavior including both fly-out angles and parachute diameters over time.

The central vent and several points around the parachute skirt are tracked through every video frame to compute an effective diameter, circumference and inlet area as a function of time. Tracking is done semi-automatically with commercial software designed for the military and automotive industries and that data is corrected for geometric lens distortions. Figure 1 illustrates a plot of parachute diameter over time for drop test at the Yuma Proving Grounds (YPG).

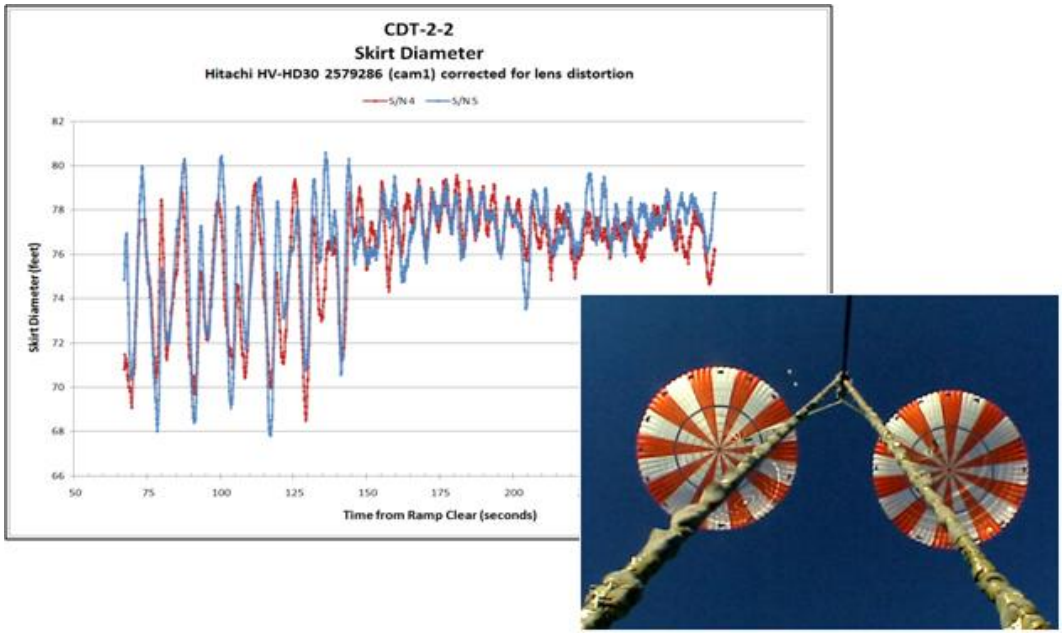


*Figure 1.– Two parachute skirt diameters measured in each frame of video and plotted (time along horizontal axis and diameter along vertical).*

The fly-out angles, the angle of each parachute cluster relative to a central, vertical reference line are also measured over each frame of video (figure 2). The test data can be correlated to on-board accelerometers to assist engineers in designing parachutes that minimize fly-out angle and diameter oscillations and thereby stabilize the rate of descent. One such design change increased the porosity, allowing more air to flow through the parachute canopy. Testing of increased porosity, as illustrated in the plots of figures 1 and 2, showed a reduction in cluster fly-out angle oscillations, reducing parachute collisions and thus producing more stable flight dynamics. Note the change in both plots after approximately 2 minutes, reflecting a reduction in "breathing" and angles.

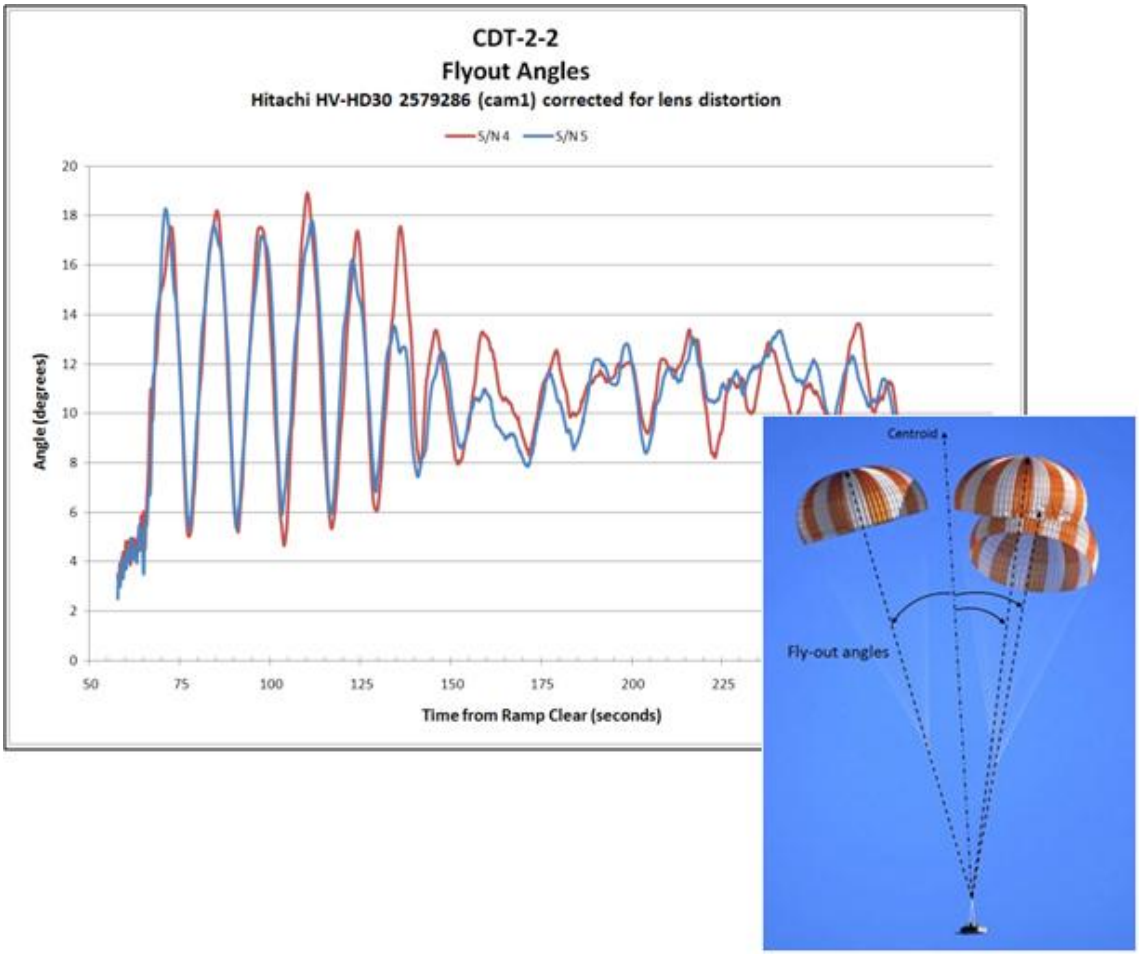


*Figure 2.– The fly-out angles for two main parachutes (vertical axis) measured over time (horizontal axis).*

Parachute fly-out angles have also been useful in calculating the loads on each line, or riser, that joins the parachute canopy to a common attach point. In one test case, each riser was instrumented with a Tension Measuring System (TMS). It was later discovered that the system's calibration was inappropriate for the type of material used. By resolving the TMS readings into components based on the fly-out angles, it was possible to re-calibrate the TMS data based on the loads calculated from accelerometers. This resulted in more accurate riser loads appropriate for load sharing analysis.

In both planned and unplanned ways, image analysis has proven to be a cost effective method of extracting data from a system that is very difficult to instrument. The image analysis gives designers an understanding of parachute cluster dynamics which will in turn ensure a parachute system that will return space explorers safely to Earth.

## *Orion On-Orbit Inspection Capability Study*

*Michael Rollins*

NASA has been directed to build a Multipurpose Crew Vehicle (MPCV) capable of carrying humans beyond low Earth orbit (LEO) and conducting operations in LEO. Orion spacecraft development is anticipated to have high applicability to the MPCV project. MPCV service in LEO may require the vehicle to be docked to the International Space Station (ISS) for several weeks, during which it will be exposed to micrometeoroids and orbital debris (MMOD), which can potentially cause critical damage to the vehicle with respect to reentry heating. Understanding the criticality of damage will depend upon effective on-orbit inspection of the vehicle. In 2008, the Orion Project tasked JSC's Image Science and Analysis Laboratory (ISAL) to study the ability to inspect the Orion thermal protection system (TPS) while docked to ISS. The findings of the study will have direct applicability to MPCV.

Specifically, ISAL was directed to explore the effectiveness of currently space-qualified sensors as inspection sensors for Orion docked to ISS. At the same time, as part of its risk analyses, the Orion Project estimated the likelihood of critical MMOD strikes to the vehicle and has assumed that on-orbit inspections can be 95% effective in finding and determining the criticality of any such MMOD damage. For an Orion spacecraft, the surfaces of particular interest, due to their representing large components in the overall MMOD-based risk to crew safety and mission success, are the Backshell and Forward Bay Cover (FBC). These surfaces are composed of tiles, similar to the black TPS tiles on the Space Shuttle. Critical damage to such tiles from MMOD strikes can result in damage cavities whose observable entry holes are as small as a quarter inch in diameter.

While a major emphasis has been placed on examining the utility of existing space-qualified sensors in the detection and characterization of MMOD damage cavities within TPS tiles, other sensors have been examined as well. All of the sensors examined by ISAL as candidates for on-orbit TPS inspection have been non-penetrating 2-dimensional (2D) sensors (i.e. various cameras) and inherently 3-dimensional (3D) sensors (e.g. the Laser Camera System or LCS—currently space-qualified—and the Mold Impression Laser Tool or MILT). Other organizations have collected data from penetrating sensors, especially X-ray and millimeter-wave, but such sensing technology has been outside the area of expertise for ISAL to date. Non-penetrating sensors have the advantage of high resolution and strong surface contrast as compared to penetrating sensors. The latter have the advantage of not requiring unobstructed lines of sight to structural damage. The attractiveness of space-qualified sensors is that they are known to be robust to launch acceleration and vibration,

space radiation and poor cooling from the lack of atmospheric convection. Space-qualified hardware generally has also (but not always) been the product of assembling reliable, high-quality components for which an expectation for long on-orbit operating life is justified.

Based on extensive experience with Space Shuttle on-orbit inspections, ISAL assumed that Orion inspections would consist of two major operations—the initial full-surface survey (figure 1) and close-range focused inspection for any suspected damage found during the initial survey. The full-surface survey is expected to be accomplished using a camera positioned by the ISS Space Station Remote Manipulator System (SSRMS) over comprehensive scan trajectories. The focused inspections are expected to require both cameras and 3D sensors, to provide high resolution images and point clouds to characterize damage (figure 2). They are also expected to require visible-band and possibly ultraviolet illumination, which has been seen to cause fluorescence in material underlying the tile (figure 3), greatly enhancing the possibility of determining full tile penetration. Focused inspections may also benefit later from penetrating sensors as technology allows. The survey cameras may be the Mobile Servicing System (MSS) cameras already at each end of the SSRMS (and also positioned on a robotic attachment for the SSRMS, called Dextre), or another camera with greater resolution and or greater robustness to varied lighting, such as the Laser Dynamic Range Imager (LDRI), a survey-type sensor used in Space Shuttle inspections. Focused-inspection sensors may require six degrees of freedom in positioning to ensure needed proximity and view angles, and will most likely need to be attachable to the "arms" of Dextre, shown in figure 4.

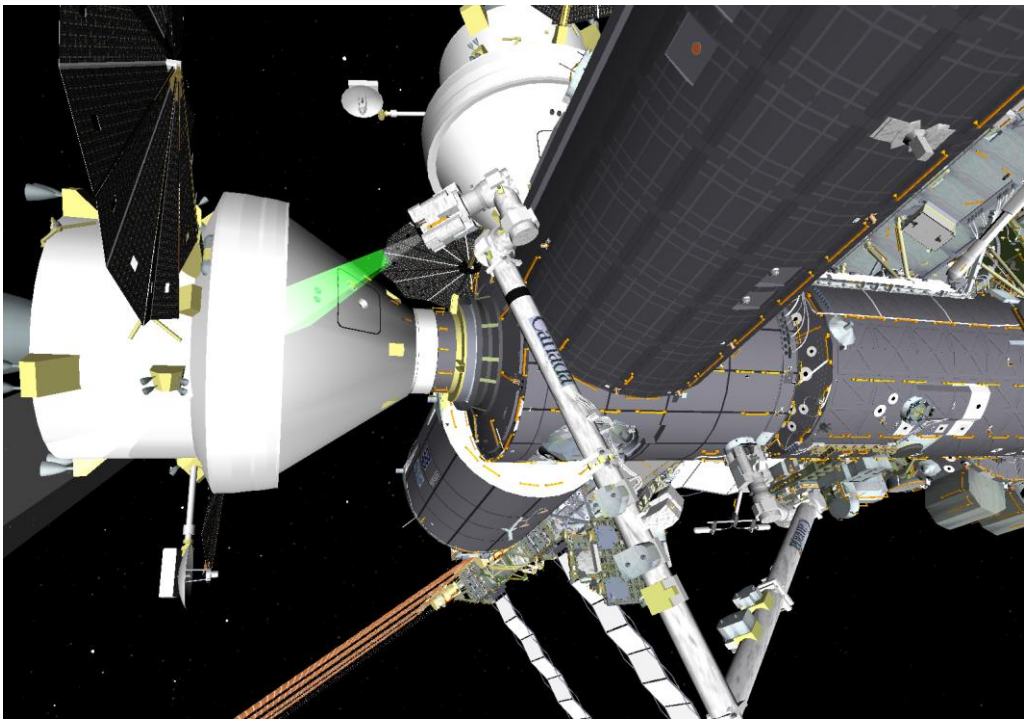

*Figure 1.– Snapshot of full-surface survey of the Orion Crew Module docked at ISS Node 2 Forward using SSRMS Latching End Effector camera.*

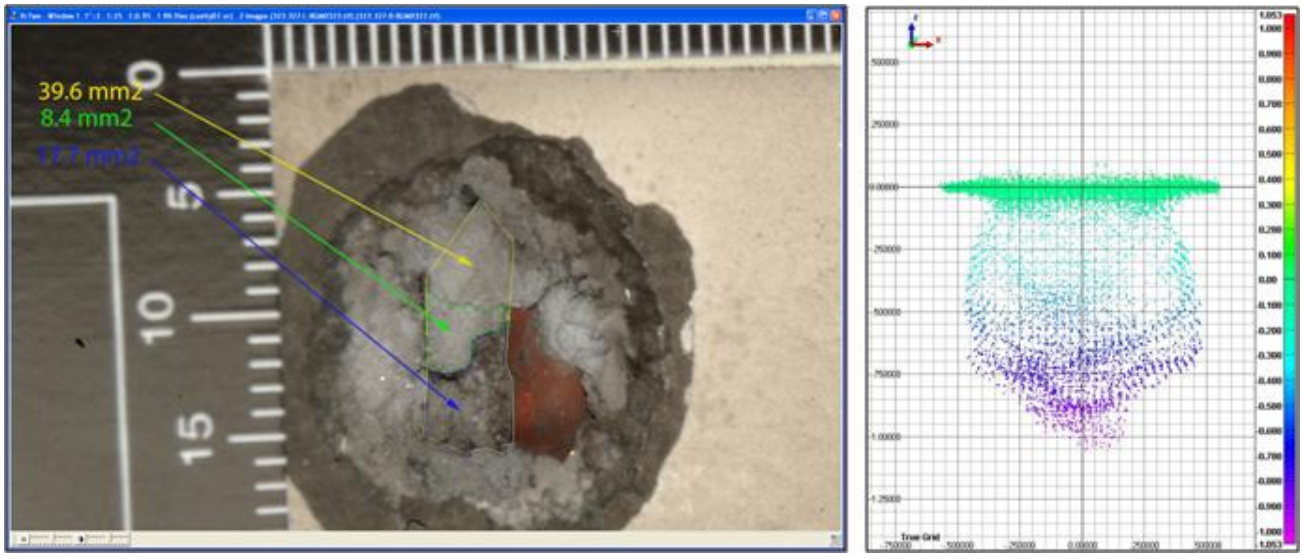


*Figure 2.– High-resolution digital image (left) from stereo pair and LCS 3D point cloud elevation view (right) of hypervelocity impacted Orion TPS tile are examples of potential focused-inspection sensor products.*

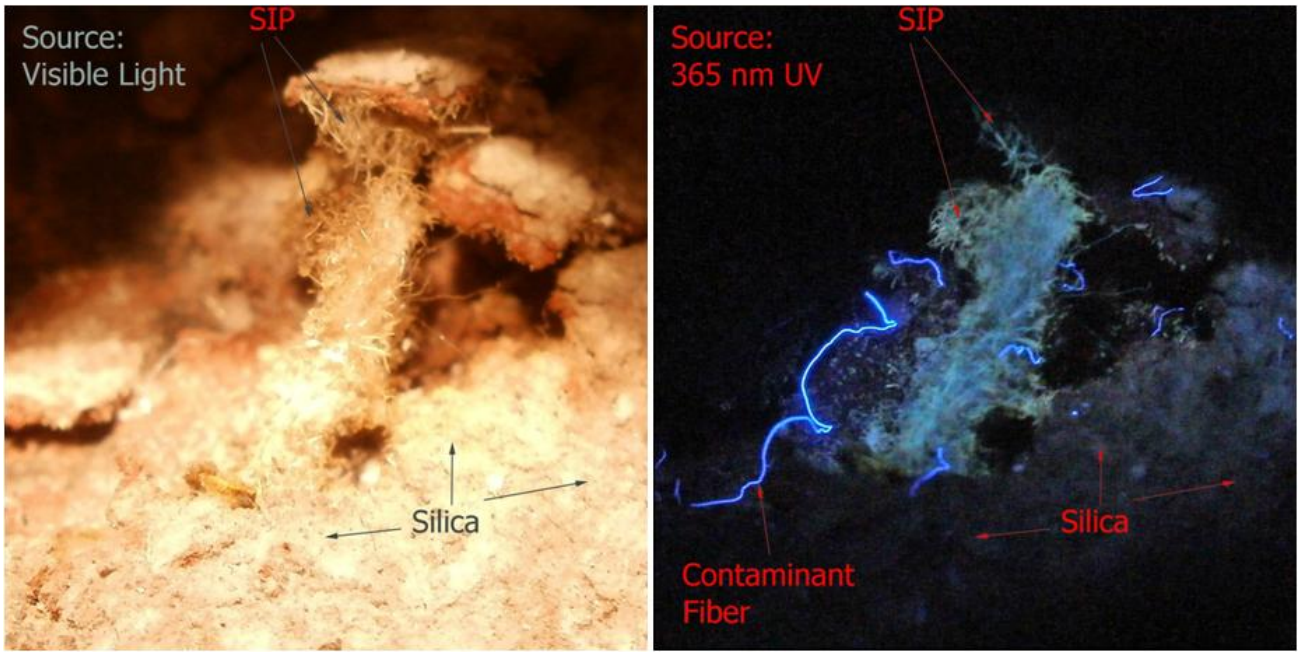


*Figure 3.– High-resolution digital image pair showing enhanced detectability of Strain Isolation Pad (SIP) material under UV illumination (right) as compared to visible-band illumination (left). Detection of exposed SIP (which will underlie tile on the MPCV) is an excellent indicator of full-tile penetration.*

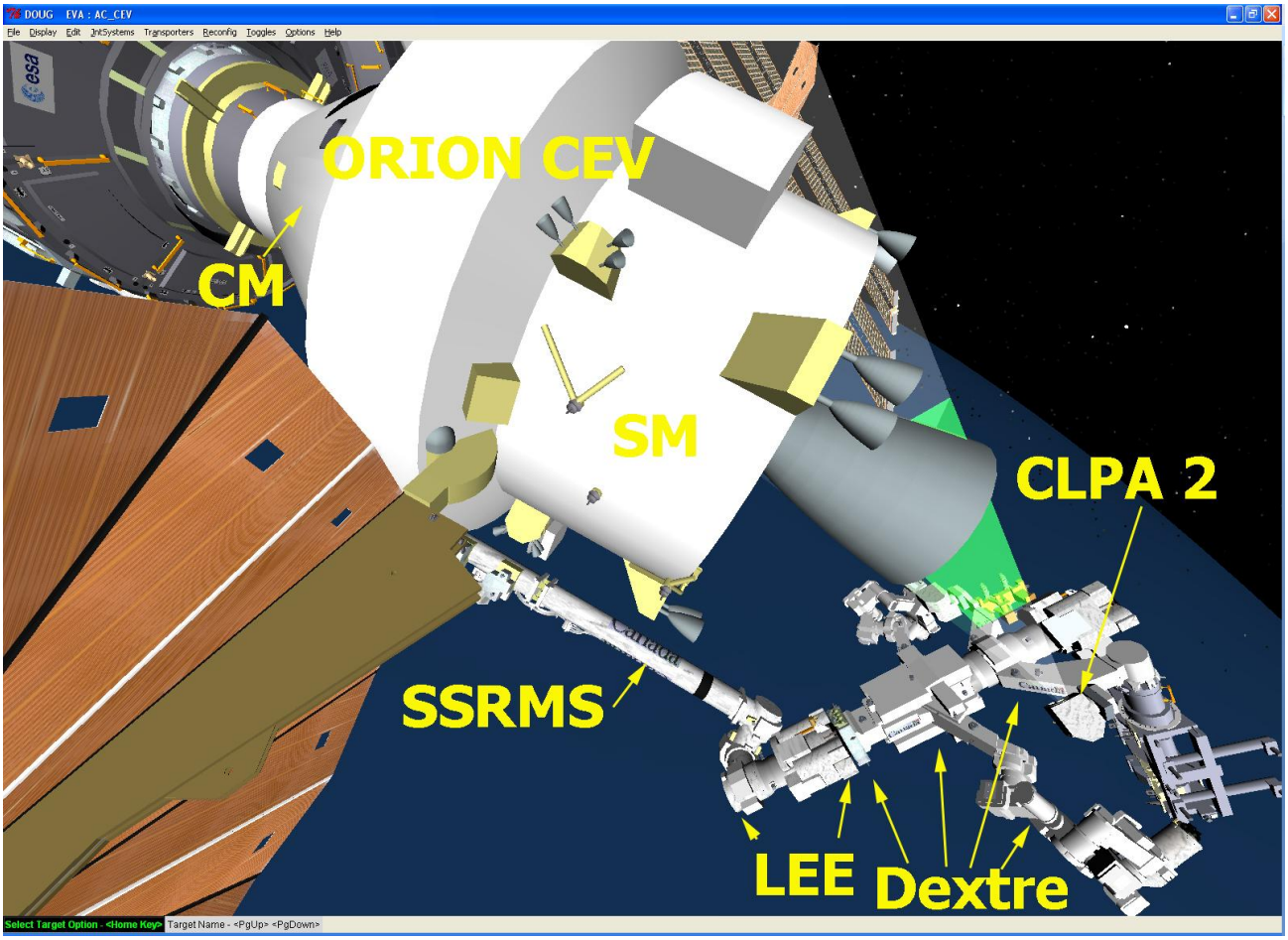


*Figure 4.– Dextre on the SSRMS provides additional reach and potential focused-inspection sensor positioning capability.*

ISAL conducted various subjective tests using data collected by cameras and 3D sensors to try to estimate inspection effectiveness using that hardware. The testing was designed to represent both an initial survey and focused inspection as described above. Probability of detection for the survey portion of the inspection has been estimated to exceed 95%, especially if redundant screening teams are employed. Although results using 2D and 3D non-penetrating sensors are encouraging, further testing will be required to determine focused-inspection effectiveness (FIE), and therefore overall inspection effectiveness, and whether or not penetrating sensors will also be needed. Testing to date shows that FIE will not only be dependent upon sensors selection and deployment, but also a ground process that draws upon the discernment of structural experts.

# *Photogrammetry Software Project–NASA Collaboration With Small Business*

*Edward R. Oshel*

The JSC Image Science and Analysis Laboratory (ISAL) uses photogrammetry to support a variety of human spaceflight issues, ranging from vehicle damage assessment to measuring the response of vehicle appendages to forcing events. Photogrammetry is the science and art of measuring the size and shape of objects from photographs. Commercial off the shelf (COTS) software packages are employed for most of the ISAL's photogrammetry work.

The figure below illustrates a common issue in imagery acquired during human space flight. It shows a set of images, each acquired from different positions, as is the case, for example, of handheld camera imagery acquired by an extravehicular crewmember on a space walk outside the International Space Station.

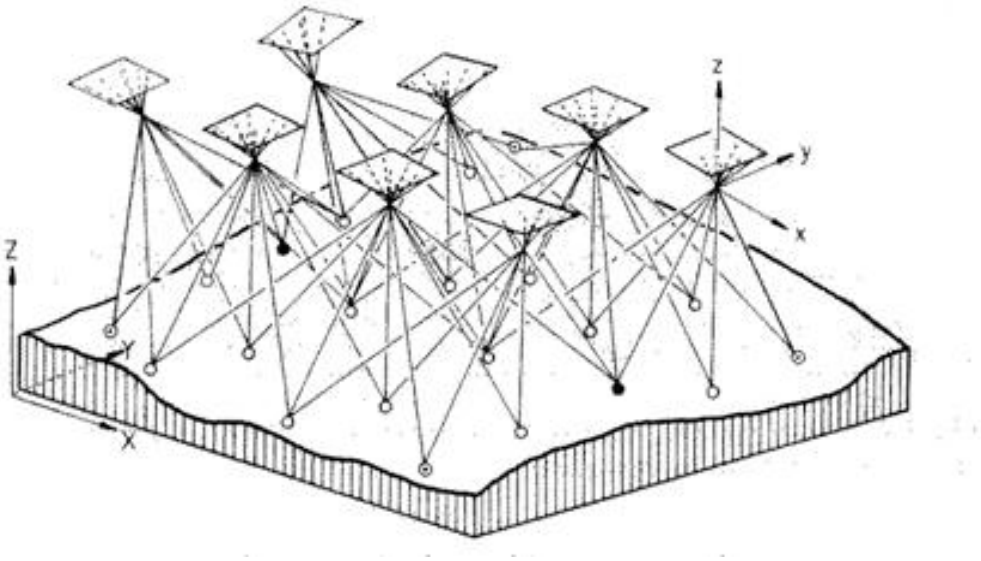


*Figure 1.– An image set for a common feature of interest with each image using an independent frame of reference.*

In using this image set to extract information, one type of software package only allows measurements to be made *one image at a time*. It then determines each image's orientation and the scene coordinates in a single simultaneous computation, or "bundle adjustment". Because no relationship between each image is factored into the calculation, each image is "jittering about" independently in the results.

Another type of software package allows the user to view a *stereo pair of images* and form a 3D model of the scene. Typically the pair of images is directly oriented to each other using measurements made on both images at the same time, and then related to the scene. This results in many independent stereo models from the image set and now each model is "jittering about" independently and thus measurements from each model are likely to be slightly inconsistent with measurements from the other models.

It is possible to use the results of the single simultaneous computation (as described earlier) to orient a stereo pair chosen from the image set, but due to the error of that approach, the stereo model achieved is often poor.

In ISAL's support of manned space flight, measurement reliability is directly related to crew safety. A technique is needed to produce stereo models that are consistent within a frame of reference. What are needed are bundle adjustment results that will allow the formation of consistent stereo models.

ISAL turned to a past collaborator, Cardinal Systems, LLC, a small software firm based in Florida to develop a single program to orient images as desired and then apply stereo analysis techniques. The team found appropriate equations for computing the best orientation of each image in terms of the neighboring images and also with respect to a common reference frame. This will allow the analyst to select any overlapping pair in the imagery set for viewing in stereo and to make measurements that are consistent across all possible stereo pairs. An additional consequence of this approach is that the frame of reference does not need to be related to any exterior frame of reference, that is, no ground control is necessary once the relationship across the image set is computed.

The collaboration between NASA and Cardinal Systems will produce a new software package, using state of the art concepts to provide optimum measurements when using multi-image sets. The new software will directly contribute to crew safety and mission success.

## *LEO Environment Remediation with Active Debris Removal*

*J.-C. Liou*

The catastrophic collision between Cosmos 2251 and the operational Iridium 33 in 2009 signaled a potential onset of the "Kessler Syndrome" in the environment, predicted by Kessler and Cour-Palais in 1978. This event also supports the conclusion of several recent modeling studies that, even with a good implementation of the commonly-adopted mitigation measures, the debris population in low Earth orbit (LEO, the region below 2000 km altitude) will continue to increase. The population growth is driven by fragments generated via accidental collisions among existing satellites. Therefore, to remediate the environment, active debris removal (ADR) should be considered. The need of ADR is also highlighted in the National Space Policy of the United States, released in

June 2010, where, under the Section of "Preserve the Space Environment," NASA and the Department of Defense are directed to pursue research and development of technologies and techniques to remove on-orbit debris.

There are many technical and non-technical challenges for ADR. If the objective is to remediate the environment, then the most effective approach is to target the root cause of the problem—objects that have the greatest potential of generating the highest amount of fragments in the future. These are objects with the highest mass and collision probability. Figure 1 shows the mass distribution in LEO. It is obvious that the major mass reservoirs are located around 600, 800, and 1000 km altitudes. The 600 km region is dominated by spacecraft (S/Cs) while the other two regions are dominated by spent rocket bodies (R/Bs). Note the operational spacecraft accounts for approximately 10% of the mass in LEO. Since the 800 to 1000 km region also has the highest spatial density in LEO, it is expected that many of the potential ADR targets will be R/Bs in that region.

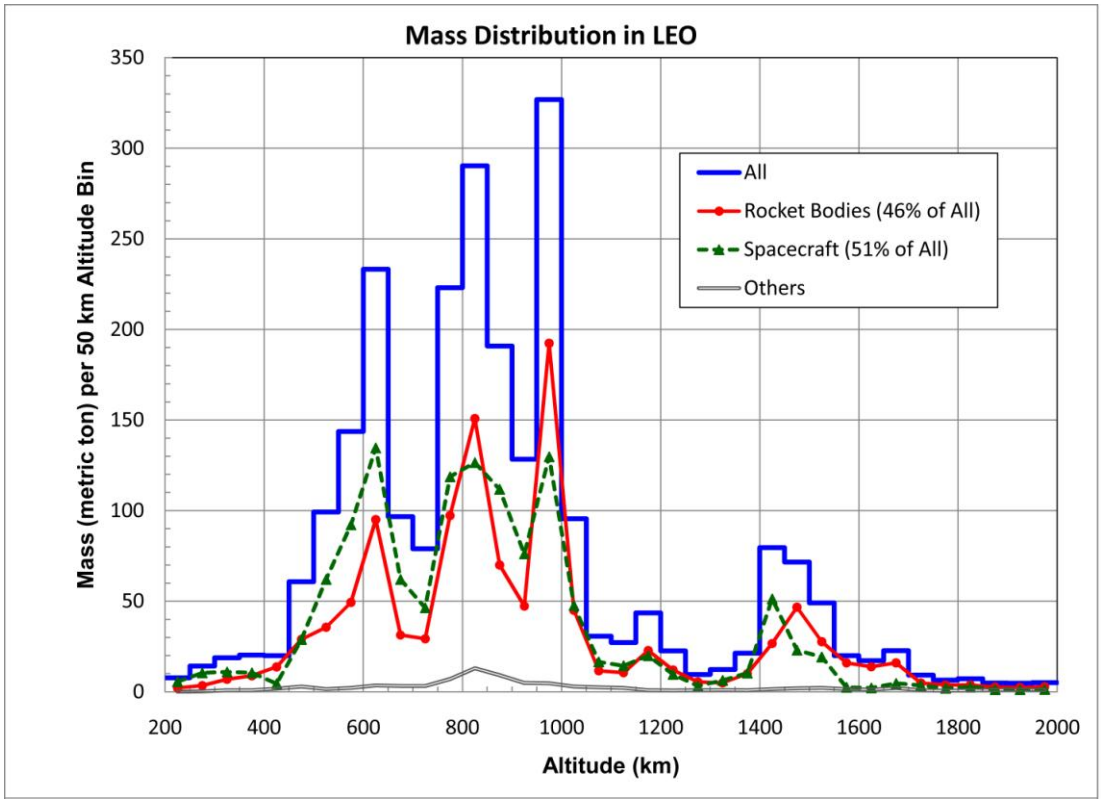


*Figure 1.– Mass distribution in LEO. The three major peaks are dominated by R/Bs and S/Cs.*

A key element for any ADR planning is the ability to quantify both the requirements of the operations and the benefits to the environment. Figure 2 shows the latest results from the NASA Orbital Debris Program Office on LEO environment remediation.

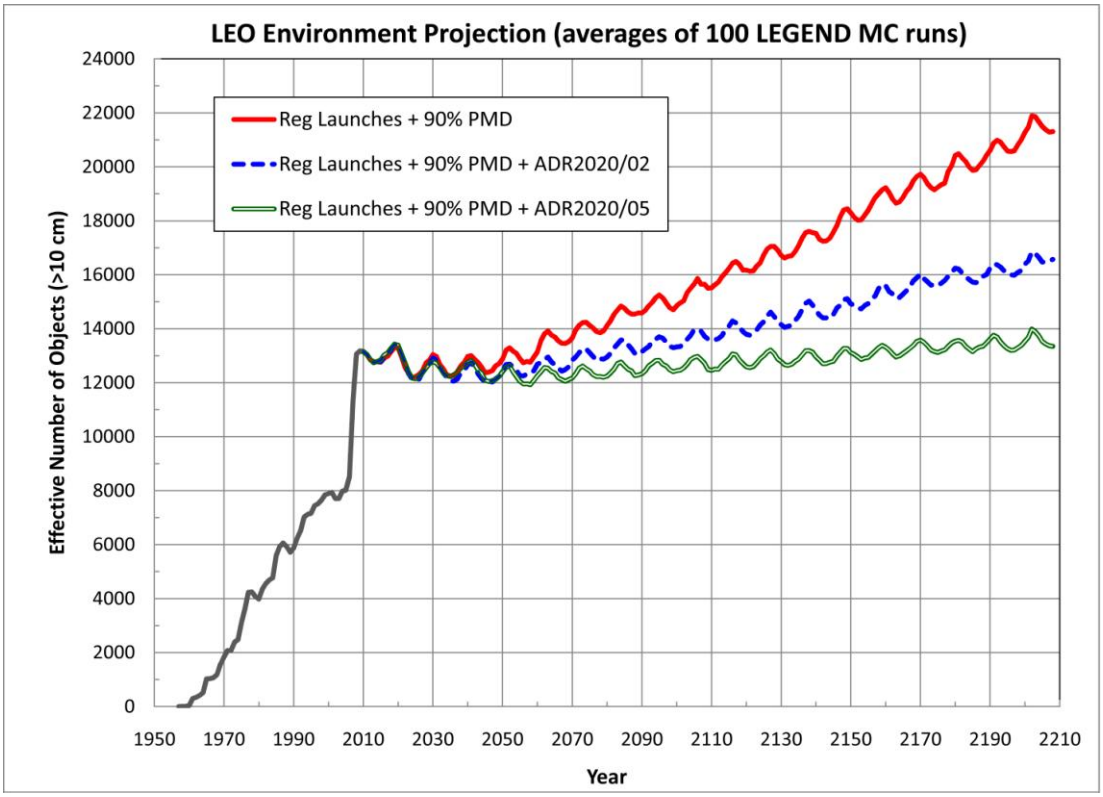


*Figure 2.– Simulated LEO population growth as a function of time. To maintain the future LEO population at the current level requires a good implementation of the mitigation measures and an ADR removal rate of about five objects per year, starting from the year 2020.*

Simulations were carried out with the NASA long-term debris evolutionary model, LEGEND. The future projection part of the top curve assumes a nominal launch cycle and a 90% compliance of the postmission disposal (PMD) measures (e.g., the 25-year rule). The average of 100 Monte Carlo LEGEND runs indicates that the LEO population will continue a steady increase in the next 200 years. With the addition of ADR operations of two objects per year, starting from the year 2020 (the middle curve), the population growth is reduced by approximately half. If the ADR rate is increased to five objects per year, then the LEO population in the next 200 years can be maintained at a level similar to the current environment (bottom curve). However, if the objective is to restore the environment back to the level prior to 1 January 2007 (before the ASAT test), then a removal rate of more than five objects per year must be implemented.

The ADR target selection criterion used in the LEGEND simulations was the [mass × collision probability] value of each object. This criterion can be applied to objects in the current environment to identify potential targets for removal in the near future. The altitude-versus-inclination distribution of the top 500 objects identified via this selection criterion is shown in figure 3. The prograde group is dominated by several well-known classes of vehicles: SL-3 R/Bs (Vostok second stages; 2.6 m diameter by 3.8 m length; 1440 kg dry mass), SL-8 R/Bs (Kosmos 3M second stages; 2.4 m diameter by 6 m length; 1400 kg dry mass), SL-16 R/Bs (Zenit second stages, 4 m diameter by 12 m length; 8900 kg dry mass), and various Meteor-series and Cosmos S/Cs (masses ranging from

1300 to 2800 kg). Below 1100 km altitude, the total mass of all SL-3, SL-8, and SL-16 R/Bs is about 500 tons, which accounts for close to 20% of the total mass in LEO. Objects in the retrograde region are more diverse. They include, for example, Ariane R/Bs (1700 kg dry mass), CZ-series R/Bs (1700–3400 kg dry mass), H-2 R/Bs (3000 kg dry mass), SL-16 R/Bs, and S/Cs such as Envisat (8000 kg) and meteorological satellites from various countries.

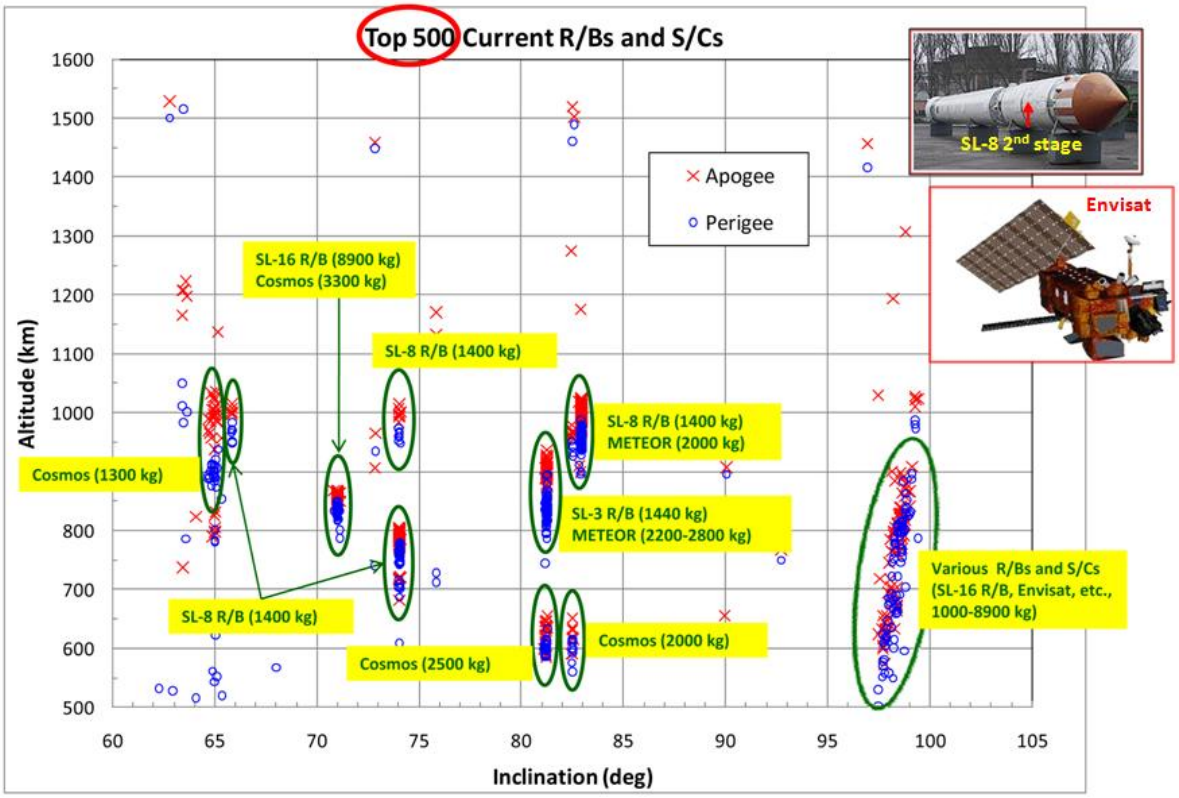


*Figure 3.– Apogee altitude (crosses) and perigee altitude (open circles) versus inclination distributions of the existing LEO R/Bs and S/Cs that have the highest mass and collision probability products. Only the top 500 are shown. These are potential targets for ADR.*

If ADR is to be conducted in the near future, objects in figure 3 should be high on the target list for removal. In general, R/Bs ought to be considered first because they have simple shapes and structures, and belong to only a few classes. However, some of the R/Bs may carry leftover propellant in pressurized containers. Any capture operations of these R/Bs will have to be carefully conducted. A potential problem to capture and remove objects, as shown in figure 3, is the non-trivial tumble rates of the targets. New ground-based observations on these objects are needed in the near future to identify their tumble states. As the international community gradually reaches a consensus on the need for ADR, the focus will shift from environment modeling to technology development, engineering, and operations. It is clear that major cooperation, collaboration, and contributions at the national and international levels will be needed to move forward to implement ADR for environment remediation.

# *Micrometeoroid and Orbital Debris Impact Inspection of the Hubble Space Telescope Wide Field Planetary Camera 2 Radiator*

*J.-C. Liou, Phillip Anz-Meador, John Opiela*

The Wide Field Planetary Camera 2 (WFPC2) was installed on the Hubble Space Telescope (HST) in 1993. After more than 15 years of collecting invaluable data for astronomers around the world, WFPC2 was replaced by the Wide Field Camera 3 (WFC3) during the final HST Servicing Mission 4 in May 2009. The entire WFPC2 instrument package was retrieved by the Shuttle *Atlantis* astronauts and brought back to NASA. The radiator attached to the WFPC2 camera, as shown in figure 1, was exposed to space for 15.44 years. The dimensions of the radiator are 0.8 m × 2.2 m, and the outermost layer is a curved aluminum plate with a thickness of 4.06 mm. The surface of the plate is covered with YB-71 white paint (specifically a Zinc Orthotitanate coating, known as ZOT, a type of ceramic thermal control paint). Due to its large surface area and long exposure time, the radiator surface served as a unique witness plate for the micrometeoroid and orbital debris (MMOD) impacts at the HST altitude between 1993 and 2009.

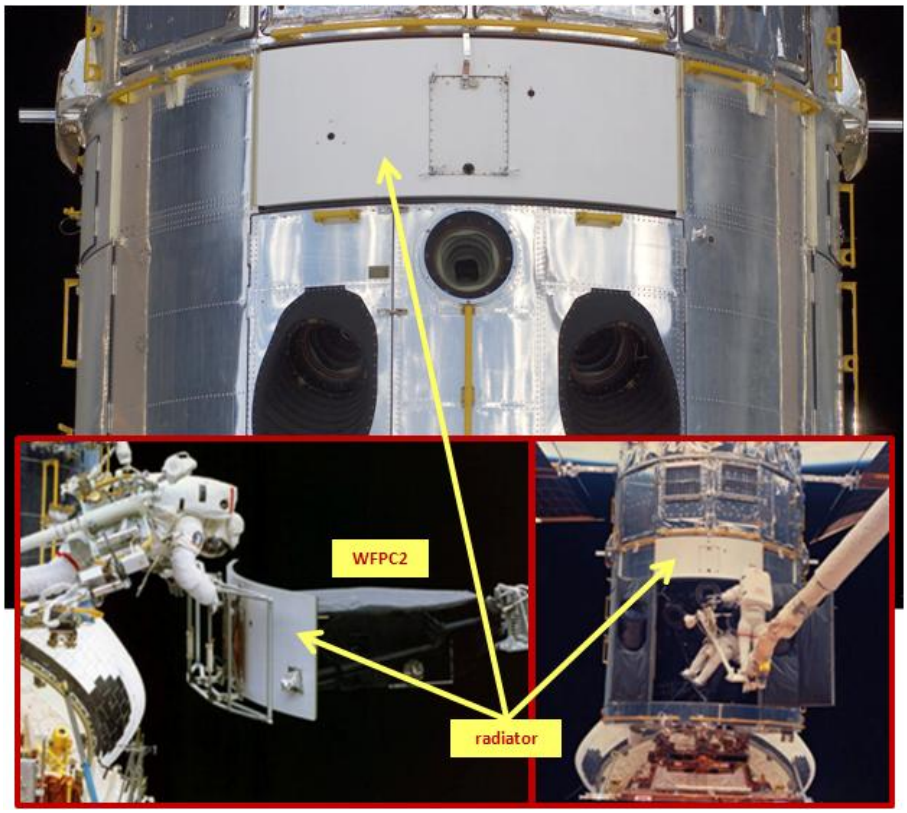


*Figure 1.– Photos from the first HST Servicing Mission in 1993. The surface of the radiator was rather smooth. The square panel in the middle was the electronic radiator.*

The NASA Orbital Debris Program Office led the MMOD impact inspection of the WFPC2 radiator. In addition, the effort was supported by the HST Program Office at NASA/GSFC, the NASA Curation Office in ARES, the Hypervelocity Impact Technology Group in ARES, and the NASA Meteoroid Environment Office at MSFC. The objective of the inspection was to document the impact damage on the radiator surface, and then use the data to improve the near-Earth MMOD environment definition. To prepare for the MMOD impact inspection of the WFPC2 radiator, two major instruments were acquired by the team—a LAP CAD-Pro laser template projector and a VHX-600 digital microscope. The former was programmed to project, from about 3 meters away, pre-distorted, red 10 x 10 cm square grid patterns on the curved radiator surface to provide reference coordinates for the identified features. The resolution of the grids is 1 cm × 1 cm. The location of any impact feature within each grid was estimated down to millimeter accuracy. The VHX digital microscope is capable of optical magnifications of up to 5000X, though 200X was the usual survey magnification employed. It was used to record two-dimensional digital images of selected features and, via a series of progressing images, provided three-dimensional profiles and depth measurements of the impact craters.

After the post-flight de-integration at NASA/KSC, the WFPC2 package was shipped to NASA/GSFC in Maryland and placed inside a class 10,000 clean room, where a 6-week MMOD inspection took place between July and September of 2009. The focus of the inspection was to identify MMOD particles large enough to be a safety concern to robotic and human space missions, i.e., particles larger than 100 µm in diameter. Since the damage area caused by the impact of a 100 µm MMOD particle is likely to be at least 300 µm across, a decision was made to limit the inspection to features 300 µm and larger. By the end of the inspection, a total of 677 MMOD impact features were identified and documented. Figure 2 shows the setup during the inspection and two sample crater images. The largest crater identified on the radiator surface has a crater diameter of 1.6 mm with a surrounding spall zone about 1.4 cm across (on the painted radiator surface). An additional 200 or so non-impact features, such as surface contamination and tool marks, were also noticed and recorded during the inspection.

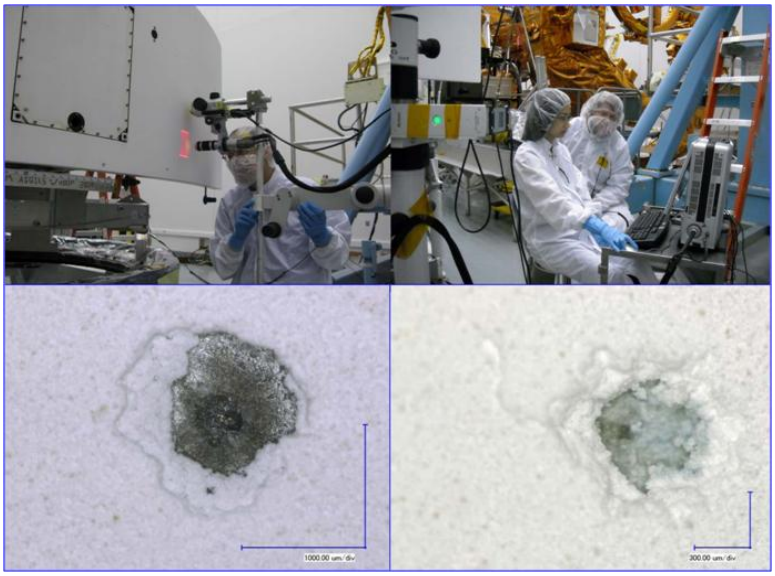

*Figure 2.– (Top) The MMOD inspection was conducted in a clean room at NASA/GSFCA. Note the red laser 10 x 10 cm reference grid projected upon the radiator's surface. (Bottom) Two MMOD impact craters documented during the inspection. At left is one of the largest impacts observed. At right is a more typical crater resident in the 100-200 micrometer-thick (measured) YB-71 paint layer.*

Figure 3 shows the distribution of the 677 identified impact craters on the surface of the radiator. The craters can be separated into three categories. Large circles indicate the locations of the 45 largest features, which are visible to the naked eye at a distance of about 2 meters from the radiator; small circles indicate the locations of smaller impacts that penetrated the paint coating and reached the aluminum layer of the radiator; and crosses indicate the locations of impacts that did not penetrate the paint. The overall distribution of the craters appears to be uniform, although the distribution of the largest 45 craters is biased toward one side of the surface.

In order to convert the observed feature dimensions to the characteristics of the impacting particles and to estimate the impact conditions, a series of hypervelocity impact tests were conducted at JSC's White Sands Test facility in 2010. The targets were made of materials identical to the WFPC2 radiator. Projectiles of different sizes and different materials were selected. At the end of the test series, a total of 50 successful shots on radiator analogue targets were completed. The shots covered impact speeds between 2.7 and 8.2 km/sec, and impact angles between 0° (normal impact) and 70°. The inspections of the test coupons are currently underway. Once the damage equations are established, the WFPC2 crater data will be combined with the time-attitude history of the WFPC2 to model the MMOD environment at the HST altitude.

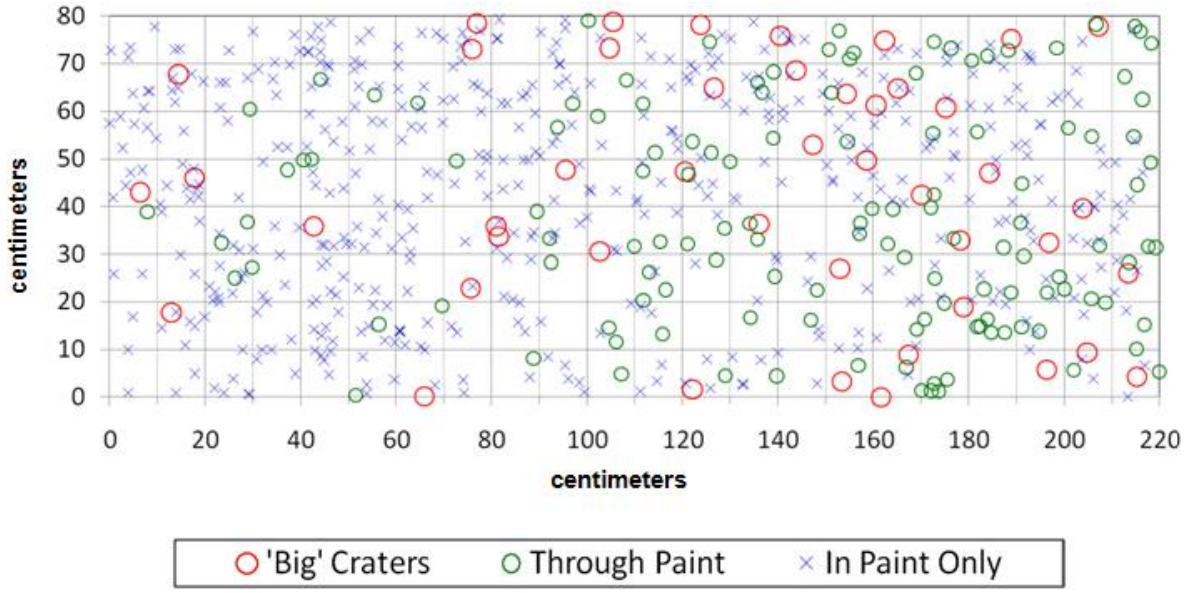


*Figure 3.– Distribution of the 677 MMOD impact craters on the radiator surface. The overall distribution of the craters appears to be random. However, there are more "big craters" on the right side of the radiator than on the left side. The ratio is about 2:1.*

# *Habitat Particle Impact Monitoring System*

*J.-C. Liou, John Opiela*

JSC's Habitat Demonstration Unit (HDU) is a large-scale test bed designed for the testing and demonstration of technologies, processes, and operations that will be needed to support future human exploration missions to the International Space Station, near-Earth asteroids, the Moon, or Mars. The 2010 configuration of the HDU included a Pressurized Excursion Module (PEM, approximately 6 m in diameter and 4 m in height) and an airlock (see figure 1). A multi-layer inflatable loft is planned to be installed on top of the PEM in late 2011. The construction of the HDU was completed at JSC in the summer of 2010. After a brief dry run at a JSC rockyard facility, the HDU was shipped to the SP Mountain, approximately 40 miles north of Flagstaff, Arizona, and participated in a very successful NASA Desert Research and Technology Studies (D-RATS) campaign for 3 weeks in late August.


*Figure 1.– The HDU in front of the SP Mountain. The large module in the center is the PEM and the smaller structure to the left is the airlock.*

A key requirement to improve the safety of long-term habitat operations is the capability to monitor potentially damaging particle impacts on the structure. Sources of the impacting particles include orbital debris and micrometeoroids in the near Earth environment, micrometeoroids and lunar secondary ejecta on the surface of the Moon, and micrometeoroids in interplanetary space. NASA's Orbital Debris Program Office at JSC initiated an effort, with collaboration from the Naval Research Lab and Virginia Polytechnic Institute and State University, to develop the Habitat particle Impact Monitoring System (HIMS) for HDU in April 2009. Twelve space-qualified acoustic impact sensors were installed at four different locations and three layers on the wall of Section D of the PEM. The four locations are indicated by the red circles in the left portion of figure 2. The wall of the PEM consists of a fiberglass hard shell with a thickness of about 1 cm and an exterior layer of 10-cm-thick foam insulation. Sensors were attached both to the inside and outside of the PEM, and between the fiberglass shell and foam insulation (right portion of figure 2). The objective of the project in 2009-2010 was to demonstrate the HIMS capability of detecting particle impact location and the degree of impact penetration. The former is achieved by triangulation analysis using signals received by sensors at different locations. The latter is achieved by analyzing signal strength from sensors located at different layers.

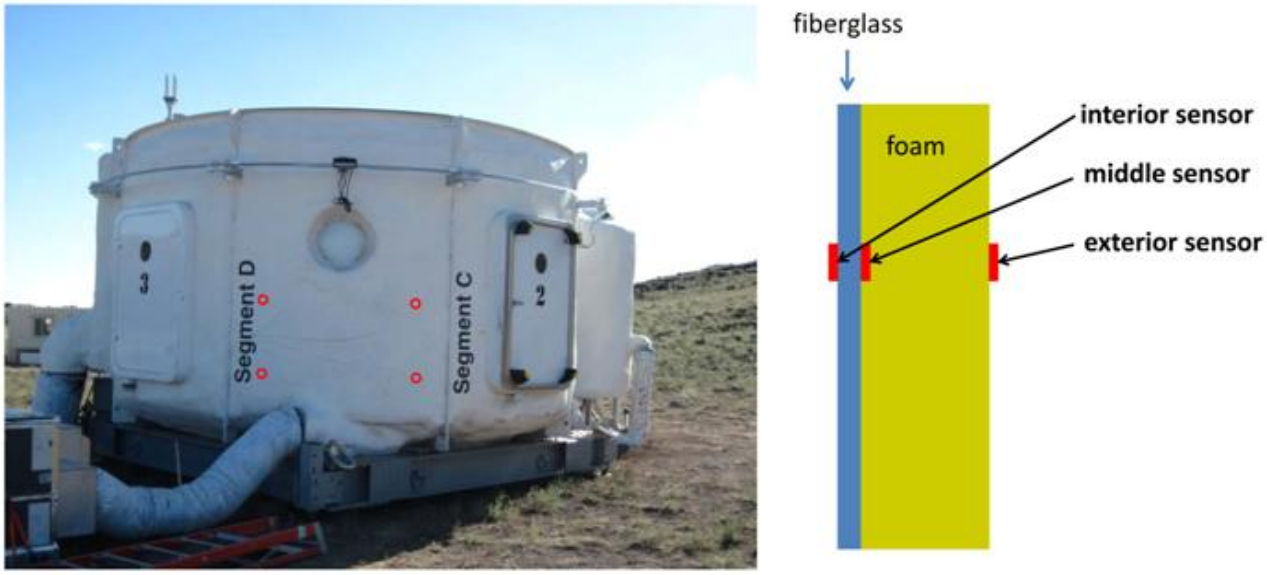


*Figure 2.– Left, the red circles indicate the locations of the sensors. Right, an illustration of the cross-section of the PEM wall structure.*

The space-qualified HIMS sensors have been tested on different materials (aluminum plate, Kevlar, multi-layer insulation, etc.) subjected to hypervelocity impacts up to 7 km/sec. For demonstration purposes during the D-RATS campaign, however, hypervelocity impacts on the HDU were not possible. Instead, a 10-pump air rifle was used to simulate particle impacts. The degree of projectile penetration was controlled by varying the number of pumps of the air rifle. The speed of the projectile was also measured using a ballistic chronometer. It ranged from about 30 m/sec for 1 pump to 150 m/sec for 10 pumps. The transition from partial to full penetration through the foam insulation of the structure occurred around 130 m/sec.

The HIMS team members conducted a very successful impact test series during the 2010 D-RATS campaign. A total of 113 air rifle shots and more than 20 hours of the HDU background acoustics data were collected. Team members analyzed the data to optimize the HIMS system parameters and developed a triangulation algorithm to identify each impact location. Key objectives for the project in 2010-2011 were to develop a three-dimensional graphical console to display impact time/location/penetration information in real time, to develop an impact response procedure for crew members in preparation for the integrated 2011 D-RATS campaign, and to fully-integrate the HIMS hardware and software into the existing infrastructure of the PEM. The aim for the 2011 D-RATS campaign will be to test the end-to-end detection capability of the system (figure 3), and to demonstrate the potential applications of this low-cost, low-mass, low-power-consumption, and easy-to-install HIMS system to other habitat structures, such as a multi-layer inflatable, for future mission opportunities.


*Figure 3.– The goal of the HIMS project is to demonstrate the fully automated end-to-end capability, from simulated particle impacts to crew response based on processed impact information, during the 2011 D-RATS campaign.*

## *Shielding Against Micrometeroid and Orbital Debris Impact With Metallic Foams*

*Shannon Ryan, Eric Christiansen, Dana Lear*

For the past 50 years the protection of manned spacecraft against micrometeoroids and orbital debris (MMOD) has, for the most part, been performed by the Whipple shield or derivatives thereof. Although highly capable, the installation of Whipple-based shielding configurations requires a significant amount of non-ballistic mass for installation (e.g. stiffeners, fasteners, etc), that can consume up to 35% of the total shielding mass. As NASA's vehicle design focus shifts from large pressurized modules operating for extended durations in relatively debris polluted low earth orbits to small volume, lower duration craft, new protective concepts are being designed and evaluated to address the new threats.

One possible solution involves the utilization of structural components that have intrinsic shielding capability. Traditional primary structures such as honeycomb sandwich panels are unsuited for use in

manned vehicles due to their poor shielding performance. Metallic foams, however, are a relatively new material with low density and novel physical, thermal, electrical, and acoustic properties that offer a promising alternative for MMOD protective systems. There are two competing types of metallic foam: open cell and closed cell. Although closed cell foams are capable of retaining some residual atmosphere, which may aid in the deceleration of penetrating fragments via drag, open cell foams are considered the more promising technology due to their lower weight and higher degree of homogeneity. Preliminary investigations have demonstrated the potential of open cell foam core structures, as shown in figure 1, compared to a traditional honeycomb core sandwich structure.

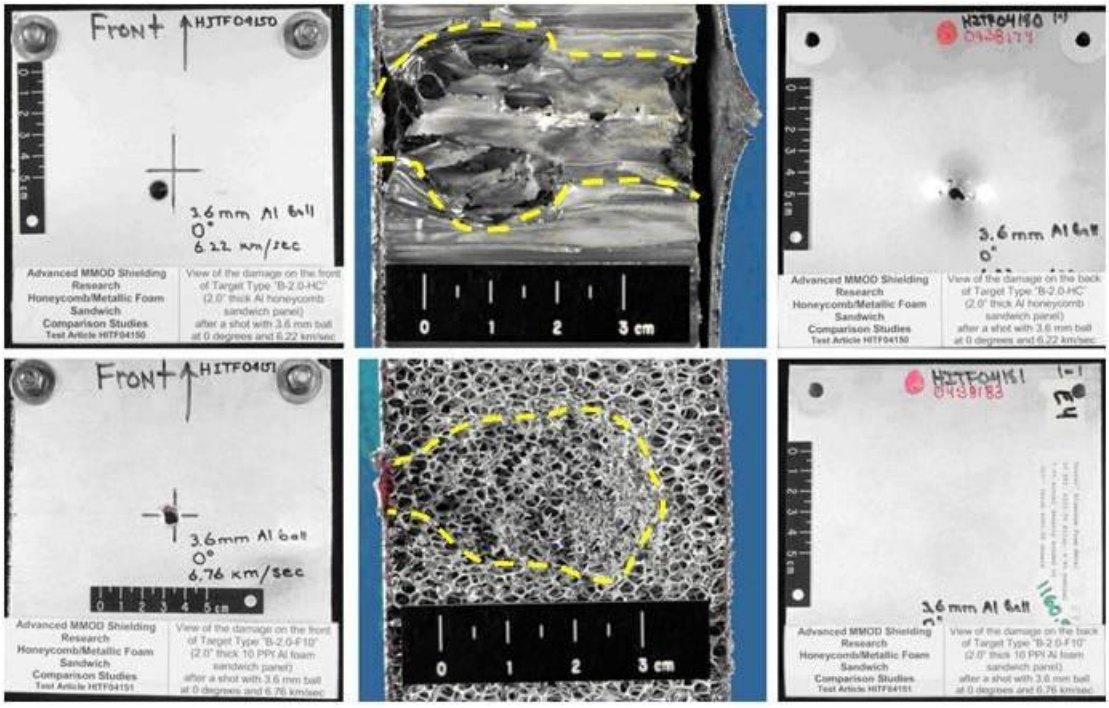


*Figure 1.– Comparison of damages in a honeycomb core (top) and open-cell foam core (bottom) sandwich panel impacted by 3.6 mm diameter aluminum spheres at 6.22 km/s (honeycomb) and 6.76 km/s (foam) with normal incidence (0°). From left to right: bumper (front view), core cross-section (emphasis added), rear wall (rear view).*

Three experimental investigations have recently been performed by the JSC's Hypervelocity Impact Technology Facility (HITF) to comprehensively evaluate the performance of open-cell foams during hypervelocity impact: a fundamental study to investigate penetration and failure mechanisms in open-cell metallic foam structures; an application study evaluating the performance effect of modifying International Space Station (ISS)-representative shields with open cell metallic foams, and; a study comparing the performance of open cell foams of varying materials with alternate MMOD shielding materials and structures.

**Hypervelocity Impact Performance of Open-Cell Foams**

An advantageous property of open cell metallic foams, in terms of MMOD shielding, is their periodic structure of small diameter, low mass pores. During a hypervelocity impact event, the

isentropic shock and non-isentropic release process acts to raise the thermal state (internal energy) of the impacting particle. As a projectile penetrates through an open cell foam structure, repeated impacts upon individual foam cell ligaments induce multiple shock and release events, resulting in the fragmentation, melt, and vaporization of meteoroid or debris particles at impact velocities significantly lower than with traditional shields. The multi-shock shield utilized a similar concept, demonstrating potential weight savings of 30-40% over traditional Whipple shields for equal levels of protection. Although enhanced fragmentation and melting was clearly observed in experiments on foam core sandwich panels, rear facesheet failure was almost exclusively caused by the penetration of individual solid (or molten) fragments, even at impact velocities above 7 km/s. Given the non-homogeneity of the foam structure on a micro scale, it is considered that these individual fragments have propagated through the foam core with minimal secondary impacts. Subsequently, the degree of experimental scatter for these structure types may be greater than that of traditional configurations.

The number and size of foam ligaments is a function of material pore density (i.e. PPI or pores per linear inch), which is specified in the manufacturing process. Additionally, the relative density of the foam (also adjustable during manufacturing) controls both the panel weight and the cross-sectional form of the foam ligaments (figure 2). It was found that increased pore density led to minor improvements in protective capability, for instance 40 PPI foam core sandwich panels were found to be ~5% more capable than 10 PPI configurations. The effect of ligament shape was found to be minimal, with 3-5% (nominal) relative density cores providing equal levels of protection as heavier 6-8% (nominal) panels.

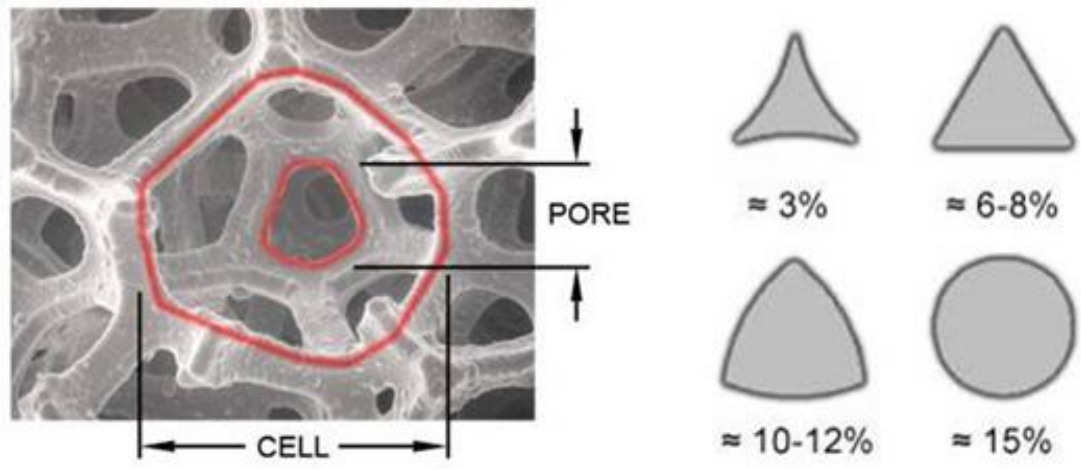


*Figure 2.– Foam pore size, cell size, and ligament cross-section (variation with relative density) ©ERG Aerospace*

**Improved Shielding Performance Through Utilization of Metallic Foam**

Metallic open cell foams provide comparable mechanical and thermal performance to honeycomb structures, without the MMOD shielding detrimental through-thickness channeling cells. A double-layer honeycomb sandwich panel shield, with a mesh outer layer and monolithic aluminum rear wall

was modified to include aluminum open cell foam, and thus evaluate the effect on shielding performance. The aluminum honeycomb core of the outer sandwich panel was replaced with 10 PPI foam, while the 2nd honeycomb sandwich panel was replaced with an equal thickness foam panel (no facesheets), maintaining approximate totals for shield standoff and weight. The foam modified shield was found to provide a 3-15% increase in critical diameter for impacts normal to the target surface (0°). For oblique impacts, the performance gain was more substantial, particularly at low velocities. A comparison of impact damages induced by 0.833 cm diameter Al2017-T4 (aluminum) spheres at ~6.9 km/s with normal incidence is shown in figure 3. In addition to reduced rear wall damage, clear evidence of enhanced fragment melting is visible on the foam-modified target.

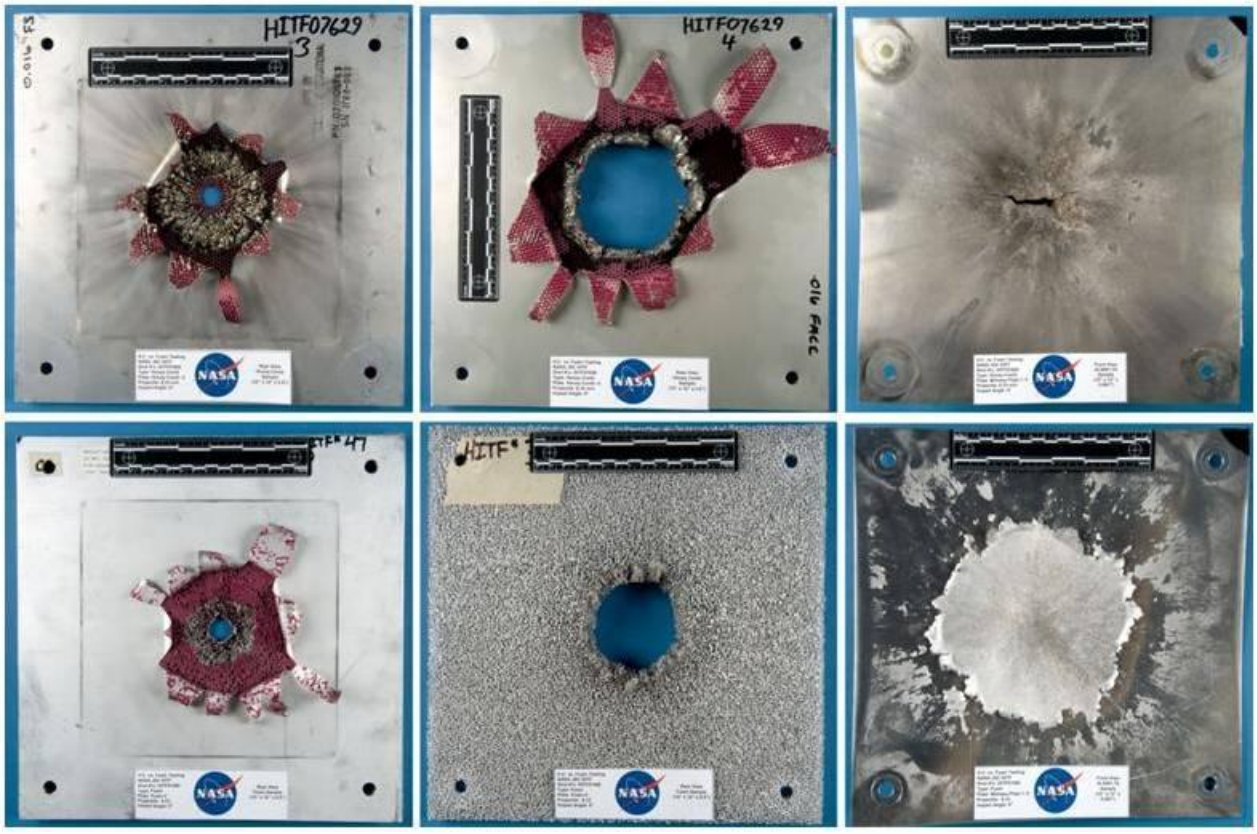


*Figure 3.– Comparison of impact damages induced by impact of 0.833 cm diameter Al-spheres at approx. 6.9 km/s (0°) on the double layer honeycomb (top) and foam (bottom) targets. From left to right: outer sandwich panel (rear view), 2nd panel (rear view), rear wall (front view).*

**Evaluation of Advanced Shielding Materials and Structures**

The performance of aluminum, titanium, copper, stainless steel, nickel, nickel/chromium, reticulated vitreous carbon (RVC), silver, and ceramic open-cell foams was evaluated in an extensive experimental impact campaign. Configured in single-, double-, and triple-bumper shields, their protective capability was assessed against metal plates, meshes, and various flexible fabrics via a figure of merit based on cratering and impulsive failure modes. Further ballistic limit-based evaluations were performed, in which the advanced shield configurations were compared against

equivalent weight all-aluminum shields. The top performing configurations were found to generally include monolithic aluminum outer bumper plates, with metallic foam and/or Kevlar fabric inner bumper plates. Of the various foam types investigated, copper was found to provide the best protection, with RVC the worst.

The generation of ejecta during MMOD impact on a shield outer bumper is of concern due to the danger of secondary impacts, and the general pollution of the orbital environment. For impact on common shielding materials (i.e. aluminum, carbon-fiber reinforced plastic), ejecta can constitute up to 30% of the total expelled mass (ejecta + fragment cloud). Impact on foams, meshes, and fabrics was found to generate almost no ejecta of any significance, providing a substantial reduction in ejecta mass over monolithic structures (figure 4).

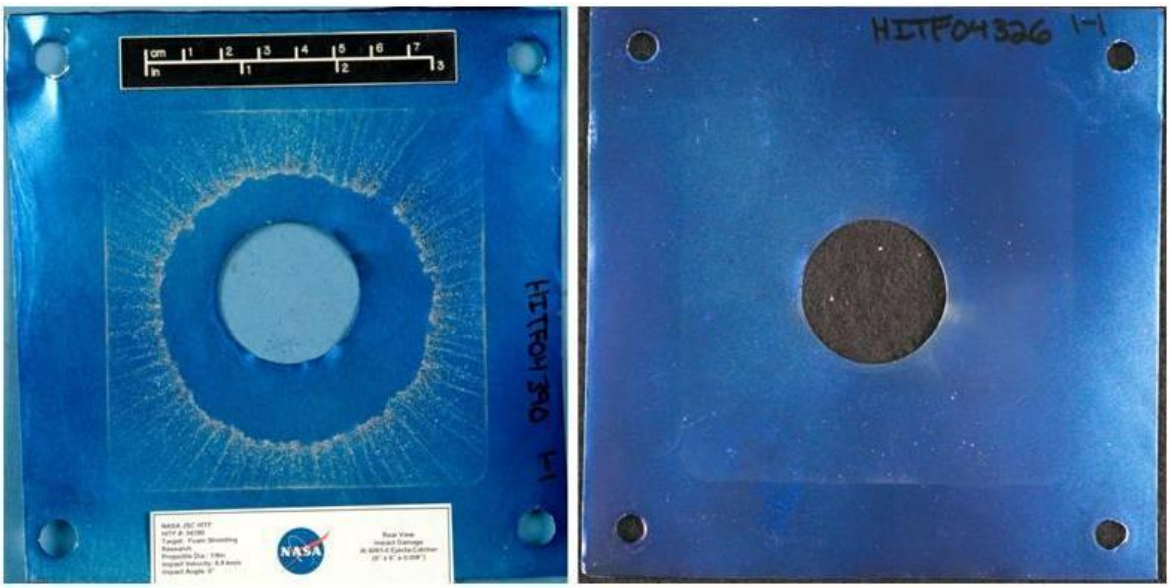


*Figure 4.– Comparison of ejecta plate damages following impact of 0.3175 cm diameter aluminum spheres on a monolithic aluminum outer bumper (left) and stainless steel foam outer bumper (right) at hypervelocity (approximately 6.8 km/s).*

## *Shuttle Radiator Protection Helps Prevent Mission Loss from MMOD*

*Eric Christiansen, Dana Lear, Eugene Stansbery*

NASA's Hypervelocity Impact Technology (HVIT) team, located at Johnson Space Center, routinely inspects the Space Shuttle vehicle after each mission for micrometeoroid and orbital debris (MMOD) damage. During the post-flight inspection after the STS-128 flight of the Space Shuttle Discovery, 14 MMOD impacts on the crew cabin windows, 16 impacts on the wing leading edge and nose cap, and 21 impacts on the payload bay cooling radiators were found. Of these, one is perhaps the most important because it highlights a success story over 10 years in the making (see figure 1).

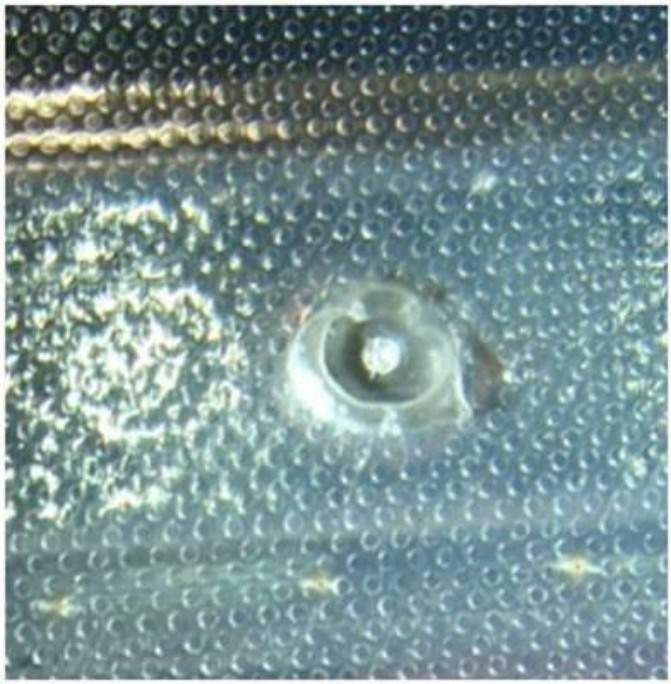

*Figure 1.– Impact crater on the radiator located on the interior of the Shuttle payload bay doors. The impact was on an aluminum "doubler" directly over the tube carrying Freon coolant used to cool electronic equipment and avionics in the Shuttle.*

Although not the largest damage found on the radiators, the impact crater was strategically placed directly over one of the cooling tubes bonded to the back side of the radiator face sheet. The impact crater is important because, if not for decisions to "harden" the Space Shuttle fleet to the increasing orbital debris environment in the late 1990s, the impact would have breached the Freon cooling loop and by flight rule, would have resulted in a leak rate high enough to result in an early mission termination (i.e., loss-of-mission).

The Space Shuttle was designed in the 1970s, before the risk from human-made orbital debris was widely recognized. The Shuttle was originally designed with requirements for protection against only the micro-meteoroid environment. Almost immediately, damage from orbital debris started showing up. The first significant impact was a 0.2-mm paint chip that damaged a window during the STS-7 mission and required the window to be replaced prior to re-flight.

In the early 1990s, NASA applied the BUMPER code to predict the risk of damage to different surfaces of the spacecraft given their orbit, orientation, and the MMOD environment. Analysis showed that the Shuttle risk was highly dependent on its flight attitude or orientation. The highest vulnerability to loss-of-mission was penetration of the cooling loop bonded to the inside surface of the radiator face sheet (see figure 2a).

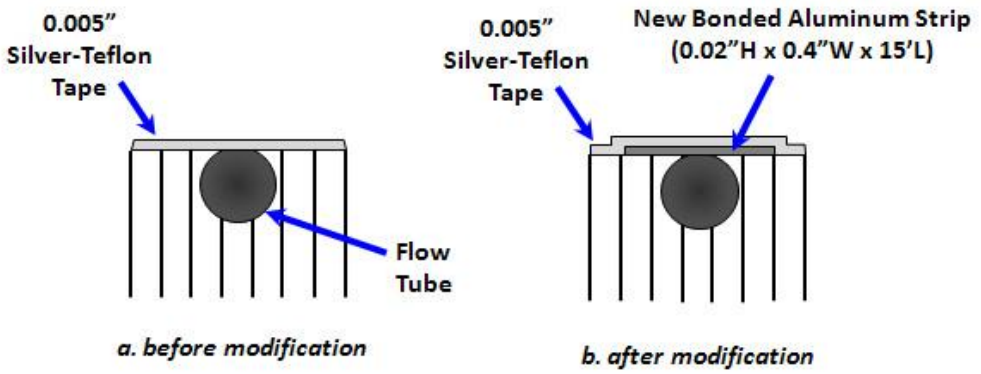


*Figure 2.– The Shuttle radiators are curved panels on the inside of the payload bay doors that are exposed to space when the doors are open. The panels are a honeycomb structure sandwiched between a face sheet and a back sheet with a total thickness of either 12.7 or 22.9 mm. Aluminum tubes are bonded to the backside of the 0.28- mm thick face sheet at intervals. This figure shows a cross section of the honeycomb radiator showing the configuration before and after the addition of the 0.5-mm aluminum "doubler."*

During this time, the on-orbit heat rejection system in the Shuttle vehicle consisted of two Freon coolant loops routed through the radiator panels attached to the payload bay doors and accumulator tanks. There was no provision for isolating a leak in the system. Puncture of a tube by MMOD would totally deplete the coolant in one of the two loops, necessitating that approximately half of the heat sources (such as avionics in the crew cabin) be switched off. Flight rules under this situation required a next primary landing site (PLS) abort, i.e., that the Shuttle mission be aborted immediately and preparations made to land at the next available primary landing site. Because coolant is lost quickly from the pumped flow system in the event of a leak, some of the avionics would be turned off during reentry and landing, decreasing the ability to recover from some other anomaly that could occur during this critical mission phase (due to loss of redundancy in the avionics systems).

The BUMPER predictions were put to the test during the first flight of the U.S. Microgravity Laboratory (USML-1) during STS-50. One of the experiments required that the Shuttle fly nose up, payload bay into the velocity vector for 10 days of the 14-day mission. After much discussion with Shuttle managers and impact tests on various spacecraft components that were contained in the payload bay of the Orbiter, it was decided to fly the mission as planned. Fortunately, no MMOD impact breached the Freon cooling loop. However, post-flight inspection of the radiators showed that the number of impact features closely matched the pre-flight BUMPER predictions and were much higher than typical for Shuttle missions flown with the payload bay facing Earth.

After STS-50, new flight rules were implemented that required the Shuttle to fly with the payload bay to the Earth and the tail towards the velocity vector "unless payload or orbiter requirements dictate otherwise." This procedure worked well while the Shuttle flew independently. Flights to the Russian space station Mir and later to the International Space Station (ISS), once again exposed the cooling loops to higher risk of MMOD impact for long periods while docked.

In 1997, modifications were approved by the Space Shuttle Program to "harden" the Orbiters from the increasing orbital debris environment. Three of these modifications involved the Freon cooling system, two of which would prove critical for STS-128. First, an extra layer of 0.5-mm thick aluminum (aluminum doubler) was bonded to the radiator face sheet directly over the cooling tubes (see figure 2b). Automatic isolation valves were added to each coolant loop that could isolate a leak in a radiator panel from the rest of the Freon system (accumulator and pumps) so that sufficient Freon remained to activate the cooling system for all electronics during reentry, when heat is rejected to the flash evaporator system. If sufficient coolant is saved, the need for a next PLS abort is alleviated. The modifications were incorporated into the Shuttle fleet during routine maintenance between 1998 and 1999. These modifications, made 11 years prior to the STS-128 mission, saved the mission from early termination.

During the STS-128 mission, an orbital debris particle impacted the aluminum doubler directly above the Freon tube. Simulations show that had the doubler not been in place, the Freon tube would have been breached (figure 3). Without the second modification isolating the leak to the radiator panels, all of the Freon (which is under pressure) would have leaked from the system, requiring the Shuttle to land within 24 hours and with reduced avionics.

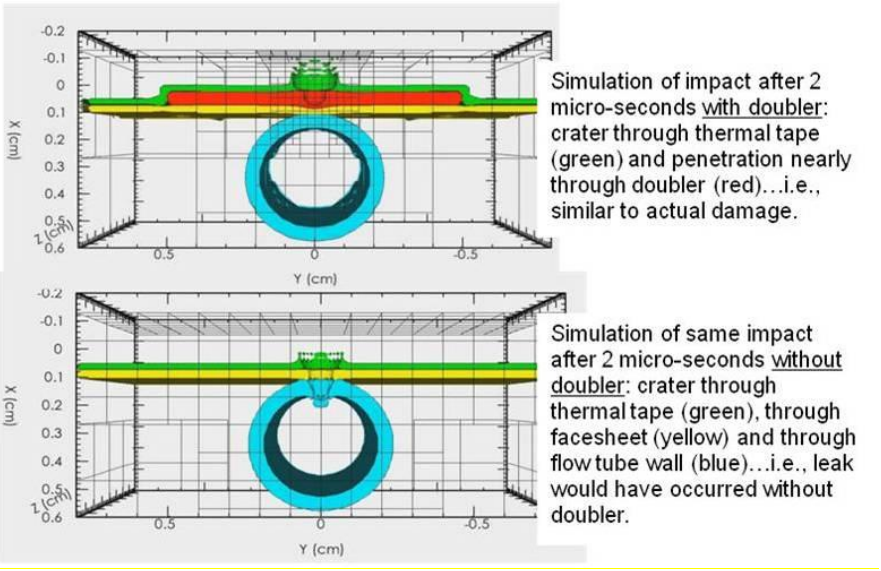


*Figure 3.– Hydrocode simulation of the impact with and without the aluminum "doubler." Without the doubler, the Freon cooling loop would have been breached.*

This success story is a tribute to the entire NASA Hypervelocity Impact Technology, Orbital Debris and Space Shuttle management team. The Orbital Debris Program Office created the debris environment flux models that were based on solid science and measurement data. The Hypervelocity Impact Technology (HVIT) team applied the *Bumper* code, which demonstrated the vulnerability of the Freon cooling system and its impact to overall mission risk, as well as evaluating risk mitigation techniques, such as the addition of aluminum doublers (which was eventually selected). Then, the Space Shuttle Program Management made critical decisions in tight economic conditions to enhance

the safety to the Orbiters from the MMOD threat. A decade later, their hard work and tough decisions paid off.

## *ISS Solar Array Guide Wire MMOD Damage*

*Daniel Kent Ross, Eric Christiansen, Dana Lear*

During the STS-120 mission in 2007, astronauts moved the Port 6 (P6) solar photovoltaic power module from its original location on the Z1 truss, where it generated power for almost 7 years, to its permanent location on the port outboard truss of the International Space Station (ISS). P6 contains two solar array wings (SAWs), referred to as SAW 2B and SAW 4B. The P6 transfer operation consisted of first retracting each SAW, then moving the P6 module from Z1 and reinstalling it at its permanent location, and finally the solar array wings had to be redeployed to generate power. During the SAW 4B deployment operation, the solar array began to tear in two places and deployment was halted at about 90% deployment. The STS-120 crew and ground determined that a guidewire had frayed and snagged on a grommet, causing tears in the solar array that measured one foot and almost three feet (figure 1). During extravehicular activity (EVA) #4, astronaut Scott Parazynski cut the snagged wire from the 4B SAW. The EVA crew also installed reinforcing straps and fully extended the solar array. The piece of guidewire that was removed was returned to the ground for analysis.

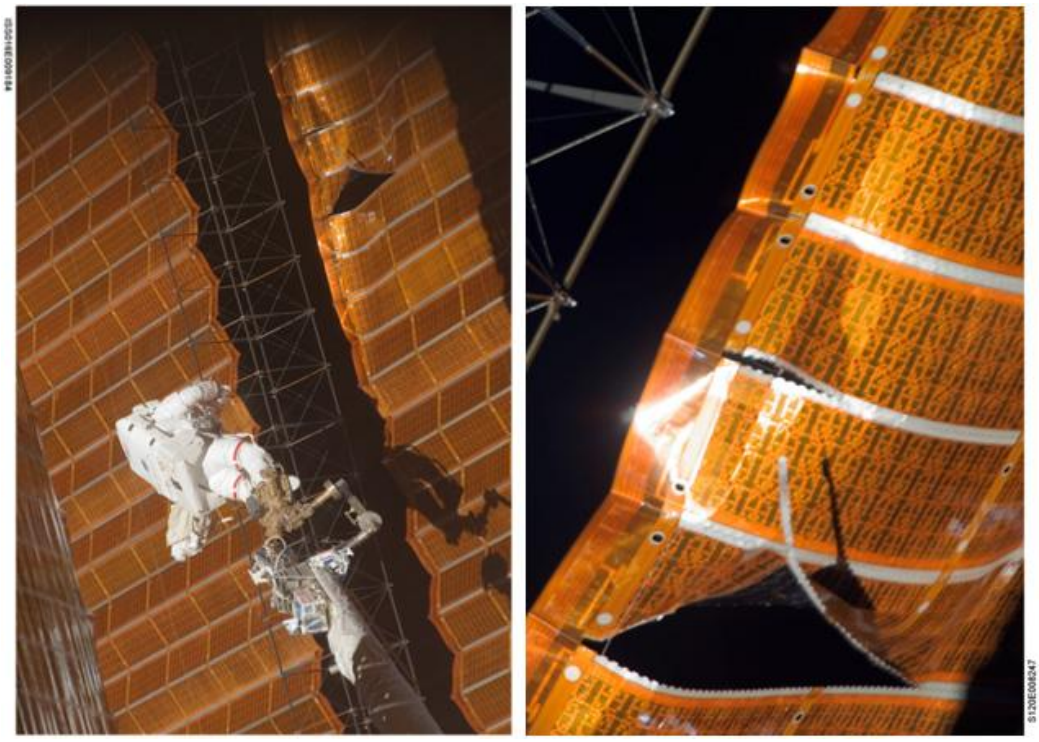

*Figure 1.– Tears in ISS P6 solar array wing 4B after attempt at re-deployment during STS-120 mission.*

The frayed end of the guidewire was examined by scanning electron microscopes (SEM) at JSC's Astromaterials Research and Exploration Science (ARES) Directorate by personnel of the Hypervelocity Impact Technology (HVIT) Team. There were 7 individual wires that had been broken at the frayed end (figures 2 and 3). On three of these wires, the SEM examination found a large amount of material that appeared to have been melted at one time near the broken ends of these wires (figures 4 through 6).

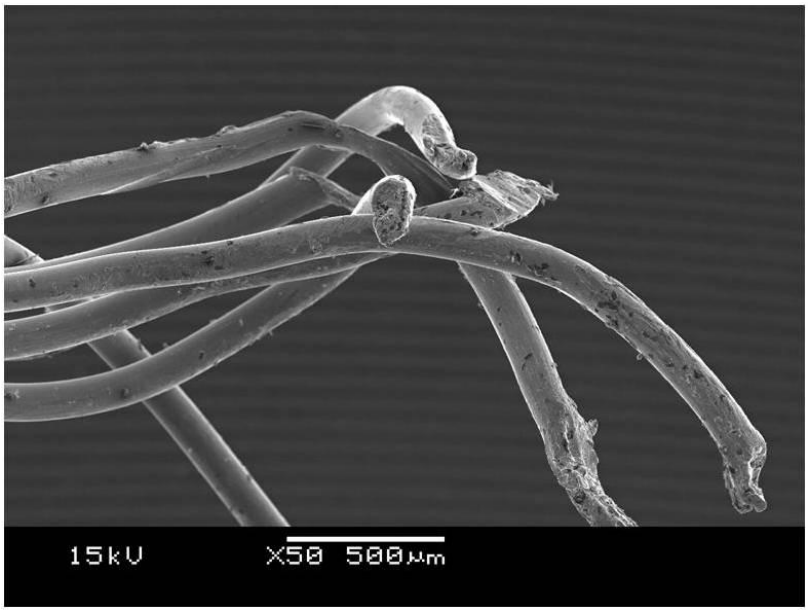


*Figure 2.– Frayed end of 4B SAW guidewire. Wires at bottom and in lower right-hand corner exhibited melt near ends.*


*Figure 3.– Three wires exhibiting melt.*

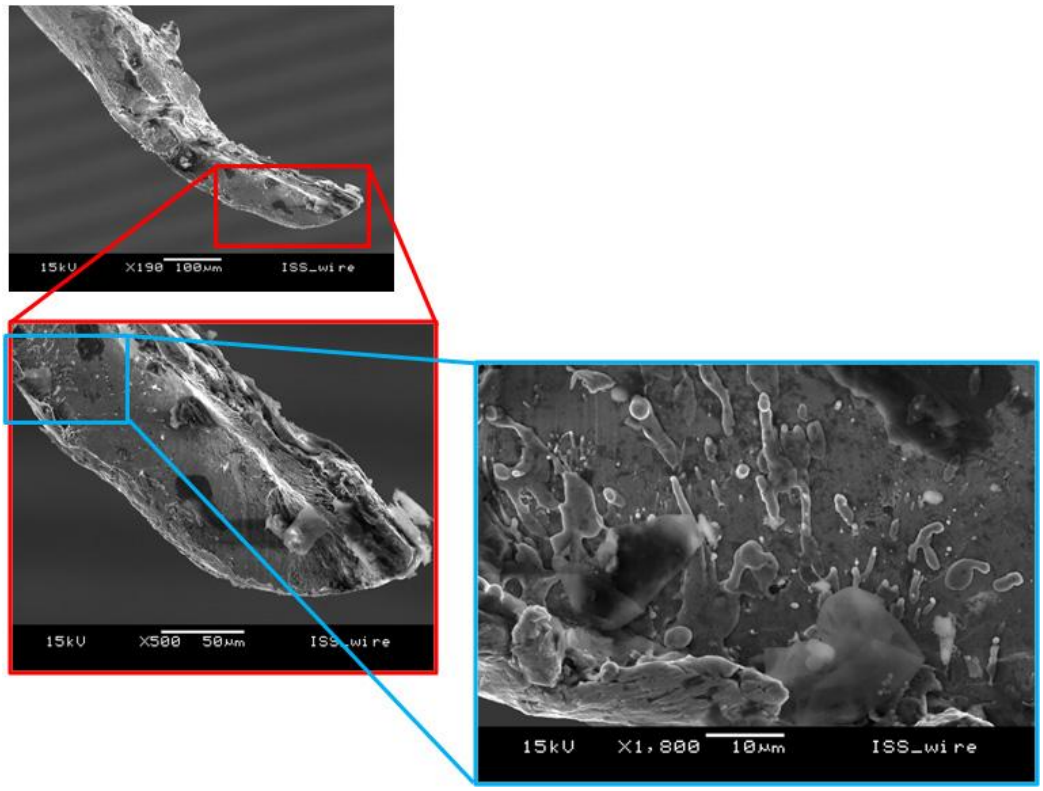


*Figure 4.– Evidence of melting.*

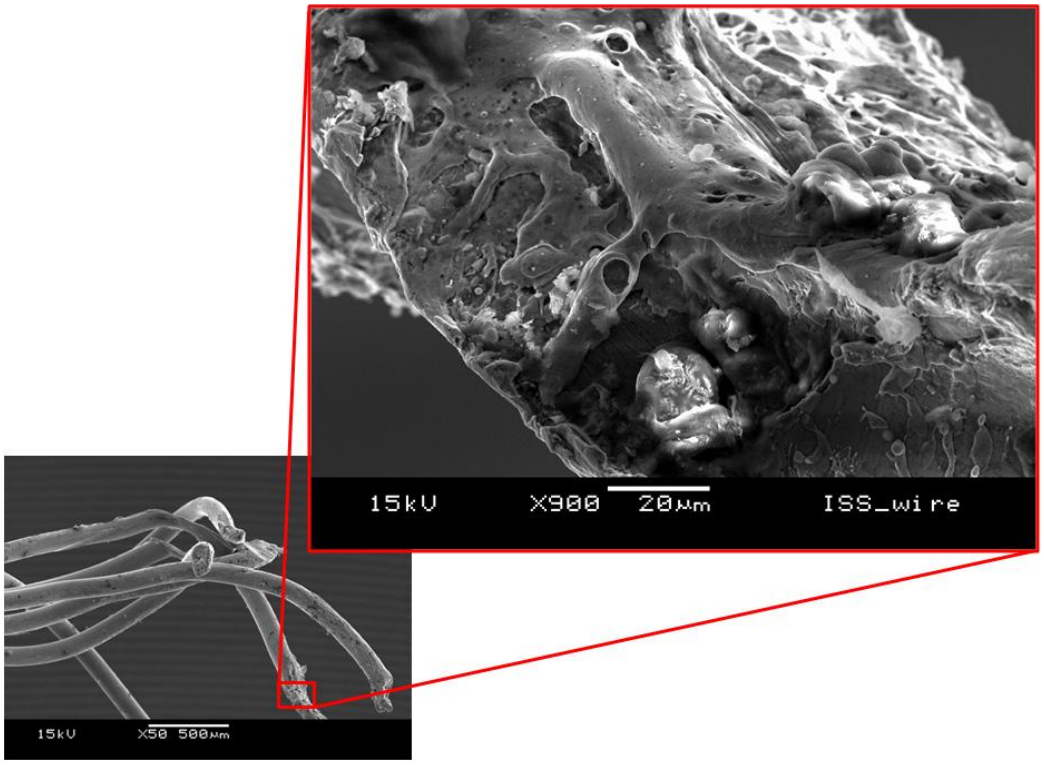


*Figure 5.– Additional evidence of melting.*

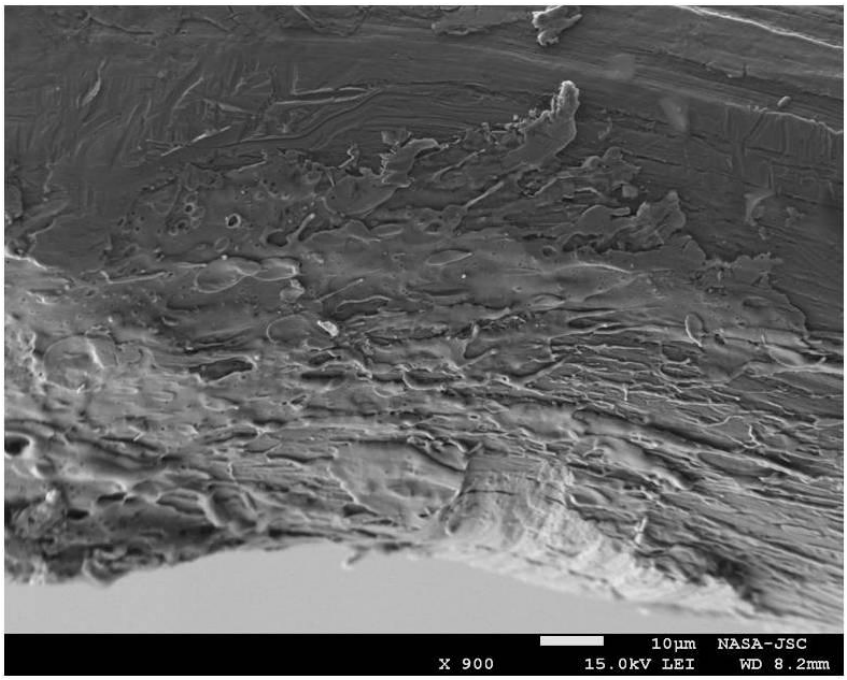


*Figure 6.– More evidence of melting.*

Micrometeoroid and orbital debris (MMOD) particles typically impact at high speed and release a large amount of energy, resulting in the displacement of target material with a mass 10 to 100 times the projectile mass due to melting and plastic flow local to the impact site. The presence of melt is a clear indication that the damage to these three wires was caused by MMOD impact. Other wires in the bundle appear to have been broken by mechanical action. A likely scenario that explains the observed damage to the guidewire is that MMOD impact damaged and broke a few of the wires, which allowed the guidewire to snag in a SAW grommet during deployment. Subsequently, as the process of deployment continued with a snagged guidewire, additional wires in the guidewire were sheared as they were pulled against the grommet.

An effort was made to identify the source of the impact damage. The SEM is equipped with a narrow focus electron microprobe and energy dispersive X-ray spectrometer to detect elemental composition of materials found in the impact zone. Several foreign particles with composition differing from the stainless steel wire material were detected in the area of the wires that had considerable melt. The composition of these particles suggests the possibility that an orbital debris impact was responsible for breaking wires within the guidewire bundle. Bismuth metal, gold-copper-sulfur, gold-silver-copper, lanthanum-cerium, antimony-sulfur and tungsten-sulfur bearing particles were identified (figures 7 through 9). No evidence of micrometeoroid impact was identified. The wire is composed of FeCrNi-rich stainless steel, and these elements are present in all spectra. Also, carbon-rich particles are abundant on all of the wires, likely from the plastic bag containing the sample (i.e., contamination).

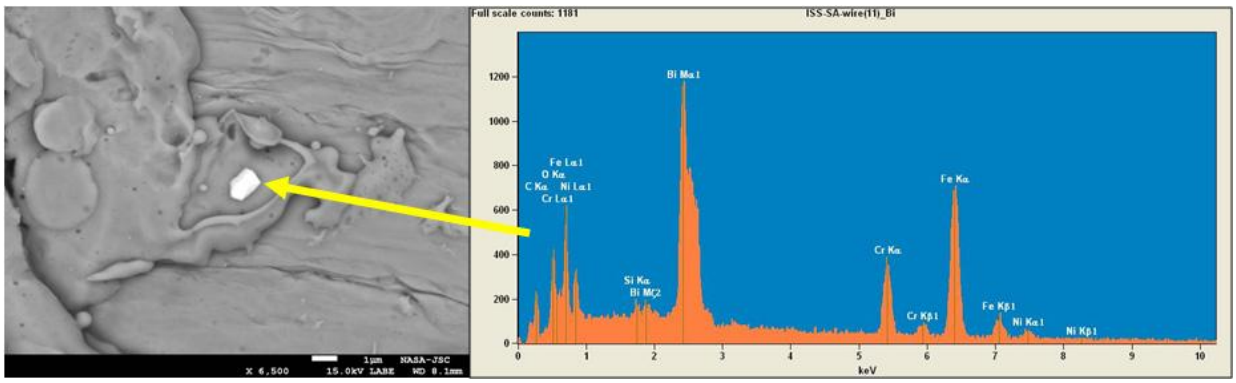


*Figure 7.– Bismuth-rich particle on melted zone on steel wire. Fe, Cr and Ni peaks are from underlying wire.*

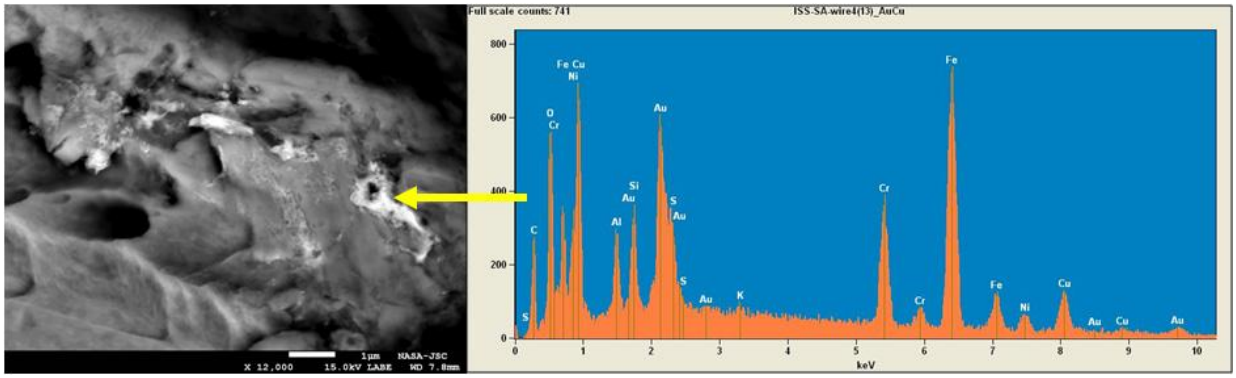


*Figure 8.– Gold-rich particles.*

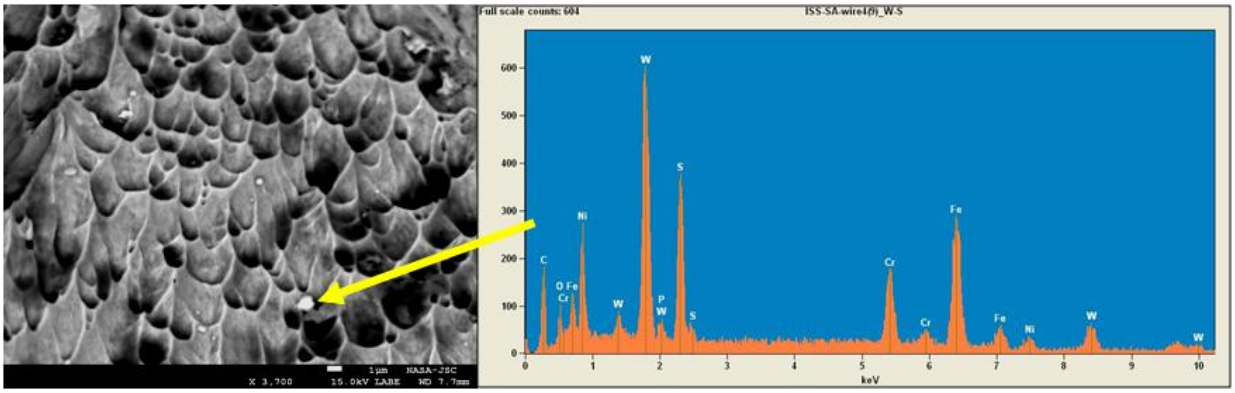


*Figure 9.– Tungsten-sulfur particle on damaged steel wire.*

# *Crew Earth Observations—Earth's Dynamic Events and Twitpics*

*Justin Wilkinson, Sue Runco, Kim Willis, William L. Stefanov, Mike Trenchard*

Almost every week images of some "dynamic event" are requested from orbiting International Space Station (ISS) crews. Dynamic events include hurricanes, floods, tsunami damage, volcanic eruptions and forest/bush fires. When immediacy is important, NASA can get an image from the astronaut camera to a public website in less than 24 hours. Dynamic and other images are made available on the Crew Earth Observations (CEO) website, http://eol.jsc.nasa.gov/ which is known as the Gateway to Astronaut Photography of Earth.

Other "tools" for quick viewing of dynamic events from orbit include the use of social media in the form of the first Twitter feeds from ISS and the installation of the cupola on the ISS in 2010, with its 360 degree viewing capability. Figure 1 is a "fish-eye" view of the mid-Atlantic coast of the U.S. acquired from the cupola.


*Figure 1.– View from ISS cupola centered in 34°N 77°W of the mid-Atlantic coast of the U.S. with Cape Lookout included as the cape on the right. NASA ID no. ISS26-E-6359*

**Volcanoes**

Amazing as it may seem, astronauts have sometimes been close to volcanoes at the moment of the first major explosive activity—as when Jeff Williams captured the first explosion of Cleveland Volcano in the Aleutian Islands before the science world was even aware of the eruption (http://earthobservatory.nasa.gov/IOTD/view.php?id=6592). Crews on board ISS Expedition 20 captured an even more amazing plume of ash rising from Sarychev Volcano off northeastern Japan, cataloged at http://earthobservatory.nasa.gov/IOTD/view.php?id=38985 and illustrated in figure 2. The upward blast incorporates a white, strikingly bulbous pileus cloud, which may be water condensing as air is forced to rise in the plume, and ground-hugging ash, known as a pyroclastic flow, streams down the hillside to the lower right. The origin of the circular, cloud-free zone around

the island raised interesting questions in the science community, discussed at the catalog link. By computerized smoothing of a sequence of still images, the desk-bound observer can sense both the movement of the astronaut as well as the billowing plume as it surges upward (http://earthobservatory.nasa.gov/images/imagerecords/38000/38985/sarychev_oblique_final_H264.mov).

*Figure 2.– Eruption of Sarychev Volcano, Kuril Islands, northeast Japan in June 2010. NASA ID no. ISS20-E-9048*

**Hurricanes**

Major storms last for many days and their cloud bands rise up to the top of the troposphere, the weather layer of the atmosphere. Major storms are therefore easily photographed and usually evoke much public interest. Images of any hurricane that approaches land are candidates for fast downlink so the public can see the view from space. Hurricane Earl (figure 3) was a long-lived, powerful storm which formed on August 25, 2010 and finally dissipated ten days later. Interestingly, it interacted with Hurricane Danielle which crossed the Atlantic Ocean behind it. Traveling just off the east coast of the USA, Earl was blamed for six fatalities, and became the first major hurricane to threaten New England since Hurricane Bob in 1991. It caused power outages for hundreds of thousands of people in Nova Scotia, Canada.

**Fires**

The Arnica fire (http://earthobservatory.nasa.gov/IOTD/view.php?id=40681) in the Yellowstone National Park (figure 4) was imaged on September 24, 2009, the day after it began when it grew to 101 acres in area. Astronauts have observed even small fires giving rise to enormous smoke palls. Here smoke can be seen streaming southwest towards the Grand Tetons Range. Oblique images such as this give a powerful sense of three dimensions to fire images: the smoke rises over Yellowstone Lake, casting an orange reflection in the lake and dark shadows on West Thumb embayment of the lake.


*Figure 3.– Hurricane Earl, Atlantic Ocean, on 27 August 2010, five days after it formed in the eastern Atlantic, approaching the Caribbean islands. NASA ID no. ISS24-E-12814*


*Figure 4.– The Arnica fire in Yellowstone National Park, September 2009. Other fires are visible near Jackson Lake (left) and on the flanks of the Grand Tetons Mountains (top center).*
*NASA ID no. ISS20-E-43017*

**Social Media**

Social media have promoted the immediacy of astronaut photography, sometimes with images of dynamic events. Astronaut Soichi Noguchi was the first to downlink Twitpics on a regular basis. An example of one of his dynamic Twitpic images include the May 2010 floods in central Poland. Figure 5 compares one of Soichi's images of the Vistula River floods in Poland with a Landsat image of the same region in 2011. The entire area of low country where the Vistula River meets a major tributary is inundated by brown muddy water.

*Figure 5.– Flooded Vistula River valley, Poland (left) as captured by Astronaut Noguchi in May 2010 and centered at 50.6N 21.8E as compared to Landsat image (right) of the same area in 2011. NASA ID no. ISS23-E-50542*

Another example of social media used to share dynamic events observed from ISS is Soichi's Twitpic posting of the Gulf of Mexico following the Deep Horizon disaster. Figure 6 captures sun glint patterns of oil on the surface of the Gulf of Mexico several days after the start of the disaster on May 4, 2010, http://earthobservatory.nasa.gov/IOTD/view.php?id=43897.

*Figure 6.– May 2010 oil spill in the Gulf of Mexico captured by ISS astronauts and shared with the public via Twitpic posting. NASA ID no. ISS23-E-32397*

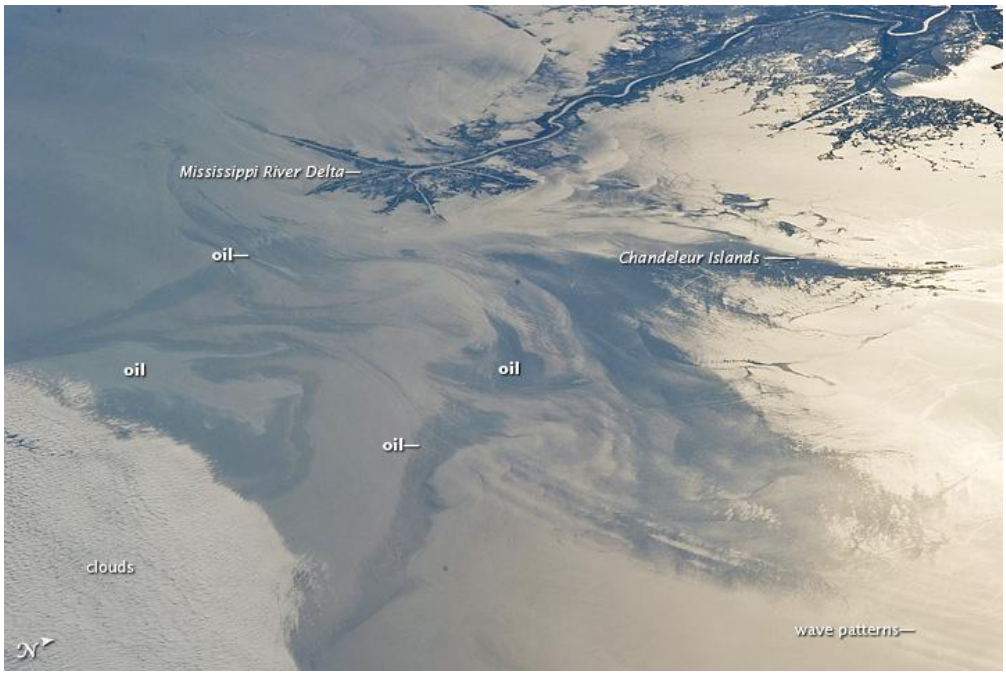

# *Lights in the Night: Capturing City Lights Just Became Easier*

*Sue Runco, Kim Willis, William L. Stefanov, Mike Trenchard, Justin Wilkinson*

Looking at the Earth at night has been one of the favorite past-times of astronauts since they began to orbit the Earth. Taking images of the city lights, to share these otherworldly images, has been a challenge. But the capability has improved over time. At first, advancements occurred by the astronauts developing their own photographic techniques, such as moving the camera for motion compensation to avoid smear in the photograph. To help avoid smear by rotating the camera at just the right speed, astronaut Don Pettit on Expedition 6 developed a "Barn-door Tracker" using on-board cameras, a drill and brackets. A video of Don Pettit's tracker and city light imagery can be found at: http://eol.jsc.nasa.gov/cities/CitiesAtNightWorldTour720X480edit7.mpg.

And, additional information about the challenges and interest in the city light imagery can be found in "Cities at Night: the View from Space": http://eol.jsc.nasa.gov/EarthObservatory/Cities_at_Night_The_View_from_Space.htm.

More recently, a camera capable of capturing low light levels (Nikon D3s) flew to the International Space Station (ISS) on Shuttle STS-131(19A) in April 2010, providing better night-imaging capability than has ever been available on the ISS. The Nikon D3s has larger pixels (8.396 microns horizontally and 8.392 vertically between pixel centers) allowing for more light capture, but with the trade-off of reduced ground resolution. By contrast, another onboard camera, the Nikon D2Xs, has smaller pixel sizes (5.527 horizontally and 6.489 vertically) and captures more detail on the ground but is harder to use for documenting city lights at night.

Even with the new D3s, astronauts must still move the camera to compensate for motion. However it is now much easier to take quality imagery of the world's cities at night. Two oblique views depict a sparkling web of human activity around the Mediterranean Sea (figures 1 and 2). A more vertically oriented image of Houston, Texas (figure 3) depicts the variety of lighting associated with different types of land-use. Other astronaut night images of cities can be accessed on the Gateway to Astronaut Photography of Earth at http://eol.jsc.nasa.gov.


*Figure 1.– City Lights at Night along the France-Italy Border, May 2010. NASA ID ISS023-E-2906*
*http://eol.jsc.nasa.gov/EarthObservatory/CityLightsatNightalongtheFranceItalyBorder.htm*


*Figure 2.– Nile River Delta at Night, November 2010. NASA ID ISS025-E-9858*
*http://eol.jsc.nasa.gov/EarthObservatory/NileRiverDeltaNight.htm*

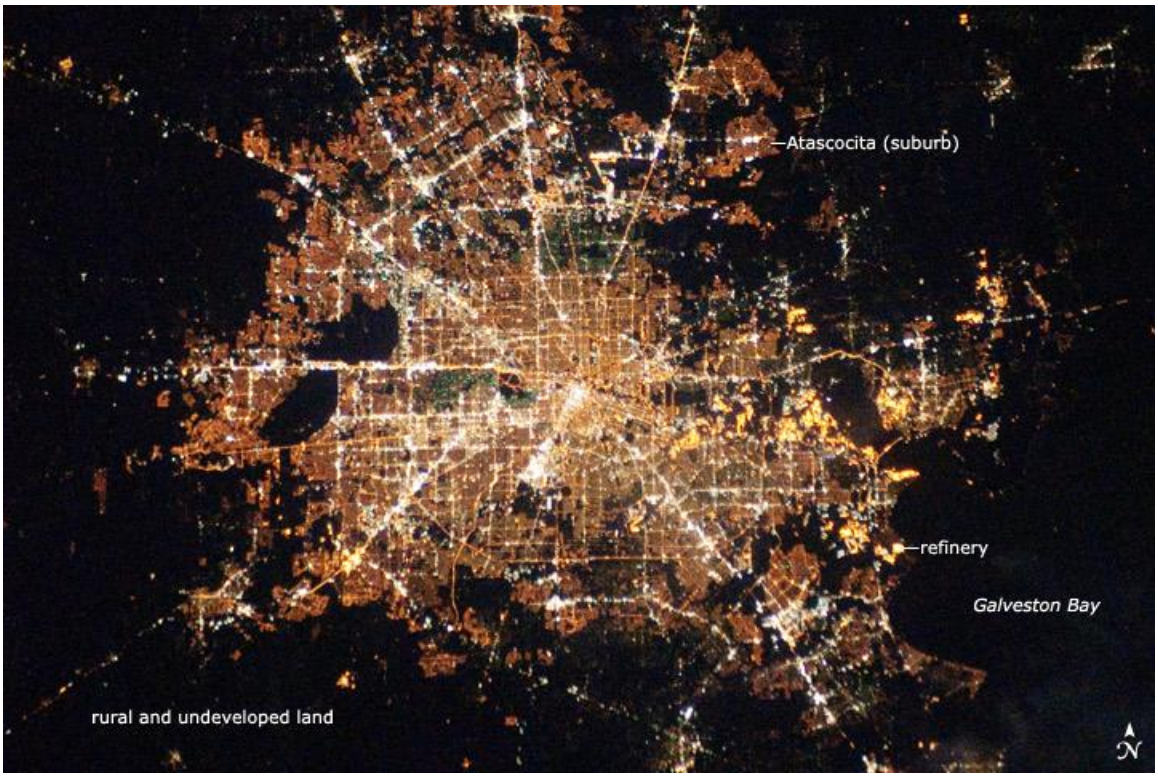


*Figure 3.– Houston at night, March 2010. Lights along the refinery corridor are distinctly yellower than whiter lights along highways. Suburban areas appear redder. Memorial Park, just west of downtown, is so brightly lit from surrounding lights that the green of its forests appears even at night. NASA ID ISS022-E-78463*
*http://eol.jsc.nasa.gov/EarthObservatory/HoustonTexasNight.htm*

## *Forward-Looking Infrared Cameras: A Potential Crew Tool for Geological Site Assessments*

*William L. Stefanov, Cynthia A. Evans, Kei Shimizu (Brown University)*

Plans for future crewed missions to the lunar or Martian surface, or Near-Earth Objects (NEOs) such as asteroids or comets, will include field traverses to assess site geological character, potential geohazards and to identify potential in-situ resources. While much of this information—mineralogy, chemical composition, and surface particle size distributions for example—can be obtained from multispectral or hyperspectral instruments located on orbiters, the very high spatial resolution of field validation data obtainable by crews "on the ground" is desirable prior to establishment of site infrastructure and habitats.

A handheld forward-looking infrared, or FLIR, camera was investigated as a field assessment tool for rapid estimation of rock abundance and discrimination of geological materials using both

laboratory and field analog site approaches. The FLIR Systems SC660 640 x 480 pixel array, uncooled microbolometer thermal infrared (IR) camera was selected as it includes a coregistered digital camera for simultaneous acquisition of visible wavelength (red, green and blue bands) data. A typical experimental setup of the camera in the laboratory is shown in figure 1.

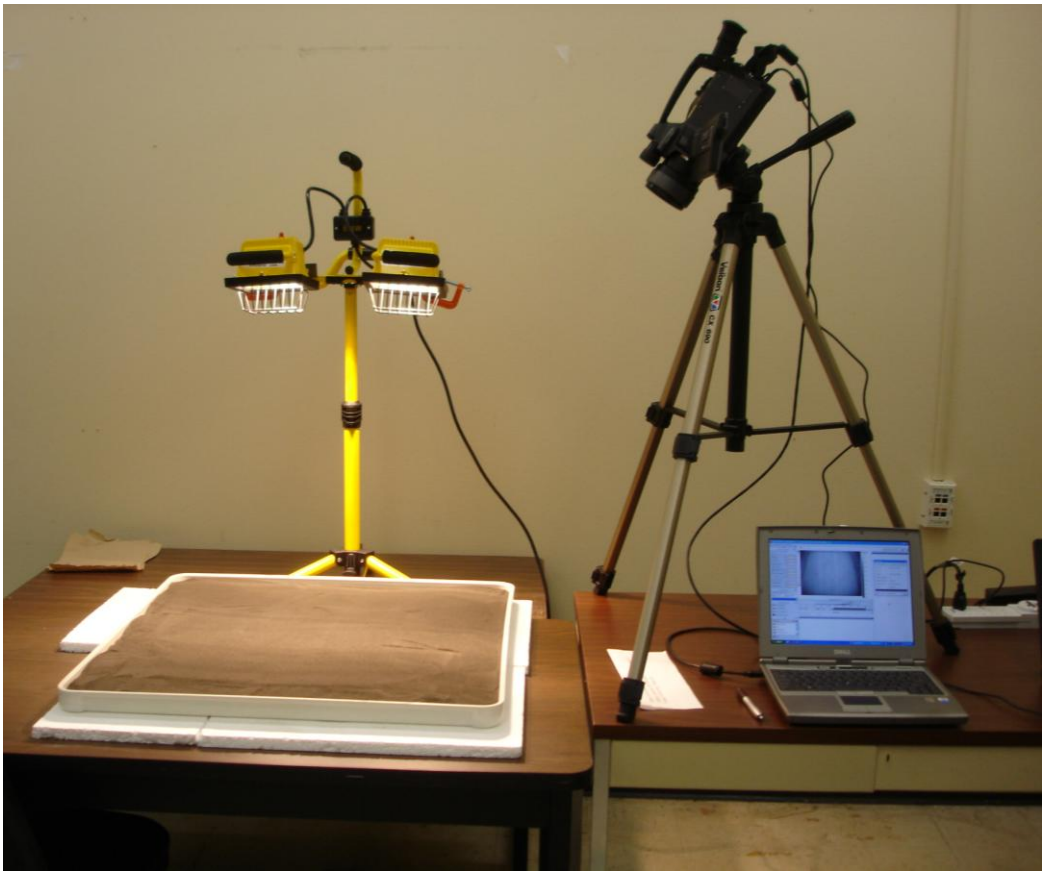

*Figure 1.– Typical FLIR experimental setup.*

The camera signatures and thermal response of a laboratory analog of a lunar mare surface were characterized. The analog surface used lunar soil simulant, basalt "gravel" (including vesicular scoria and dense lava fragments), and included depressions to represent impact craters.
Figure 2 (left) shows the visible wavelength (true color) image of the laboratory lunar analog surface; the lunar soil simulant substrate is gray, basalt scoria is red to pink and lava fragments are gray to black. A diurnal cycle was simulated with two 500 Watt halogen lamps to illuminate and heat the analog surface over periods ranging from 1 to 8 hours (sunrise, lunar "day"), followed by lamp switch-off and 3 to 16 hours of darkness (sunset, lunar "night"). The percent area of basalt gravel, number of impact craters, and illumination angle was also varied over different data collection runs.

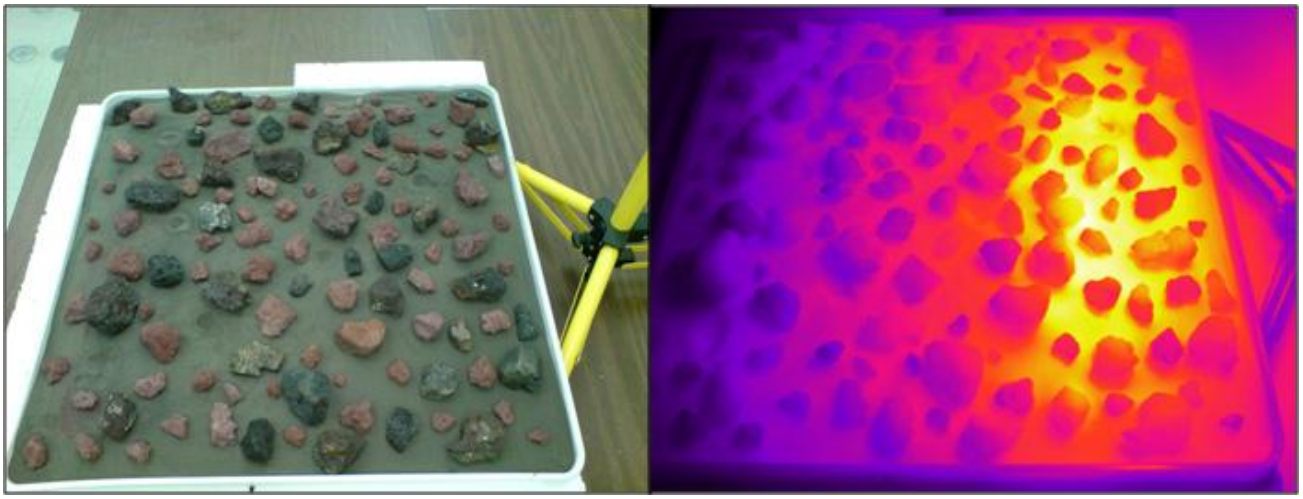

*Figure 2.– Visible image compared to simultaneous thermal IR image in laboratory environment.*

The FLIR camera recorded thermal IR and coregistered visible wavelength imagery at 1-minute intervals during each data collection run. This allowed us to observe qualitative variations in apparent thermal inertia—generally speaking, a measure of how quickly a given material heats up and subsequently cools down—related to the different analog materials, particle sizes, and illumination conditions and provided confidence that we could obtain similar data in the field. Figure 2 (right) shows a false-color thermal IR image of the analog surface during heating. Relatively hot, low apparent thermal inertial surfaces appear bright yellow and cooler, high apparent thermal inertial surfaces appear dark orange to violet.

Following initial trials at JSC's Planetary Analog Test Site or "rock yard", a field assessment was conducted with the FLIR camera at Colton Crater, located north of Flagstaff, AZ. While this crater was formed from explosive volcanic processes rather than a meteor impact, its basaltic character, geomorphology and ease of access made it an ideal lunar (and Martian) analog site for the study. Data collection occurred at, or shortly following, sunrise at several sites around and within the crater during the field assessment to maximize apparent thermal inertia contrast between different materials and surfaces, e.g. fine sediments on the crater floor and basaltic gravels and boulders; basaltic agglutinate (hot spatter deposits subsequently welded together) outcrop and surrounding soil, etc. The field data collection methodology was informed by the results of the laboratory analog study, resulting in approximately 4-hour collection runs with thermal IR and visible imagery collected at 5-minute intervals.

Principal component analysis was then performed to extract the most correlated information from the field data and reduce noise. By applying both unsupervised and supervised image classification algorithms to the visible wavelength data, thermal IR data and fused visible + thermal IR data, the performance of these relatively simple classification approaches was assessed for different geological materials and surfaces in the field to simulate "on the fly" operations by crew members, i.e., without significant science backroom support and analysis.

Figure 3 illustrates imagery obtained in the field at Colton Crater. The left image shows a visible wavelength (true color) image and the center image shows the corresponding thermal IR image. Relatively hot surfaces (indicating low apparent thermal inertia) are bright and relatively cool surfaces (indicating high apparent thermal inertia) are dark in the center image. The right image shows a supervised classification of fused visible and thermal IR data; red – basalt boulders; pink – basalt gravel; yellow – shadows; green – basalt agglutinate; blue – high albedo (high reflectance) materials; gray – masked vegetation, not classified.

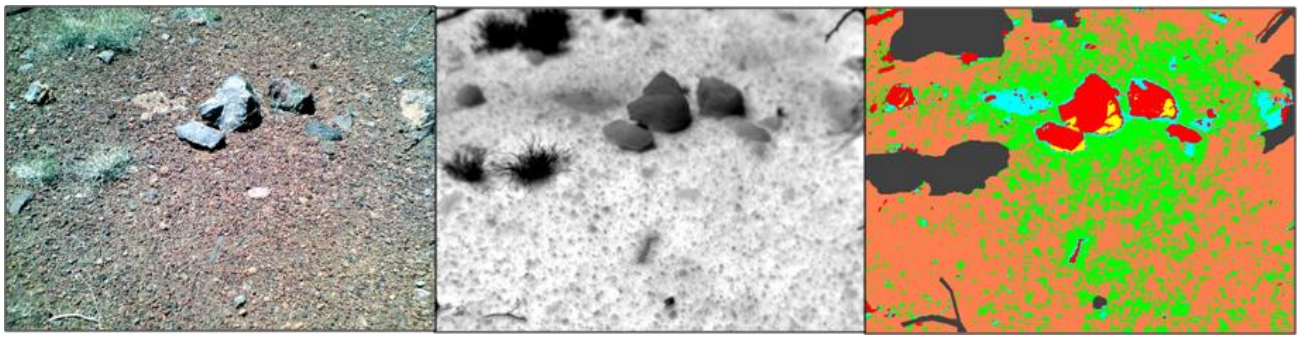

*Figure 3.– FLIR field data comparison.*

Mixed results were anticipated from these initial tests. Performance with regard to discrimination of different types of geological materials at Colton Crater was generally poor, with a large variance in overall accuracy obtained using both unsupervised and supervised approaches (35–80%); the range of variance for individual class accuracy was similar. This is largely a result of the relatively limited spectral sampling obtained by the FLIR camera—red, green, and blue visible wavelengths, and a single broad thermal IR band. In contrast, the classified FLIR camera data performed satisfactorily for determination of rock abundance compared with visual estimation in the field. These results suggest that current FLIR cameras would be a useful addition to a crew "toolkit" for geohazard and site suitability assessment, and suggests that further development of multispectral, microbolometer-based thermal IR and visible wavelength imagers would produce a highly useful tool for crew field geology activities.

# *Did Rivers Deposit the Layered Rock Suite of Sinus Meridiani, Mars?*

*Justin Wilkinson*

**Background**

The origin of the 800m of layered rocks in Sinus Meridiani is a key question in Mars geology since they underlie the rocks that have been investigated by the Mars rover Opportunity. The river hypothesis as an explanation for the layered rocks has been rejected routinely on the basis of the lack of a topographic basin to hold river sediments. Dust and ash sheets have been proposed as better candidate explanations.

The ridge-forming unit (RFU) is one of the upper layers. It is best exposed to view by wind erosion. The RFU is shown in oblique view in figure 1. ARES proposes an origin by river sedimentation, for this unit, and suggests the same origin may well apply to other units in the stack.

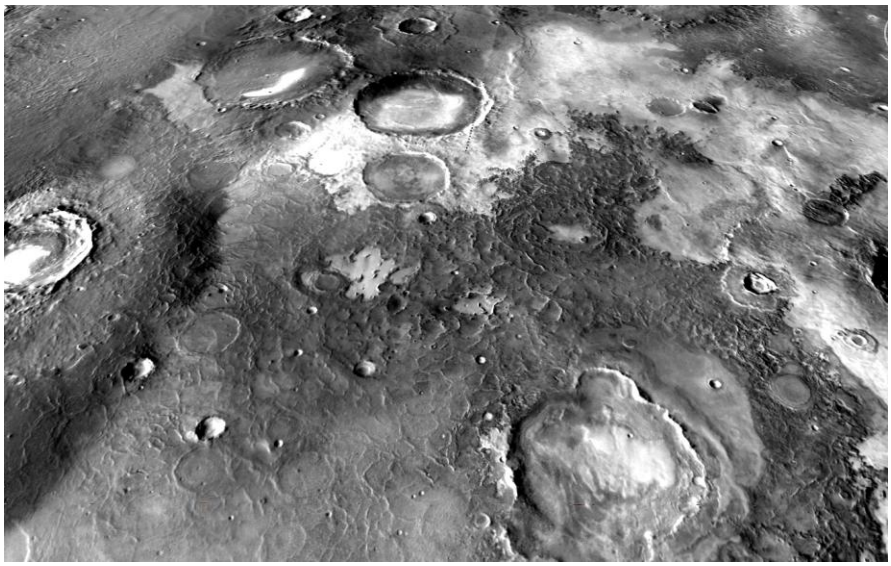

*Figure 1.– Sinus Meridiani shown in an oblique image looking north. Almost the entire area shown is covered by a network of raised ridges (except for craters and light-toned areas top right). The sinuous morphology of the ridges, their interlocking pattern, and the general north-south orientation have parallels in relatively newly understood terrestrial fluvial patterns. The lower margin of the image represents a distance of 180 km. (THEMIS daytime infrared mosaic; centered 3.7N 3.6W)*

**Rivers and the Large Fan Model**

Astronaut imagery has revealed a new global perspective on the way rivers emplace sediment on continents—a perspective that filled a major gap at the mid-level in the hierarchy of fluvial features. The global study revealed, in particular, the great number of large fans (radius >100 km). Since so many other fluvial features are now identified on Mars, this suggests strongly that large fans certainly ought to have operated on Mars also.

Two unexpected geomorphic patterns related to large fans seem to be particularly relevant to a new interpretation of the Meridiani rocks:

- Channel networks. Large fans are dominated exclusively by networks of crossing channels, to the exclusion of other landforms types, even hillsides (figure 2). When such landscapes are "inverted" by subsequent erosion, channels become networks of ridges covering wide areas. Ridge patterns of apparently inverted topography of the RFU show several features reminiscent of river features—ridges are sinuous, they cross in a complex network, and they are oriented primarily down the regional slope. Small areas of dark inverted ridges in Oman have been quoted already as possible analogs for the RFU (Figures 3a and b). Figure 2 shows that these analog areas of Oman lie firmly in a large fan geologic environment.

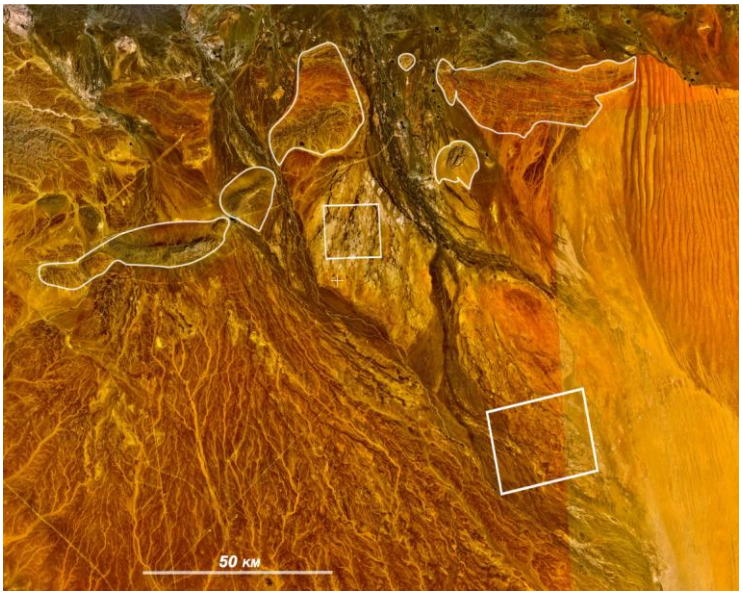


*Figure 2.– Large fans of river sediment are widespread in many parts of Earth. In this image of Oman they cover 22,000 km$^2$ (middle and lower part of the image), and extend further west (left) covering twice this area. Sources of the fan sediments are dark ophiolitic rocks of the Omani Mts. (top of the image). Bedrock outliers of the mountains are outlined. River channels bring dark sediment from the mountains, forming several large fans. The most extensive fan—hundreds of km in width and length—appears in the lower left, smaller fans center and center-right. The lower box is detailed in figure 3a and the upper box is detailed in figure 3b. Parallel dunes of the Wahiba Dune Field appear top right. North to top. Landsat VIS imagery.*

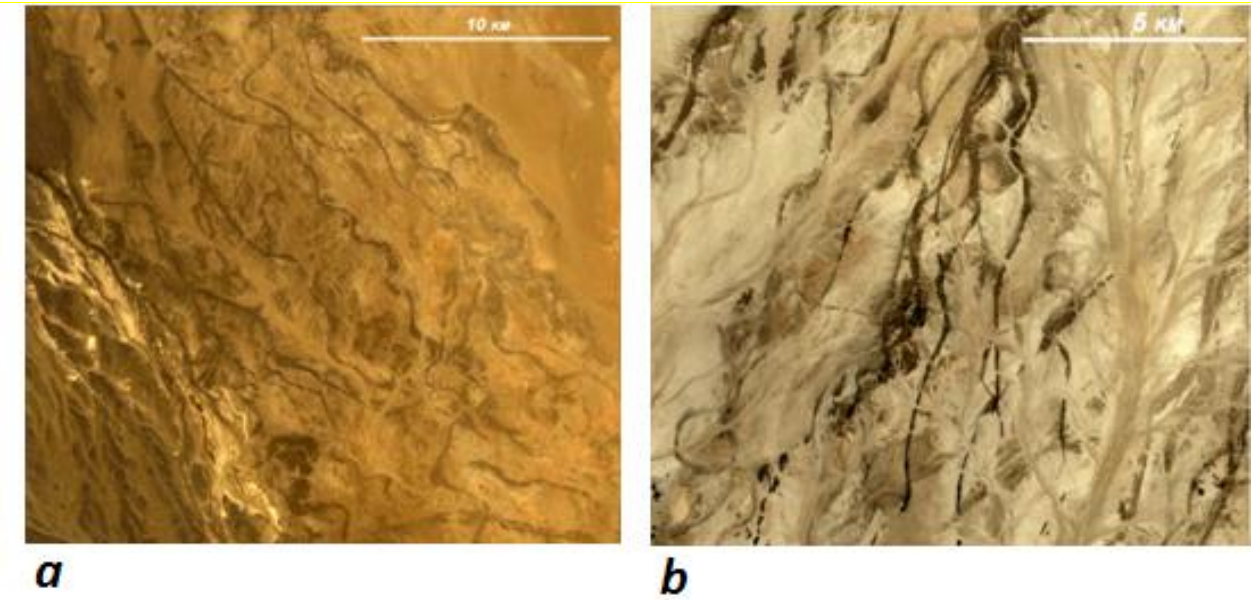


*Figure 3.– Patterns of sinuous dark lines are paleo-channels in Oman – detail. Ancient river systems cover the entire area of landscapes shown here (see boxes figure 2) as dark sinuous lines. The channels have been "inverted" by subsequent erosion so that they appear as ridges in the modern landscape. The dark sinuous channels have been quoted as possible analogs for the ridge-forming unit (RFU) of Sinus Meridiani. These more detailed views show three noteworthy characteristics: (i) the sinuous morphology of all ridges; (ii) the strong crossing pattern of the ridges; and (iii) the general orientation of the paleo-channels is apparent (SE in a, SW in b) – the fans of which they are part (figure 2) are so much larger than small alluvial fans that overt diverging/radial orientations are not apparent. Importantly, figure 2 shows that the wider setting of the inverted channel networks is a series of large fans.*

- The unusual setting of large fans. Another unexpected pattern revealed by global studies is that large fans, with their amazingly smooth surfaces, are probably typical of large-scale river sedimentation on continents. With this new understanding come new perspectives on river systems. Roughness maps—produced with the same algorithm used by Kreslavsky and Head in constructing their well-known roughness map of Mars—show unexpected and important differences from the classical understanding of rivers as movers of sediment.
  - Major river-related deposits cover large flat areas ($10^{3–6}$ $km^2$)—note scale bars (figure 4a).
  - These flat river plains (multiple large fans) are laid down far from oceans and lakes (figure 4a).
  - Such deposits are laid down immediately next to the erosional source upland. We term this the 2-zone model – diagrammed in fig 4b (lower left). It contrasts with the classical 3-zone model of textbooks (figure 4b, top).
  - Perhaps most importantly, closed topographic basins are not necessary for widespread river sediments to accumulate on continental surfaces (see especially Argentina inset, figure 4a).

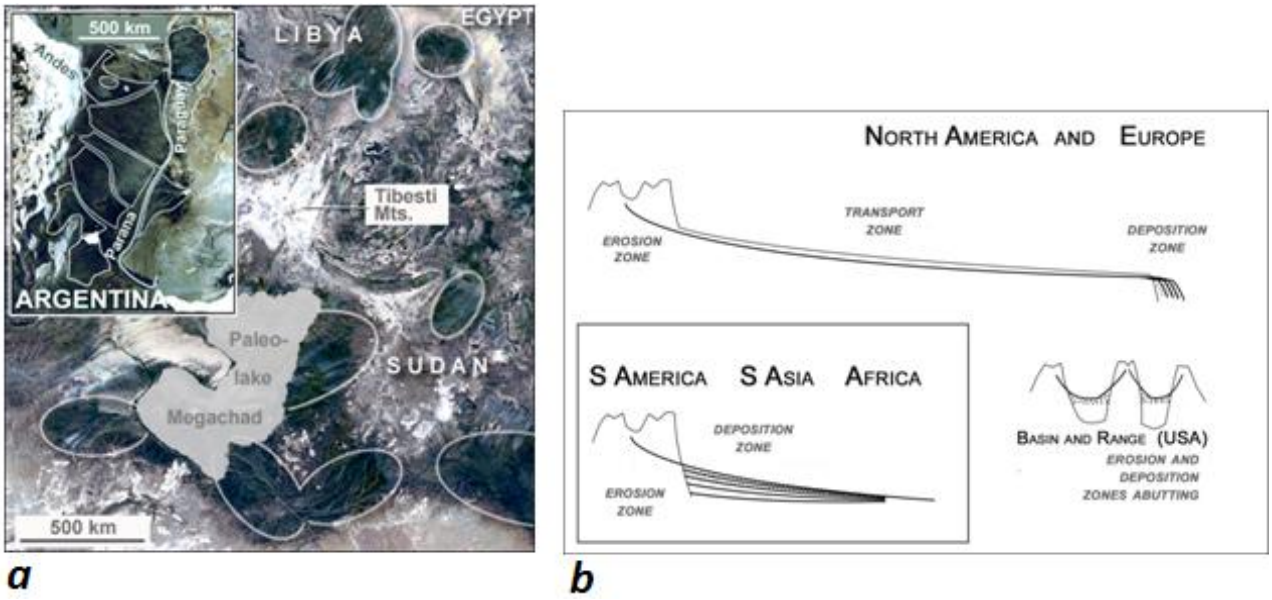


*Figure 4.– (a) Roughness maps of central South America and eastern Sahara Desert. Dark areas are smooth plains of very low slope. Rougher surfaces such as mountains and dune fields are light-toned. Significance for a river sedimentation model are these unexpected features: all smooth, low-angle surfaces are single or nested megafans (outlined); fan surfaces form at the immediate margin of uplands; fan-dominated areas cover very large areas (note scale bars). (b) Well-known 3-zone North America/Europe model (top), and the 2-zone model typical of large fan settings (box, lower left). Large fan model also shows that rivers lay down sediment on a regional slope, specifically without the requirement for a basin. The large fan model may be the most appropriate for Sinus Meridiani (see text).*

**River-Sediment Hypothesis (Fluvial Hypothesis) for Sinus Meridiani Layered Sediments?**
For years the main objection to the fluvial hypothesis has been the lack of a basin in this part of Mars within which sediments could accumulate. ARES has recently argued that a basin is specifically not required for the accumulation of river-borne sediments—based on the fact that fluvial sediments are specifically laid down on slopes determined by the actively depositing river. River sedimentation therefore is compatible with deposition on a slope.

This counters the notion that river deposition requires basins, and certainly counters the notion that it requires water bodies to occur. Further, large fan patterns account for the location at Meridiani of extensive, layered sediments, of variable thickness and composition, located at a sharp margin immediately at the foot of an eroding upland—an upland notably cut by numerous and major river networks. Research also shows that the Meridiani units slope with the regional slope, away from the upland, as expected of river sediments. The fluvial hypothesis also provides the most robust explanation for sinuous inverted ridges, with their intricate crossing patterns, that cover wide areas.

# *Managing Science Operations During Planetary Surface Missions: The 2010 Desert RATS Test*

*Dean B. Eppler, Douglas W. Ming*

**Introduction**

Desert Research and Technology Studies (Desert RATS) is a multi-year series of hardware and operations tests carried out annually in the high desert of Arizona on the San Francisco Volcanic Field. Conducted since 1997, these activities are designed to exercise planetary surface hardware and operations in conditions where long-distance, multi-day roving is achievable. Such activities not only test vehicle subsystems through extended rough-terrain driving, they also stress communications and operations systems and allow testing of science operations approaches to advance human and robotic surface capabilities. Desert RATS is a venue where new ideas can be tested, both individually and as part of an operation with multiple elements. By conducting operations over multiple yearly cycles, ideas that "make the cut" can be iterated and tested during follow-on years. This ultimately gives both the hardware and the personnel experience in the kind of multi-element integrated operations that will be necessary in future human planetary exploration.

Desert RATS 2010 tested two crewed rovers designed as first generation prototypes of small pressurized vehicles. Each rover provided the internal volume necessary for crewmembers to live and work for periods up to 14 days, as well as allowing for extravehicular activities (EVAs) through the use of rear-mounted suit ports. The 2010 test was designed to simulate geologic science exploration traverses over a 14-day period through a terrain of volcanos, lava flows and underlying sedimentary rocks. Prior to the test, a series of traverses were planned using techniques that were first developed during the Apollo missions. These activities were based on a photogeologic interpretation of air photo and satellite images conducted by the U.S. Geological Survey in Flagstaff, and they were designed to simulate a reconnaissance investigation by two rover crews of a planetary surface operating under a variety of communications constraints like intermittent connectivity. Predicted areas of good radio reception were overlaid on the planned traverses and locations of geological interest were adjusted to ensure communications supported the planned test conditions during each day of the test. The resulting set of traverses and stations were then field checked by the test team leads to ensure they matched the planned test conditions.

Conduct of the actual test took place between 31 August and 13 September 2010. Two crewmembers lived in and drove each rover for a single week with a "shift change" on day 7, resulting in a total of eight test subjects for the two week period. Each crew consisted of an engineer/commander and an experienced field geologist. Three of the engineer/commanders were experienced astronauts with at least one Space Shuttle flight. The field geologists were drawn from the academic community (figure 1).

*Figure 1.– Crewmembers acquire a basalt sample at a stop during a 2010 Desert-RATS geologic traverse.*

Operations were tested with different communication states and rover deployment conditions. Three days of each week operated under conditions were the crew could always talk with mission operations team (called continuous communications), and three days the crew could only talk to mission control for ≈1 hour in the morning and ≈1 hour at the end of the traverse day (called 2-A-Day communications). In addition, portions of the traverses were conducted with the two rovers in working together as a combined crew, while during other periods, the rovers operated out of line-of-site of each other, pursuing independent science objectives.

**Science Operations Management Approach**

In previous Desert RATS operations, the science support room has operated largely in an advisory role to the mission test team. This approach was driven by the need to provide a loose science mission framework that would underpin the engineering tests, rather than be an element of the operations that was conducting science discipline specific test operations. However, the extensive nature of the traverse operations for 2010 drove the decision to expand the role of the science operations and test specific operational approaches as part of the science support for the test. The success of the Apollo mission science support team as well as the science operations approach utilized by the MER missions became the baseline for the science test.

Past experience has shown that overseeing manned operations of multiple vehicles requires a separate control room for each (e.g., Space Shuttle and ISS operations prior to docking of the orbiter to ISS or after undocking). Consequently, each rover worked directly with a Tactical Science Operations Team (TSOT) responsible for managing real-time science operations while each crew was conducting "boots on the ground" geologic field operations. The TSOT operated during normal duty days, between ≈7:30 AM and ≈5:30 PM. In addition to the TSOT, independent test operations with two rovers required an integration team, termed the Strategic Science Operations Team (SSOT). The SSOT would analyze the results of daily sciences operations from each rover crew and evaluate those operations within the larger objectives of the field traverse plans. In particular, a major function of the SSOT was to evaluate the completion status of a particular day's objectives and, if necessary, recommend to the Mission Manager variations in the following days' operations in response to missed objectives or important, unexpected discoveries. The SSOT operated during the night shift, between ≈8:00PM and ≈4:00 AM. Both the SSOT and TSOT were crewed by scientists with a range of experience levels in both field geology and planetary mission operations.

Each TSOT was housed in a separate trailer in the field that had 7 console positions (figure 2). The TSOTs were managed by a team lead, responsible for the overall conduct of a particular rovers' science operations during EVA. Communications with the rover crew were conducted by a Science Communicator (SCICOM), who was the only person on the TSOT that communicated directly with the crew. A Documentarian assisted the TSOT Lead with a real-time, running "war diary" of field operations, describing the operations, identifying specific issues to be resolved downstream, and providing the overall daily reference document for science operations. Two of the remaining console positions were responsible for managing the operation of a variety of still, panoramic and video cameras and downlinking image products to be utilized in real-time for situational awareness and management of the science operations at a particular station. Lastly, two TSOT members were assigned the responsibility for overseeing the science activities of a single crewmember. This activity included downlinking image data from backpack cameras, listening to and conducting real-time science analysis of crewmembers' verbal descriptions, and providing advice to the TSOT Lead on operations. In addition, each TSOT maintained a team member (OPSLINK) in the primary operations control trailer to act as the liaison between each science team and the overall mission operations team. In particular, OPSLINK managed the control handoff between mission operations team, which controlled the rovers when they were driving between stations, and the TSOT, which took over when the crewmembers stepped off the rover to begin geologic work.

*Figure 2.– Science operations control room located near the 2010 Desert-RATS field test site.*

The SSOT was conducted in a hotel conference room in Flagstaff, separate from the field operations site. Like the TSOT, there were a number of standing positions on the team held by a variety of scientists. The SSOT was managed by a team lead responsible for management and completion of all activities of the SSOT, including replanning of traverses for the following day's science operations. In addition, the Team Lead was responsible for presenting any changes to the day's plan to the Mission Management Team following the SSOT's daily operations. The team also included a Documentarian whose role was similar to the counterpart on the TSOT. An SSOT Strategic Operations Lead was responsible for managing long-term constraints that affected the daily replanning process (e.g. communications constraints), and any items that may affect the mission in light of re-planned science operations. The Activity Planners were responsible for taking the recommendations of the SSOT Team Lead for changes to future tactical plans and preparing the revised daily plan for each rover crew. The Long-Term Planning Lead was responsible for coordinating the science teams that worked on datasets critical to planning the next day's tactical activities, determining whether there were discoveries or issues that warranted traverse replanning, and revising traverse plans in accordance with new directions. Various geoscience teams were responsible for analyzing data sets produced by the crew Rover imaging and science teams (e.g., Crew Field Notes, panoramic or back pack imaging data), making specific recommendations to the Strategic Operations Lead on revising the following day's geologic traverses, and identifying key samples collected that were candidates for further study.

The 2010 RATS Science Operations Test was extremely successful, testing a variety of old and new operations approaches to managing science data and crew operations on planetary surfaces. In addition to substantive lessons learned about how to do extended planetary science operations, the test served to begin training a new generation of scientists in the demands of planetary surface science operations.

# *ARES Education and Public Outreach*

**Jaclyn Allen, Charlie Galindo, and Paige Graff**
**with contributions from Susan Runco, William Stefanov, and Kim Willis**

**http://ares.jsc.nasa.gov/ares/education/index.cfm**

The ARES education team is charged with translating the work of ARES scientists into content usable in formal and informal K-12 education settings and to assist with public outreach. This is done through local efforts and national partnerships.

**Local Efforts**

Local efforts include partnerships with universities, school districts, museums, and the Lunar and Planetary Institute (LPI) to share the content and excitement of space science research. A strong partnership with LPI includes a variety of solar system educator workshops at Texas science teacher conferences and the Harris County Department of Education. ARES also teams with LPI to provide space science education events at LPI. The ARES education team supports NASA JSC education workshops and the Texas Aerospace Scholars program with workshop presentations, speakers and printed materials.

Locally the education team assists the ARES directorate in public outreach endeavors. Sharing ARES science with the public is an essential part of the directorate's work in Earth and space science. As the small enclave of physical scientists at a NASA engineering and space flight center, the ARES staff is frequently called upon to support science presentation and interview requests from the JSC public affairs or education offices. Scientists and staff are active volunteers in the JSC Speaker's Bureau, Digital Learning Network, and National Engineers Week programs. Scientists and staff also support local science fairs and give presentations at many local schools. Scientists are frequent mentors for university faculty and students in programs sponsored by the NASA education and equal opportunity offices as well as the Lunar and Planetary Institute. The staff also provides tours of our research and curatorial laboratories for JSC personnel and visitors (figure 1).

**National Partnerships**

Programs with a national reach are an important vehicle for ARES education efforts. With funding from the Discovery Program and the Lunar and Meteorite Sample Disk Program, the ARES education team is an active and contributing member of the NASA space science education community. The team is involved in several national efforts to reach formal and informal educators:

- Affiliation with Girl Scouts USDS and the NASA Girl Scout Core Trainers.
- Participation in the annual teacher professional development and school visitation event in the Huntsville, Alabama area in conjunction with the Discovery and New Frontiers Program.
- Contributions to recently released Discovery education products: Space School Musical, Image Impact, Expo's Discovery http://discovery.nasa.gov/index.cfml.

*Figure 1.– Engaging employees' children at 'Bring Your Children to Work' Day*

The ARES Education team continues to have a presence at state and national venues for science educators and afterschool educators presenting workshops focused on Solar System Exploration including ARES research, Mars, and the Moon.

**ARES Continuing Education Projects**

ARES has five continuing education projects that reach a national audience—Educational Thin Sections Program, Lunar and Meteorite Education Disk Program, Earth Observations Education and Public Outreach, Expedition Earth and Beyond, and NASA Space Science Days continue to serve a large national audience.

***Educational Thin Sections***

NASA Educational Thin Section sets, with 12 thinly sliced samples from the Lunar and meteorite collections, are available to colleges around the country. Each set is accompanied by educational materials including background information, petrographic descriptions and a video or slide set with captions. The NASA Educational Thin Section Sets program is managed by the ARES Astromaterials and Curation Office, with collaboration from the Smithsonian Institution in the preparation of the meteorite sets.

***Lunar and Meteorite Sample K-12 Education Disk Program***

The Lunar and Meteorite Sample Education Disk Program is a continuation of two, long-established education programs. The focal of the program is a collection of six Lunar or meteorite samples encapsulated in a six-inch diameter clear Lucite disk. This program is available to schools,

museums, and planetariums throughout the country. Distribution of the disks has made it possible for millions of people to examine the precious Apollo lunar and meteorite samples. The educational sample disks are accompanied by educational materials including a teachers' guide and image support.

An integral part of this program is the training and certifying of educators to borrow the disks. The ARES Education team serves as trainers of trainers, delivering the scientific background information, hands-on activities and security information to NASA Aerospace Education Services Project (AESP) specialists and ERC educators who prepare formal and informal educators to use the disks as they teach planetary science. The Lunar and Meteorite Sample Education Disk Program is currently managed by the ARES Education Office in cooperation with the ARES Astromaterials Acquisition and Curation Office.

***Earth Observations Education and Public Outreach***

Astronaut photography of Earth is extremely popular with students, teachers, and the general public, and this excitement is used to leverage interest in science and exploration. ARES provides at least one annotated human space flight image, with caption, per week to "Earth Observatory," NASA's Earth science education flagship website, http://earthobservatory.nasa.gov. Over 1 million astronaut photographs of Earth are downloaded each month by educators and the public from the "Gateway to Astronaut Photography of Earth," which has received numerous educational citations, http://eol.jsc.nasa.gov.

***Expedition Earth and Beyond***

Expedition Earth and Beyond (EEAB) is an inquiry-based geosciences student involvement program developed and led by the ARES Education Program. EEAB allows teachers and students to be actively involved in the excitement of exploration, discovery, and the process of science. Experiences provided through EEAB allow students to model the process of science and helps prepare them to become NASA's next generation of scientists and explorers.

The program facilitates student-led, authentic research investigations that promote the study of Earth and planetary body comparisons. EEAB uses astronaut photographs of the Earth collected during Space Shuttle missions and as part of the ARES International Space Station Crew Earth Observations (CEO) payload. The astronaut photographs, available online from the Gateway to Astronaut Photography of Earth website, http://eol.jsc.nasa.gov, have proven to be popular with students, teachers, and the general public. The program provides a classroom friendly structure that allows teachers in grades 5–14 to have their students use these striking images of Earth as part of research conducted in the classroom (figure 2).

*Figure 2.– Students presenting research.*

Educator professional development workshops train hundreds of teachers to use the inquiry-based, standards-aligned curricular materials designed to help students model the process of science (figure 3). These materials enable teachers to replace previously used classroom curricula with more engaging, relevant, and inspiring activities that use the excitement of current exploration as the hook. As part of their participation, student teams have the opportunity to submit data requests for new imagery to be taken by crew on the International Space Station (ISS) to support their research. This enables students to not only obtain and use current NASA data, but allows them to actively participate in current NASA exploration.


*Figure 3.– EEAB educator workshop.*

Through EEAB, classrooms across the nation can also connect with ARES scientists in a number of ways. Classroom connection webinars enable ARES scientists to conduct interactive presentations that allow participants to increase their knowledge of Earth, planetary comparisons, and science being conducted within the ARES Directorate (figure 4). ARES scientists also directly communicate with student teams to help mentor them through their research. This communication not only helps students as they conduct their research, but is a great motivational tool enhancing student interest and helping to narrow the gap between NASA scientists and classroom students. This gap is further narrowed by having students share and present their research "live" to ARES and other participating scientists using distance learning technologies.

*Figure 4.– Connecting scientists with classrooms.*

***NASA Space Science Days***

NASA Space Science Day (NSSD) are undergraduate mentor-led educational outreach programs exposing middle school students to STEM-related Science Mission Directorate (SMD) educational products based on an upcoming science mission such as a current Discovery mission. NSSD transforms underrepresented undergraduate students into space science mentors who lead these events for their local communities. ARES partners with:

- The University of Texas at Brownsville and Texas Southmost College (UTB/TSC) – South Texas Engineering Math and Science (STEMS) Program, and
- Society of Hispanic Professional Engineers (SHPE) – Foundation-Advancing Hispanic Excellence in Technology Engineering, Math and Science (AHETEMS) to engage a broad spectrum of fifth graders through second year college students in space science. The program utilizes science researchers and SMD educational products to increase student awareness of STEM careers and opportunities, as well as exposing students normally not reached through major NASA education programs due to their remote locations or distance from a NASA center.

To accomplish this, four main rotating components occur yearly:

- Science content mentor (undergraduate students) training – Mentor training occurring every year in December at JSC where two students from each past and future NSSD site attend a two day workshop conducted by ARES. Mentors attend lectures and laboratory tours to gain insight into ARES science and to prepare them for presentations using a thematic approach to the content and related hands-on activities.

*Figure 5.– Mentor content training at JSC.*

- The original NSSD event at UTB/TSC – The original NSSD event occurs each year in January in Brownsville, Texas at the UTB/TSC campus. The event is in its ninth year and serves as the training site for future NSSD events by allowing the new student mentors to see firsthand how the program works and to actively participate in the mentoring process. Over 700 5$^{th}$ and 8$^{th}$ graders from the Texas Rio Grande Valley school districts attend the event.

*Figure 6.– UTB Mentor being briefed by local 5th grader on where they would land on Mars using remote imaging data.*

- Mini-information training sessions at SHPE's National Institute for Leadership Advancement (NILA) conference – These sessions are NSSD's way of recruiting new SHPE student and professional chapters. SHPE requires that all chapter officers attend their yearly three day intensive leadership training, and NSSD has taken advantage of the event to expose all SHPE chapters to NSSD's goals and to solicit proposals from interested chapters to host an event in their communities as conducted in Brownsville.
- Teacher/mentor training workshops at a second NSSD site selected from proposals submitted by candidate host sites – Upon selection of the host site, which is typically a local university, a Teacher/Mentor Training Workshop is held at the university approximately two months prior to the event. SMD products are distributed to local middle school teachers and the teachers are prepared for the NSSD event, which occurs two months later. Mentors from a local university and some upper level high school students are also trained to lead hands-on activities.

**Publications**

The ARES education team has developed and published activities and education packages. This work is the collaboration of ARES scientists and classroom educators. The hallmark of ARES education activities is accurate science presented in hands-on learning experiences that meet the needs of educators:

- Mars Soil Sleuths
  http://ares.jsc.nasa.gov/Education/index.cfm
- Exploring Meteorite Mysteries
  http://ares.jsc.nasa.gov/Education/Activities/ExpMetMys/ExpmetMys.htm
- Exploring the Moon
  http://ares.jsc.nasa.gov/Education/activities/ExpMoon/ExpMoon.htm
- Destination: Mars!
  http://ares.jsc.nasa.gov/Education/activities/destmars/destmars.htm
- Modeling the Solar System
  http://ares.jsc.nasa.gov/Education/modelingsolarsystem.pdf
- Expedition Earth and Beyond Classroom Activities
  http://ares.jsc.nasa.gov/ares/eeab/curricularmaterials.cfm

## Peer Reviewed Papers

Arvidson, R. E., et al., including **D. W. Ming** and **R. V. Morris**. "Results from the Mars Phoenix Lander Robotic Arm Experiment." Journal of Geophysical Research 114, E00E02 (2009), doi:10.1029/2009JE003408.

Arvidson, R. E., et al., including **D. W. Ming** and **R. V. Morris**, "Spirit Mars Rover Mission: Overview and selected results from the Northern Home Plate Winter Haven to the side of Scamander Crater." Journal of Geophysical Research-Planets 115, E00F03 (2010), doi:10.1029/2010JE003633.

Basilevsky, A. T., G. Neukum, and **L. E. Nyquist**. "The spatial and temporal distribution of lunar mare basalts as deduced from analysis of data for lunar meteorites." Planetary and Space Science (2010).

**Bell, M. S.** "Relative shock effects in mixed powders of calcite, gypsum, and quartz: A calibration scheme from shock experiments." Large Meteorite Impacts and Planetary Evolution IV, The Geological Society of America, Special Paper 465, Boulder, CO (2010): 593-608.

Berthet, S., V. Malavergne, and **K. Righter**. "Melting of Indarch (EH4 chondrite) at 1 GPa and variable oxygen fugacity: implications for early planetary differentiation processes." Geochimica et Cosmochimica Acta 73 (2009): 6402-20.

Boynton, W. V., et al., including **D. W. Ming**, **P. B. Niles**, **B. Sutter**, and **R. V. Morris**. "Evidence for Calcium Carbonate at the Mars Phoenix Landing Site." Science 325 (2009): 61-64, doi:10.1126/science.1172768

Busemann, H., et al., including **A. N. Nguyen**. "Ultra-primitive interplanetary dust particles from the comet 26P/Grigg-Skjellerup dust stream collection." Earth and Planetary Science Letters 288 (2009): 44-57.

**Calaway, M. J., E. K. Stansbery,** and **L. P. Keller**. "Genesis capturing the sun: Solar wind irradiation at Lagrange 1." *Nuclear Instruments and Methods in Physics Research, Section B: Beam Interactions with Materials and Atoms* 267.7 (Apr 15 2009): 1101-08.

Campbell, A. J., L. R. Danielson, **K. Righter**, C. T. Seagle, Y. Wang, and V. B. Prakapenka. "High pressure effects on the iron-iron oxide and nickel-nickel oxide oxygen fugacity buffers." *Earth and Planetary Science Letters* 286 (2009): 556–64.

Cull, S., et al., including **R. V. Morris**. "Seasonal ice cycle at the Mars Phoenix landing site: 2. Postlanding CRISM and ground observations." *Journal of Geophysical Research* 115, E00E19 (2010), doi:10.1029/2009JE003410.

Cull, S., et al., including **D. W. Ming** and **R. V. Morris**. "Concentrated perchlorate at the Mars Phoenix landing site: Evidence for thin film liquid water on Mars." *Geophysical Research Letters* 37, L22203 (2010), doi:10.1029/2010GL045269.

**Danielson, L. R.**, **K. Righter**, and M. Humayun. "Mineralogy, petrology and trace element chemistry of Cumulus Ridge (CMS) 04071 pallasite." *Meteoritics and Planetary Science* 44 (2009): 1019-32.

Drube, L., et al., including **R. V. Morris**. "Magnetic and optical properties of airborne dust and settling rates of dust at the Phoenix landing site." *Journal of Geophysical Research* 115, E00E23 (2010), doi:10.1029/2009JE003419.

Edmunson, J., L. E. Borg**, L. E. Nyquist**, and Y. Asmerom. "A combined Sm-Nd, Rb-Sr, and U-Pb isotopic study of Mg-suite norite 78238: Further evidence for early differentiation of the Moon." *Geochimica et Cosmochimica Acta* 73 (2009): 514-27.

**Evans, C A.,** J. A. Robinson, and J. M. Tate-Brown. "Research on the International Space Station: An Overview." *Proceedings: 47th AIAA Aerospace Sciences Meeting and Aerospace Exposition*, AIAA-2009-0186 (January 5-8, 2009).

Fleischer, I., et al., including **R. V. Morris**. "Distinct hematite populations from simultaneous fitting of Mössbauer spectra from Meridiani Planum, Mars." *Journal of Geophysical Research* 115, E00F06 (2010), doi:10.1029/2010JE003622.

Fleischer, I., et al., including **R. V. Morris**. "New insights into the mineralogy and weathering of the Meridiani Planum meteorite, Mars." *Meteoritics and Planetary Science* 46 (2011), doi:10.1111/J.1945-5100.2010.01127.X.

**Gibson, E. K**. "Life on Mars hypothesis: The status of research on ALH84001 and additional Martian meteorites." *The Observatory: A Review of Astronomy, The Royal Astronomical Society* 130 (2010): 245-48.

**Gibson, E. K.**, C. T. Pillinger, and L. Waugh. "Lunar Beagle and Lunar Astrobiology" *Earth, Moon and Planets* 107.1 (2010): 25-42, doi:10.1007/s11038-010-9364-1.

Goetz, W., et al., including **R. V. Morris**. "Microscopy analysis of soils at the Phoenix landing site, Mars: Classification of soil particles and description of their optical and magnetic properties." *Journal of Geophysical Research* 115, E00E22 (2010), doi:10.1029/2009JE003437.

Golden, J. S., W. C. Chuang, and **W. L. Stefanov**. "Enhanced classifications of engineered paved surfaces for urban systems modeling." *Earth Interactions* 13.5 (2009): 1-18.

Gounelle, M., et al., including **M. Zolensky**. "A unique basaltic micrometeorite expands the inventory of solar system planetary crusts." *Proceedings of the National Academy of Sciences* 106 (2009): 6904-09.

Hanada, T., **J.-C. Liou**, T. Nakajima, and **E. Stansbery**. "Outcome of recent satellite impact experiments." *Advances in Space Research* 44 (2009): 558-67.

Hecht, M. H., et al., including **D. W. Ming**. "Detection of perchlorate and the soluble chemistry of Martian soil at the Phoenix Lander site." *Science* 325 (2009): 64-7, doi:10.1126/science.1172466

Herrin, J., et al., including **M. Zolensky**, **D. Mittlefehldt**, and **L. Le**. "Thermal and fragmentation history of ureilistic asteroids/Insights from the Almahata Sitta fall." *Meteoritics and Planetary Science* 45 (2010): 1789-1803.

Herzog, G. F., et al., including **D. D. Bogard**, **L. E. Nyquist**, **C.-Y. Shih**, **D. H. Garrison**, and **Y. Reese**. "Cosmic-ray exposure history of the Norton County enstatite achondrite." *Meteoritics & Planetary Science* 46 (2011): 1-27.

**Hörz, F.**, **M. J. Cintala**, **T. H. See**, and **K. Nakamura-Messenger**. "Penetration tracks in aerogel produced by $Al_2O_3$ spheres." *Meteoritics and Planetary Science* 44 (2009): 1243-64.

Jenniskens, P., et al., including **M. Zolensky**, and **L. Le**. "The impact and recovery of asteroid 2008 TC3." *Nature* 458 (2008): 485-88.

Jenniskens, P., et al., including **M. Zolensky** and J. Herrin. "Almahata Sitta (= asteroid 2008 $TC_3$) and the search for the Ureilite Parent Body." *Meteoritics and Planetary Science* 45 (2010): 1590-1617.

Lapen, T. J., M. Righter, A. D. Brandon, V. Debaille, B. L. Beard, J. T. Shafer, and **A. H. Peslier.** "A younger age for ALH 84001 and its geochemical link to shergottite sources in Mars." *Science* 328 (2010): 347-51.

Lee, T. K., and **T. L. Wilson**. "Space-Radiation-Induced Photon Luminescence of the Moon." *Advances in Space Research* 44 (2009): 478-82.

Lichtenberg, K A., et al., including **R. V. Morris**. "Stratigraphy of hydrated sulfates in the sedimentary deposits of Aram Chaos, Mars." *Journal of Geophysical Research* 115, E00D17 (2010), doi:10.1029/2009JE003353.

Lida, Y., et al., including **M. Zolensky**. "Three-dimensional shapes and Fe contents of Stardust impact tracks: a track formation model and estimation of comet Wild 2 coma dust particle densities." *Meteoritics and Planetary Science* 45 (2010): 1302-19.

**Liou, J.-C.,** and **N. L. Johnson**. "A sensitivity study of the effectiveness of active debris removal in LEO." *Acta Astronautica* 64 (2009): 236-43.

**Liou, J.-C.,** and **N. L. Johnson**. "Characterization of the cataloged Fengyun-1C fragments and their long-term effect on the LEO environment." *Advances in Space Research* 43 (2009): 1407-15.

**Liou, J.-C., N. L. Johnson**, and **N. M. Hill**. "Controlling the growth of future LEO debris populations with active debris removal." *Acta Astronautica* 66 (2010): 648-53.

Kebukawa, Y., et al., including **K. Nakamura-Messenger,** and **M. Zolensky**. "Rapid contamination during storage of carbonaceous chondrites prepared for micro FTIR measurements." *Meteoritics and Planetary Science* 44 (2009): 545-58.

Kebukawa, Y., et al., including **M. Zolensky**. "Kinetics of organic matter degradation in the Murchison meteorite for the evaluation of parent body temperature history." *Meteoritics and Planetary Science* 45 (2010): 99-113.

Kebukawa, Y., et al., including **K. Nakamura-Messenger**, and **M. Zolensky**. "Spatial distribution of organic matter in the Bells CM2 chondrite using near-field infrared micro-spectroscopy." *Meteoritics and Planetary Science* 45 (2010): 394-405.

Kounaves, S. P., et al., including **D. W. Ming**. "Discovery of natural perchlorate in the Antarctic Dry Valleys and its global implications." *Environmental Science and Technology* 44 (2010): 2360-64.

Kounaves, S. P. et al., including **D. W. Ming**. "Soluble Sulfate in the Martian Soil at the Phoenix Landing Site." *Geophysical Research Letters* 37, L09201 (2010), doi:10.1029/2010GL042613.

Kounaves, S. P., et al., including **D. W. Ming**. "The MECA Wet Chemistry Laboratory on the 2007 Phoenix Mars Scout Lander." *Journal of Geophysical Research* 114, E00A19 (2009), doi:10.1029/2008JE003084.

Kounaves,, S. P., et al., including **D. W. Ming**, "The Wet Chemistry Experiments on the 2007 Phoenix Mars Scout Lander Mission: Data Analysis and Results." *Journal of Geophysical Research* 115, E00E10 (2010), doi:10.1029/2009JE003424.

Kueppers, M., and **M. Zolensky**. "Triple F - A Comet Nucleus Sample Return Mission." *Experimental Astronomy* 23 (2009): 809-45.

Madsen, M. B., et al., including **D. W. Ming** and **R. V. Morris**. "Overview of the Magnetic Properties Experiments on the Mars Exploration Rover." *Journal of Geophysical Research* 114, E06S90 (2009), doi:10.1029/2008JE003098.

**McKay, D. S.**, et al., including **K. L. Thomas-Keprta, S. J. Clemett,** and **E. K. Gibson**. "Life on Mars: New evidence from Martian meteorites." *Proc. of SPI, Instruments and Methods for Astrobiology and Planetary Missions XII* 7441, San Diego, CA (2009).

**McKay, D. S**., **S.J. Clemett**, **E. K. Gibson** and **K. L. Thomas-Keprta**. "Carbon in Mars meteorites: Where is the carbon on Mars?" *SPIE Optical Engineering and Applications*, San Diego, CA (August 1-5, 2010).

Mellon, M. T., et al., including **D. W. Ming** and **R. V. Morris**. "Ground ice at the Phoenix Landing Site: Stability State and Origin." *Journal of Geophysical Research* 114, E00E07 (2009), doi:10.1029/2009JE003417.

**Mendell, W**. "An Exploration-Driven Renaissance in Lunar Science." *Space Science Reviews* 150 (2010): 3-6.

Michalski, J. R., and **P. B. Niles**. "Deep Crustal Carbonate Rocks Exposed by Meteor Impact on Mars." *Nature Geoscience* 3.11 (2010): 751-55.

Michalski, J. R., et al., including **P. B. Niles**. "The Mawrth Vallis Region of Mars: A Potential Landing Site for the Mars Science Laboratory (Msl) Mission." *Astrobiology* 10 (2010): 687-703.

Mikouchi, T., and **M. Zolensky**. "Electron microscopy of pyroxenes in the Almahata Sitta ureilite." *Meteoritics and Planetary Science* 45 (2010): 1812-20.

Mikouchi, T., et al., including **M. Zolensky** and **L. Le**. "Dmitryivanovite: A new calcium aluminum oxide from the Northwest Africa 470 CH3 chondrite described using electron back-scatter diffraction analysis." *American Mineralogist* 94 (2009): 746-50.

**Morris, R V.**, et al., including **D.W. Ming**, and **D. C. Golden**. "Identification of carbonate-rich outcrops on Mars by the Spirit rover." *Science* 329 (2010): 421-24, doi:10.1126/science.1189667.

**Morris, R. V.**, et al., including **D W. Ming**. "Identification of carbonate-rich outcrops on Mars by the Spirit Rover." *Science* 329 (2010): 421-24.

**Nakamura-Messenger, K.**, et al., including **L. Keller**, **M. Zolensky**, and **S. Messenger**, "Brownleeite: a new manganese silicide mineral in an interpanetary dust particle." *American Mineralogist* 95 (2010): 221-28.

Nakamura, T., et al., including **M. Zolensky**. "Chrondrules in short-period comet 81P/Wild 2 recovered by the Stardust mission." *Chikyukagaku (Geochemistry)* 43 (2009): 143-53.

Nakamura, T., et al., including **M. Zolensky**. "Chrondrules in short-period comet 81P/Wild 2 recovered by the Stardust mission." *Japanese Geochemistry Society Magazine* (2009).

**Niles, P. B.**, et al., including **D. W. Ming** "Stable isotope measurements of martian atmospheric CO2 at the Phoenix Landing Site." *Science* 329 (2010): 1134-37., doi:10.1126/science.1192863.

**Niles, P. B.**, and J. Michalski. "Meridiani Planum Sediments on Mars Formed through Weathering in Massive Ice Deposits." *Nature Geoscience*2.3 (2009): 215-20.

**Niles, P. B.**, M.Y. Zolotov, and L. A. Leshin. "Insights into the Formation of Fe- and Mg-Rich Aqueous Solutions on Early Mars Provided by the Alh 84001 Carbonates." *Earth and Planetary Science Letters* 286.1-2 (2009): 122-30.

**Nyquist, L. E.**, **D. D. Bogard**, **C. Y. Shih**, **J. Park**, **Y. D. Reese**, and A. J. Irving. "Concordant Rb-Sr, Sm-Nd, and Ar-Ar ages for Northwest Africa 1460: A 346 Ma old basaltic shergottite related to the "lherzolitic shergottites." *Geochimica et Cosmochimica Acta* 73 (2009): 4288-4309.

**Nyquist, L. E.**, T. Kleine, **C. Y. Shih**, and **Y. D. Reese**. "The distribution of short-lived radioisotopes in the early solar system and the chronology of asteroid accretion, differentiation, and secondary mineralization." *Geochimica et Cosmochimica Acta* 73 (2009): 5115-36.

**Nguyen, A. N.**, L. R. Nittler, F. J. Stadermann, R. M. Stroud, and C. M. O'D. Alexander. "Coordinated analyses of presolar grains in the Allan Hills 77307 and Queen Elizabeth Range 99177 meteorites." *The Astrophysical Journal* 719 (2010): 166-89.

**Oehler, D. Z.**, and **C. C. Allen**. "Evidence for pervasive mud volcanism in Acidalia Planitia, Mars." *Icarus* 208.2 (2010): 636-57.

**Oehler, D. Z**., et al., including **E. K. Gibson**. "Diversity in the Archaean Biosphere: New Insights from NanoSIMS." *Astrobiology* 10.4 (2010): 413-24.

**Oehler, D. Z**., et al., including **E. K. Gibson**. "NANOSIMS: Insights to biogenicity and syngeneity of Archaean carbonaceous structures." *Precambrian Research* 173 (2009): 70-78.

**Oehler, D Z.**, et al., including **E. K. Gibson**. "Diversity in the early Archaean biosphere: New insights from NanoSIMS." *Precambrian Research* (2009).

**Peslier, A. H.** "A review of water contents of nominally anhydrous natural minerals in the mantles of Earth, Mars and the Moon." *Journal of Volcanology and Geothermal Research* 197 (2010): 239-58.

**Peslier, A. H.**, A. B. Woodland, D. R. Bell, and M. Lazarov. "Olivine water contents in the continental lithosphere and the longevity of cratons." *Nature* 467 (2010): 78-81.

**Peslier, A. H.**, D. Hnatyshin, C. D. Herd, E. L. Walton, et al. "Crystallization, melt inclusion, and redox history of a Martian meteorite: olivine-phyric shergottite Larkman Nunatak 06319." *Geochimica et Cosmochimica Acta* 74 (2010): 4543-76.

Pratt, L M., et al., including **C. C. Allen**, and **D. W. Ming**. "The Mars Astrobiology Explorer-Cacher (MAX-C): A potential rover mission for 2018." *Astrobiology* 10 (2010): 127-63, doi:10.1089/ast.2010.0462.

**Righter, K.**, **K. Pando**, and **L. R. Danielson**. "Experimental evidence for sulfur-rich Martian magmas: implications for volcanism and surficial sulfur sources." *Earth and Planetary Science Letters* 288 (2009): 235-43.

**Righter, K.**, **K. Pando**, **L. R. Danielson**, and C.-T. Lee. "Partitioning of Mo, P and other siderophile elements (Cu, Ga, Sn, Ni, Co, Cr, Mn, V, W) between metal and silicate melt as a function of temperature and melt composition." *Earth and Planetary Science Letters* 291 (2010): 1-9.

**Righter, K**., M. Humayun, A. J. Campbell, **L. R. Danielson**, D. Hill, and M.J. Drake. "Experimental studies of metal-silicate partitioning of Sb: implications for the terrestrial and lunar mantles." *Geochimica et Cosmochimica Acta* 73 (2009): 1487-1504.

**Righter, K**., V. Valencia, J. Rosas-Elguera, and M. Caffee. "Channel incision in the Rio Atenguillo, Jalisco, Mexico: 36Cl constraints on rates and cause." *Geomorphology* 120 (2010): 279-99.

Ruff, S. W., et al., including **R. V. Morris**. "Characteristics, distribution, origin, and significance of opaline silica observed by the Spirit rover in Gusev crater." *Journal of Geophysical Research* 116, E00F23 (2011), doi:10.1029/2010je003767.

Rumble, D., et al., including **M. Zolensky**. "The oxygen isotope composition of Almahata Sitta." *Meteoritics and Planetary Science* 45 (2010): 1765-70.

Ruttley, T. M., **C A. Evans**, and J. A. Robinson. "The Importance of the International Space Station for Life Sciences Research: Past and Future." *Gravitational and Space Biology* 22.2 (2009): 67-81.

Ruttley, T. M., D. L. Harm, **C. A. Evans,** and J. A. Robinson. "International Utilization at the Threshold of "Assembly Complete" - Science Returns from the International Space Station." *60th International Astronautical Congress* IAC.09 B3.4.7 (2009).

Sandford, S., et al., including **M. Zolensky**, **S. Clemett**, and B. Degregorio. "Assessment and control of organic and other contaminants associated with the Stardust sample return from Comet 81P/Wild 2." *Meteoritics and Planetary Science* 45 (2010): 406-33.

Schmidt, M. E., et al., including **D. W. Ming**. "Spectral, mineralogical, and geochemical variations across Home Plate, Gusev Crater, Mars indicate high and low temperature alteration." *Earth and Planetary Science Letters* (2009), doi:10.1016/j.epsl.2009.02.030.

Schroeder, C., et al., including **R. V. Morris**. "Properties and distribution of paired stony meteorite candidate rocks at Meridiani Planum, Mars." *Journal of Geophysical Research* 115, E00F09 (2010), doi:10.1029/2010JE003616.

Seelos, K. D. et al., including **R. V. Morris** and **D. W. Ming**. "Silica in a Mars Analog Environment: Ka'u Desert, Kilauea Volcano, Hawai'i." *Journal of Geophysical Research-Planets* 115, E00D15 (2010), doi:I:10.1029/2009JE003347.

Shafer, J. T., A. D. Brandon, T. J. Lapen, M. Righter, **A. H. Peslier**, and B. L. Beard. "Sm-Nd and Lu-Hf age and trace element systematics of Larkman Nunatak 06319: close system fractional crystallization of a shergottite magma." *Geochimica et Cosmochimica Acta* 74 (2010): 7307-28.

Smith, P. H., et al., including **D. W. Ming** and **R. V. Morris**. "$H_2O$ at the Phoenix landing site." *Science* 325 (2009): 58-61, doi:10.1126/science.1172339.

Squyres, S. W., et al., including **D. W. Ming** and **R. V. Morris**. "Exploration of Victoria Crater by the Mars Rover Opportunity." *Science* 324 (2009): 1058-61, doi:10.1126/science.1170355.

**Thomas-Keprta, K. L.**, et al., including **S. J. Clemett**, and **E. K. Gibson**. "Origin of magnetite nanocrystals in Martian meteorite ALH84001." *Geochimica et Cosmochimica Acta* 73 (2009): 6631-77.

**Wilson, T. L.**, and H. Blome. "The Pioneer Anomaly and a Rotating Gödel Universe." *Advances in Space Research* 44 (2009): 1345-53.

Wirick, S., et al., including **L. Keller**, **K. Nakamura-Messenger**, and **M. Zolensky**. "Organic matter from Comet 81P/Wild 2, IDPs and carbonaceous meteorites; Similarities and differences." *Meteoritics and Planetary Science* 44 (2009): 1611-26.

Wiseman, S M., et al., including **R. V. Morris**. "Spectral and stratigraphic mapping of hydrated sulfate- and phyllosilicate-bearing deposits in northern Sinus Meridiani, Mars." *Journal of Geophysical Research* 115, E00D18 (2010), doi:10.1029/2009JE003354.

Zipfel, J., et al., including **D. W. Ming,** and **R. V. Morris**. "Bounce Rock – A Shergottite-like basalt encountered at Meridiani Planum, Mars." *Meteoritics and Planetary Science* 46 (2011), doi:10.1111/J.1945-5100.2010.01127.X.

**Zolensky, M**., et al., including **L. Le**. "Mineralogy and petrography of the Almahata Sitta ureilite." *Meteoritics and Planetary Science* 45 (2010): 1618-37.

## Book Chapters

Hanner, M. S., and **M. Zolensky**. Chapter – "The Mineralogy of Cometary Dust." *Lecture Notes in Physics – Astromineralogy*, Germany: Springer Publishing Company, 2010. 203-32. ISBN 978-3-642-13258-2.

**Oehler, D. Z.**, et al. including **D. S. McKay**, and **E. K. Gibson**. Part 1: Fossils and Fossilization – "NanoSIMS opens a new window for deciphering organic matter in terrestrial and extraterrestrial samples". *From Fossils to Astrobiology: Records of Life on Earth and Search for Extraterrestrial Biosignatures*. Springer Publishing Company, 2009. 3-23. ISBN 978-1-4020-8836-0.

**Stefanov, W. L.**, and M. Netzband. Chapter 12 – "Characterization and Monitoring of Urban/Peri-urban Ecological Function and Landscape Structure Using Satellite Data." *Remote Sensing of Urban and Suburban Areas, Remote Sensing and Digital Image Processing*. Vol. 10. Dordrecht: Springer Publishing Company, 2010. 219-44. ISBN 978-1-4020-4371-0.

Wentz, E. A., **W. L. Stefanov**, et al., Chapter 9 – "The Urban Environmental Monitoring/100 Cities Project: The Legacy of the First Phase and Next Steps." *Global Mapping of Human Settlement: Experiences, Data Sets, and Prospects. New York*: CRC Press, 2009. 191-204. ISBN 978-1-4200-8339-2.

## NASA Technical Reports

Ambercromby, K., et al., including **M. Matney**. "Michigan Orbital Debris Survey Telescope Observations of the Geosynchronous Orbital Debris Environment Observing Years: 2002-2003, Final Report." *NASA/TP-2010-216128.* Aug. (2010).

Ambercromby, K., P. Seitzer, E. Barker, H. Cowardin, and **M. Matney**. "Michigan Orbital Debris Survey Telescope Observations of the Geosynchronous Orbital Debris Environment Observing Years: 2004-2006, Final Report." *NASA/TP-2010-216128* Aug. (2010).

**Christiansen, E. L.**, et al., including **J. L. Hyde**, **D. M. Lear**, **J.-C. Liou**, **F. Lyons**, and **T. G. Prior**. "Handbook for Designing MMOD Protection." *NASA/TM-2009-214785* (2009).

**Evans, C A.**, et al., including J. A. Robinson, J. M. Tate-Brown, and T. Thumm, and others. "International Space Station Science Research Accomplishments During the Assembly Years: An Analysis of Results from 2000-2008." NASA/TP–2009–213146–REVA (2009).

**Gibson, E. K.**, C T. Pillinger, and L Waugh. "Beagle 2 The Moon Concept Study." *NASA Report* (2009).

**Runco Jr., M.**, and K. P. Scott. *Basic Optical Theory Applied to Windows* (NASA/SP-2010-3407 – Human Integration Design Handbook, Appendix C). Baseline ed. Washington, D.C. 20546-0001: NASA, 1-27-2010. pp. 1066-1078. 1 vols. NASA – Lyndon B. Johnson Space Center 77058-3696. Web. <http://ston.jsc.nasa.gov/collections/TRS/_techrep/SP-2010-3407.pdf>.

**Runco Jr., M.**, and K. P. Scott. *Human Integration Design Handbook* (NASA Handbook – NASA/SP-2010-3407). Baseline ed. Washington, D.C. 20546-0001: NASA, 1-27-2010. pp. iii, 9-10, 592-624, 969-997 (Appendix A), 1066-1127 (Appendices C and D). 1 vols. NASA – Lyndon B. Johnson Space Center 77058-3696. Web. <http://ston.jsc.nasa.gov/collections/TRS/_techrep/SP-2010-3407.pdf>.

**Runco Jr., Mario**, and Karen P. Scott. *NASA Space Flight Human-System Standard, Volume 2: Human Factors, Habitability, and Environmental Health* (NASA Technical Standard 3001, Vol. 2). Baseline ed. Vol. 2 of 2. Washington, D.C. 20546-0001: NASA, 1-10-2011. pp. 11-12, 100, 104-07, 173-194 (Appendices A–C). 2 vols. NASA – Lyndon B. Johnson Space Center, Houston, Texas 77058-3696. Web. <https://standards.nasa.gov/documents/detail/3315785>.

**Runco Jr., M.**, and K. P. Scott. *Optical Design Guidelines for Good Windows* (NASA/SP-2010-3407 – Human Integration Design Handbook, Appendix C). Baseline ed. Washington, D.C. 20546-0001: NASA, 1-27-2010. pp. 1079-1088. 1 vols. NASA – Lyndon B. Johnson Space Center 77058-3696. Web. <http://ston.jsc.nasa.gov/collections/TRS/_techrep/SP-2010-3407.pdf>.

**Runco Jr., M.**, and K. P. Scott. *Optical Performance Requirements for Windows in Human Space Flight Applications* (NASA/SP-2010-3407 – Human Integration Design Handbook, Appendix D). Baseline ed. Washington, D.C. 20546-0001: NASA, 1-27-2010. pp. 1089-1127. 1 vols. NASA – Lyndon B. Johnson Space Center 77058-3696. Web. 10 May 2011. <http://ston.jsc.nasa.gov/collections/TRS/_techrep/SP-2010-3407.pdf>.

**Runco Jr., M.**, and K. P. Scott. *Requirements for Optical Properties for Windows Used in Crewed Spacecraft* (JSC-63307) Baseline ed. Houston, Texas 77058-3696: NASA, 6-28-2007. pp. 1-11, A1-A3. 1 vols. NASA – Lyndon B. Johnson Space Center. Web. <NASA-JSC Scientific and Technical Information Center – http://library.jsc.nasa.gov/default.aspx>.

Ryan, S. R., and **E. L. Christiansen**. "Micrometeoroid and Orbital Debris (MMOD) Shield Ballistic Limit Analysis Program." *NASA/TM-2009-214789* (2009).

Ryan, S. R., and **E. L. Christiansen**. "Mitigation of EMU Glove Cut-Hazard by MMOD Impact Craters on Exposed International Space Station Handrails." *NASA TM-2009-214783* (2009).

Ryan, S. R., T. Hedman, and **E. L. Christiansen**. "Honeycomb vs. Foam: Evaluating a Potential Upgrade to International Space Station Module Shielding for Micrometeoroids and Orbital Debris." *NASA/TM-2009-214793* (2009).

# NASA Agency Honor Awards

### NASA Exceptional Achievement Medal

*Nicholas L. Johnson (2009)*
*Richard V. Morris (2010)*

### NASA Exceptional Service Medal

*Donald D. Bogard (2010)*
*Douglas W. Ming (2010)*

### NASA Outstanding Leadership Medal

*Eileen K. Stansbery (2010)*

### NASA Quality and Safety Achievement Recognition (QASAR) Award

*J. Michael Rollins (2009)*

### NASA Group Achievement Awards

The Robert M. Walker Laboratory for Space Science Team (2009) – including:
*Keiko Nakamura-Messenger*
*Scott R. Messenger*
*Michael E. Zolensky*
*Lindsay P. Keller*
*John H. Jones*
*Simon J. Clement*

The JSC Science Operations for the Phoenix Mission Team (2009):
*Douglas W. Ming*
*Richard V. Morris*
*Paul B. Niles*
*H. Vern Lauer*
*Brad Sutter*
*Richard A. Socki*

The International Mars Architecture for the Return of Samples (iMARS) Team (2009) – including:
*Carlton C. Allen*

The Hypervelocity Impact Technology Group (2010)

Orbital Debris Program, Iridium/Cosmos Collision Risk Assessment Team (2010)

The Hypersonic Thermodynamic Infrared Measurements (HYTHIRM) Team (2010) – including:
*Tracy A. Calhoun*
*Daniel J. Smith*

# Johnson Space Center Honor Awards

### JSC Director's Commendation Award

*Kevin Righter (2009)*
*Alan D. Brandon (2009)*
*David W. Mittlefehldt (2010)*
*Mark Matney (2010)*
*Nancy G. Robertson (2010)*

### JSC Director's Innovation Award

*Lisa A. Fletcher (2009)*

# NASA Space Flight Awareness Awards

### Launch Honoree Award

*James L. Hyde (2009)*
*Nancy S. Todd (2009)*
*Tracy A. Calhoun (2009)*
*Kevin L. Crosby (2009)*

### Silver Snoopy Awards

*Freeman Bertrand (2009)*
*James L. Hyde (2010)*
*Friedrich P. Hörz (2010)*
*Gary E. Lofgren (2010)*
*Chris R. Cloudt (2010)*
*Mike Trenchard (2010)*
*Marco A. Lozano (2010)*

# Engineering and Science Contract Awards

### President's Awards

*Chris R. Cloudt – Hamilton (2009)*
*Thomas G. Prior – Hamilton (2010)*
*James L. Hyde – Barrios (2010)*
*Andrea B. Mosie – GeoControls (2010)*
*Simon J. Clemett – ERC (2010)*

### ESC Outstanding Science Paper Award

*Anne H. Peslier (2010)*

### Barrios Technology Gold Award

*Kevin R. Beaulieu (2009)*

# External Honor Awards

### Meteoritical Society Fellows

*John H. Jones (2010)*
*Scott R. Messenger (2010)*
*Kevin Righter (2010)*

### Outstanding STEM Aerospace Award

*John E. Gruener (2010)*

### Outstanding Professional Service Award of the American Society of Civil Engineers, Aerospace Division

*Wendell W. Mendell (2009)*

### United States Patent Award

*Eric L. Christiansen (2009)*

### National Science Foundation Antarctic Service Medal of the United States

*Scott R. Messenger (2010)*
*Keiko Nakamura-Messenger (2010)*

*Carlton C. Allen (2010)*
*Mary Sue Bell (2010)*

### International Space Ops Award for Outstanding Achievement

The Mars Exploration Rover Operations Team (2010) – including:
*Douglas W. Ming*
*David W. Mittlefehldt*
*Richard V. Morris*

### United States House of Representatives, House Resolution 67

Celebrating the success of NASA's Mars Exploration Rover (MER) missions (2009) – including MER Science Team members:
*Douglas W. Ming*
*Richard V. Morris*
*David W. Mittlefehldt*

### Hispanic Business Magazine, 25 Elite Women

*Laurie Y. Carrillo (2009)*

# *ARES Directorate Contacts*

| Name | Position | Phone | E-mail | Mail code |
|---|---|---|---|---|
| Eileen K. Stansbery, Ph.D. | Director, ARES | 281-483-5540 | eileen.k.stansbery@nasa.gov | KA |
| Gregory J. Byrne, Ph.D. | Deputy Director, ARES | 281-483-0500 | gregory.j.byrne@nasa.gov | KA |
| Joni W. Homol | Secretary | 281-483-7337 | joni.w.homol@nasa.gov | KA |
| Carlton C. Allen, Ph.D. | Manager, Astromaterials Curation | 281-483-5126 | carlton.c.allen@nasa.gov | KT |
| Cindy A. Evans, Ph.D. | Deputy Manager, Astromaterials Curation | 281-483-0519 | cindy.evans-1@nasa.gov | KT |
| Suzanne Summers | Secretary | 281-483-5033 | suzanne.summers-1@nasa.gov | KT |
| David S. Draper, Ph.D. | Manager, Astromaterials Research | 281-483-9486 | david.draper@nasa.gov | KR |
| Lindsay P. Keller, Ph.D. | Deputy Manager, Astromaterials Research | 281-483-6090 | lindsay.p.keller@nasa.gov | KR |
| Beverly C. Haygood | Secretary | 281-483-7316 | beverly.c.haygood@nasa.gov | KR |
| Douglas W. Ming, Ph.D. | Manager, Human Exploration Science | 281-483-5839 | douglas.w.ming@nasa.gov | KX |
| Susan K. Runco, Ph.D. | Deputy Manager, Human Exploration Science | 281-244-8848 | susan.k.runco@nasa.gov | KX |
| Beverly C. Haygood | Secretary | 281-483-7316 | beverly.c.haygood@nasa.gov | KR |
| David S. McKay, Ph.D. | Chief Scientist, Astrobiology | 281-483-5048 | david.s.mckay@nasa.gov | KA |
| Wendell W. Mendell, Ph.D. | Assistant Director for Exploration | 281-483-5064 | wendell.w.mendell@nasa.gov | KA |
| Nicholas L. Johnson | Chief Scientist for Orbital Debris | 281-483-5313 | nicholas.l.johnson@nasa.gov | KX |
| Eugene G. Stansbery | Manager, Orbital Debris Program | 281-483-8417 | eugene.g.stansbery@nasa.gov | KX |